PB80-200819

Particulate Control at High Temperature and Pressure Using Augmented Granular Bed Filters

A.P.T., Inc.
San Diego, CA

Prepared for

Industrial Environmental Research Lab.
Research Triangle Park, NC

Feb 80

U.S. Department of Commerce
National Technical Information Service
NTIS

United States
Environmental Protection
Agency

Industrial Environmental Research
Laboratory
Research Triangle Park NC 27711

EPA-600/7-80-036
February 1980

PB80-200819

EPA

Particulate Control at High Temperature and Pressure Using Augmented Granular Bed Filters

Interagency Energy/Environment R&D Program Report

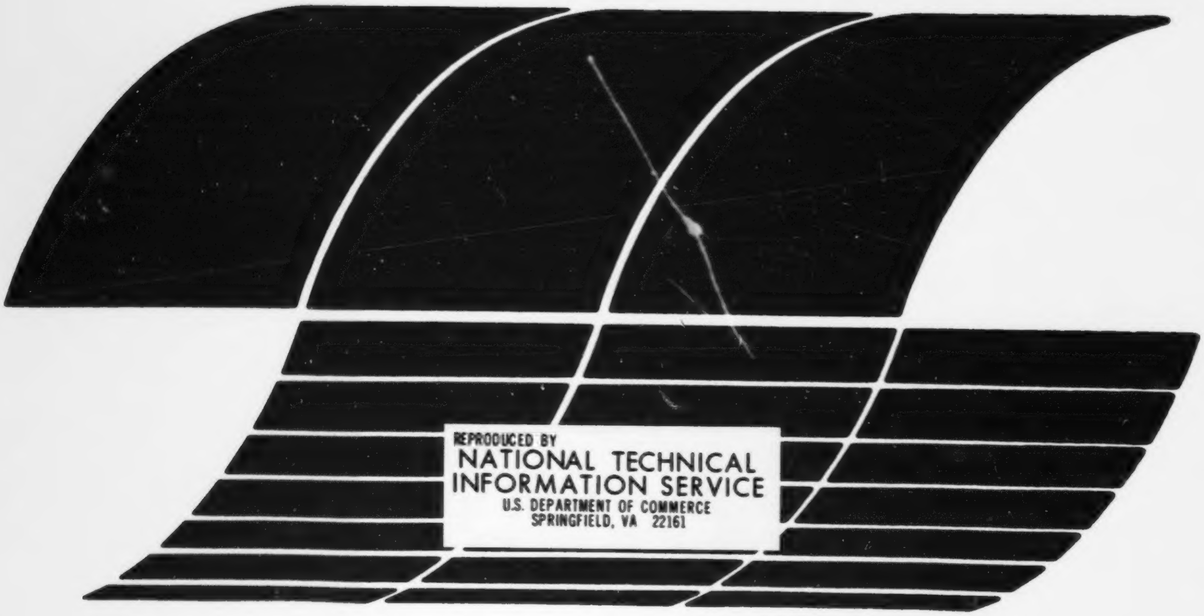

REPRODUCED BY
NATIONAL TECHNICAL
INFORMATION SERVICE
U.S. DEPARTMENT OF COMMERCE
SPRINGFIELD, VA 22161

RESEARCH REPORTING SERIES

Research reports of the Office of Research and Development, U.S. Environmental Protection Agency, have been grouped into nine series. These nine broad categories were established to facilitate further development and application of environmental technology. Elimination of traditional grouping was consciously planned to foster technology transfer and a maximum interface in related fields. The nine series are:

1. Environmental Health Effects Research
2. Environmental Protection Technology
3. Ecological Research
4. Environmental Monitoring
5. Socioeconomic Environmental Studies
6. Scientific and Technical Assessment Reports (STAR)
7. Interagency Energy-Environment Research and Development
8. "Special" Reports
9. Miscellaneous Reports

This report has been assigned to the INTERAGENCY ENERGY-ENVIRONMENT RESEARCH AND DEVELOPMENT series. Reports in this series result from the effort funded under the 17-agency Federal Energy/Environment Research and Development Program. These studies relate to EPA's mission to protect the public health and welfare from adverse effects of pollutants associated with energy systems. The goal of the Program is to assure the rapid development of domestic energy supplies in an environmentally-compatible manner by providing the necessary environmental data and control technology. Investigations include analyses of the transport of energy-related pollutants and their health and ecological effects; assessments of, and development of, control technologies for energy systems; and integrated assessments of a wide range of energy-related environmental issues.

EPA REVIEW NOTICE

This report has been reviewed by the participating Federal Agencies, and approved for publication. Approval does not signify that the contents necessarily reflect the views and policies of the Government, nor does mention of trade names or commercial products constitute endorsement or recommendation for use.

This document is available to the public through the National Technical Information Service, Springfield, Virginia 22161.

TECHNICAL REPORT DATA
(Please read Instructions on the reverse before completing)

1. REPORT NO.
EPA-600/7-80-035

2.

3. RECIPIENT'S ACCESSION NO.
PB80 200819

4. TITLE AND SUBTITLE
Particulate Control at High Temperature and Pressure Using Augmented Granular Bed Filters

5. REPORT DATE
February 1980

6. PERFORMING ORGANIZATION CODE

7. AUTHOR(S)
Shui-Chow Yung, R.G. Patterson, and Seymour Calvert

8. PERFORMING ORGANIZATION REPORT NO.

9. PERFORMING ORGANIZATION NAME AND ADDRESS
A.P.T., Inc.
4901 Morena Boulevard, Suite 402
San Diego, California 92117

10. PROGRAM ELEMENT NO.
EHE624A

11. CONTRACT/GRANT NO.
68-02-2183

12. SPONSORING AGENCY NAME AND ADDRESS
EPA, Office of Research and Development
Industrial Environmental Research Laboratory
Research Triangle Park, NC 27711

13. TYPE OF REPORT AND PERIOD COVERED
Final; 12/78 - 12/79

14. SPONSORING AGENCY CODE
EPA/600/13

15. SUPPLEMENTARY NOTES IERL-RTP project officer is Dennis C. Drehmel, Mail Drop 61, 919/541-2925.

16. ABSTRACT
The report gives results of experimental measurements (in fixed- and moving-bed filters) of the effect of electrostatic augmentation on granular bed filter particle collection efficiencies. Experimental findings included: (1) either polarizing the bed or charging the particles significantly increased the collection efficiency of the filter (efficiency increased with increasing applied voltage across the bed); (2) both polarizing the bed and charging the particles caused the bed to become very efficient in collecting particles (efficiency of a 15 cm deep bed of 1.6 mm diameter alumina spheres with a polarizing field strength of 1.31 kV/cm was above 98% for all particle sizes); (3) polarizing the bed and.or charging the particles has no effect on pressure drop across a clean bed; (4) a filter cake increases the collection efficiency of the granular bed filter (the increase depends on the cake structure and the amount of dust retained in the bed); (5) DC polarization is much more effective than low frequency AC polarization; and (6) fixed bed filters show a higher collection efficiency and a higher pressure drop than moving beds (in moving beds, lower recirculation rates also have lower rates of attrition of retaining grids and granules and lower rates of dislodging and reentraining the collected particles).

17. KEY WORDS AND DOCUMENT ANALYSIS

a. DESCRIPTORS		b. IDENTIFIERS/OPEN ENDED TERMS	c. COSATI Field/Group	
Pollution	Polarization	Pollution Control	13B	
Dust	Aluminum Oxide	Stationary Sources	11G	07B
Aerosols		Particulates	07D	
Filtration		Granular Bed Filters		
Granular Materials				
Electrostatics			20C	

18. DISTRIBUTION STATEMENT
Release to Public

19. SECURITY CLASS *(This Report)*
Unclassified

20. SECURITY CLASS *(This page)*
Unclassified

21. NO. OF PAGES

22. PRICE

EPA Form 2220-1 (9-73)

EPA-600/7-80-035
February 1980

Particulate Control at High Temperature and Pressure Using Augmented Granular Bed Filters

by

Shui-Chow Yung, R.G. Patterson,
and Seymour Calvert

A.P.T., Inc.
4901 Morena Boulevard, Suite 402
San Diego, California 92117

Contract No. 68-02-2183
Program Element No. EHE624A

EPA Project Officer: Dennis C. Drehmel

Industrial Environmental Research Laboratory
Office of Environmental Engineering and Technology
Research Triangle Park, NC 27711

Prepared for

U.S. ENVIRONMENTAL PROTECTION AGENCY
Office of Research and Development
Washington, DC 20460

ABSTRACT

The effect of electrostatic augmentation on granular bed filter particle collection efficiencies was measured experimentally in fixed and moving bed filters. The collection efficiency of a granular bed filter was greatly improved by imposing an electric field on the bed and/or by charging the particles. The electrostatically enhanced granular bed filter is capable of cleaning the gas sufficiently to meet the proposed new source performance standard of 13 mg/MJ (0.03 lb/10^6 BTU).

CONTENTS

Abstract. iii
Figures v
Tables. viii
Abbreviations and Symbols ix
Acknowledgement x

Sections

1. Summary and Conclusions 1
    Summary 1
    Conclusions 3
2. Introduction. 4
3. Fixed Bed Granular Bed Filter Experiments 5
    Fixed Bed Granular Bed Filter 5
    Collection Efficiency of a Neutral Clean Bed. 8
    Collection Efficiency of an Electrostatically Augmented Bed. 13
    Cake Filtration 22
4. Moving Bed Granular Bed Filter Experiments. 28
    Experimental Setup. 28
    Data. 30
    Data Analysis 30
5. Evaluation of Electrical Augmentation of Granular Bed Filters 41
6. Future Research Recommendations 43

References. 45

Appendices

A. Fixed Bed GBF Experimental Data. 46
B. Cascade Impactor Particle Data 67
C. Experimental Grade Penetration Curves of the Moving Bed Granular Bed Filter 79

FIGURES

Number Page

1 Schematic diagram of the experimental apparatus with PSL dispenser 6

2 Schematic diagram of the experimental apparatus with fly ash generator 7

3 Experimental pressure drop of clean GBFs 9

4 Impaction efficiency for round jet 11

5 Effect of particle charging on penetration 12

6 Redispersed fly ash particle size distribution 14

7 Experimental grade penetration of a fixed GBF 15

8 Experimental voltage-current relation 17

9 Effect of field strength on particle penetration 18

10 Experimental grade penetration of a charged GBF 20

11 Experimental particle penetration of a clean AC polarized GBF 21

12 Effects of particle loading in bed on penetration of a fixed GBF 23

13 Experimental pressure drop of a dirty GBF 25

14 Experimental penetration of a dirty GBF 26

15 Experimental penetration of a dirty GBF 27

16 Moving Bed GBF (34.3 m /min) 29

17 Measured particle penetration for various operating conditions of a GBF 32

18 Effect of granule recirculation rate on penetration 34

19 Effect of granule recirculation rate on penetration 35

FIGURES (continued)

Number Page

20 Effect of granule cleanliness on penetration. 36

21 Measured penetrations of a fixed bed and a moving GBF . 37

22 Effect of gas velocity on penetration 39

23 Effect of gas velocity on penetration 40

Appendix A

A-1 Experimental particle penetration of a clean, grounded GBF 47

A-2 Experimental particle penetration of a clean, grounded GBF 48

A-3 Experimental particle penetration of a clean, neutralized GBF 49

A-4 Experimental charged particle penetration through neutral, clean GBF. 50

A-5 Experimental charged particle penetration through neutral, clean GBF. 51

A-6 Experimental charged particle penetration through a neutral, clean GBF. 52

A-7 Experimental particle penetration of a clean, DC polarized GBF 53

A-8 Experimental particle penetration of a clean, DC polarized GBF 54

A-9 Experimental particle penetration of a DC polarized, clean GBF 55

A-10 Experimental particle penetration of a clean, DC polarized GBF 56

A-11 Experimental charged particle penetration through a clean, DC polarized GBF 57

A-12 Experimental charged particle penetration through a clean, DC polarized GBF 58

A-13 Experimental charged particle penetration through a clean, DC polarized GBF 59

FIGURES (continued)

Number | Page

A-14 Experimental charged particle penetration through a clean, DC polarized GBF. 60

A-15 Experimental particle penetration of a dirty GBF 61

A-16 Experimental penetration of a dirty, charged GBF 62

A-17 Experimental penetration of a dirty, grounded fixed GBF. 63

A-18 Experimental penetration of a dirty GBF. 64

A-19 Experimental penetration of an AC charged, dirty, fixed GBF. 65

A-20 Experimental penetration of an AC charged, dirty, fixed GBF. 66

Appendix C

C-1 through C-14 Experimental grade penetration curves of the moving GBF. 80

TABLES

Number Page

1 Test Conditions and Particle Data. . . . .

Appendix B

B-1 through B-21 - Cascade Impactor Data for Runs #1 through #21. . . . .

LIST OF ABBREVIATIONS AND SYMBOLS

C' = Cunningham slip correction factor, dimensionless
d_c = collector diameter, μm or cm
d_p = particle diameter, μm or cm
d_{pn} = number median diameter of particle, μm or cm
K_p = inertial impaction parameter, dimensionless
M = ratio of granule mass recirculated to gas mass flow kg/kg
Pt_d = penetration for particle diameter "d", fraction
u_j = jet velocity, cm/s
u_G = superficial gas velocity, cm/s
Z = bed thickness, cm

Greek

η = single impaction stage collection efficiency, fraction
ε = bed porosity, fraction
ρ_p = particle density, g/cm^3
σ_G = geometric standard deviation, dimensionless
ΔP = pressure drop, cm W.C.
μ_G = gas viscosity, g-cm/s

ACKNOWLEDGEMENT

A.P.T., Inc. wishes to express its appreciation for excellent technical coordination and for very helpful assistance in support of our technical effort to Dr. Dennis C. Drehmel of the U.S. Environmental Protection Agency.

SECTION 1

SUMMARY AND CONCLUSIONS

SUMMARY

The feasibility of advanced energy processes depends on the availability of a very efficient high temperature and pressure (HTP) particulate cleanup device. The particulate control equipment should be capable of operating at a gas temperature up to 950°C and a gas pressure up to 20 atm.

Granular bed filters (GBFs) have been proposed as control equipment for removing fine particles from high temperature and high pressure gas streams. It has been shown by Yung, et al. (1979) that the use of GBFs for HTP applications is limited by the particulate removal efficiency and operating difficulties. By properly selecting granules and structural materials, the granular bed filter could be capable of operating at the temperatures and pressures encountered in advanced energy processes. However, unless aided by other collection mechanisms, the present GBF designs are not likely to meet the proposed NSPS for boilers or the turbine requirements proposed by Sverdrup and Archer (1977).

There are several methods that may be used to increase the collection efficiency. One method is to use a deep bed of fine granules and a high face velocity. This is not a desirable approach as the pressure drop would be very high. Other effective methods are electrostatic augmentation and cake filtration.

If the bed is placed in a polarizing electric field, the granules will be polarized to produce an inhomogeneous electric field near the granule surface. A charged particle entering the bed will interact with the external field and the local field. The dipole interaction force between the granule and the particle will result in a higher collection efficiency. If the particles are uncharged, the external field will also polarize the particles. The dipole interaction force still exists.

A filter cake may be used to increase the collection efficiency of the bed. The collection mechanism depends on the type of cake. A surface cake predominantly collects by sieving. If it is an internal cake, then impaction may be more important. The dust deposit can increase the impaction parameter by reducing the bed porosity and increasing the gas velocity in the bed. A larger impaction parameter results in a higher collection efficiency.

The effectiveness of cake filtration and electrostatic augmentation were measured experimentally in the laboratory. Experiments were performed on two small scale granular bed filters. They were a fixed bed with a gas flow capacity of $0.44 m^3/min$ (15.5 CFM) and a moving bed with gas capacity of $2.8 m^3/min$ (100 CFM).

All experiments were performed under ambient conditions. Monodispersed polystyrene latex and redispersed fly ash particles were used for testing. Test conditions included:

1. Grounded bed/uncharged particle
2. Polarized bed/uncharged particle
3. Grounded bed/charged particle
4. Polarized bed/charged particle
5. Clean and dirty bed
6. AC and DC polarization

The experimental findings are:

1. By either polarizing the bed or charging the particles, the collection efficiency of the filter increased significantly. The collection efficiency increased with increasing applied voltage across the bed.

2. By both polarizing the bed and charging the particles, the bed becomes very efficient in collecting particles. For a 15 cm deep bed of 1.6 mm diameter alumina spheres and with a polarizing field strength of 1.31 kV/cm, the collection efficiency was above 98% for all particle sizes.

3. Polarizing the bed and/or charging the particles has no effect on pressure drop across a clean bed.

4. The presence of a filter cake will increase the collection efficiency of the granular bed filter. The increase depends on the cake structure and the amount of dust retained in the bed.

5. DC polarization is much more effective than low frequency AC polarization.

6. Fixed bed GBFs exhibit a higher collection efficiency and a higher pressure drop than moving beds. In the moving bed system, lower recirculation rate also has a lower rate of attrition of retaining grids and granules and a lower rate of dislodging and reentraining the collected particles.

CONCLUSIONS

It has been demonstrated that the collection efficiency of a granular bed filter can be greatly improved by imposing an electric field on the bed and by charging the particles. The electrostatically enhanced granular bed filter is able to clean the gas to meet the current and proposed new source performance standards. However, in order for the granular bed filter to be commercially acceptable and competitive, several operational problems and uncertainties need to be resolved. Development needs include: reliable bed cleaning method, a cost effective granule regeneration and recirculation technique, HTP electrical insulation, means for minimizing the erosion of bed retaining grids, and particle reentrainment prevention.

SECTION 2

INTRODUCTION

Granular bed filters have been proposed as fine particle control devices for advanced energy processes operating at high gas temperatures and gas pressures. Yung et al. (1979) evaluated granular bed filter technology and concluded that granular bed filters have the potential to meet New Source Performance Standards (NSPS) and gas turbine requirements. However, present granular bed filter designs do not have high enough collection efficiency for fine particles, especially when operating at high temperatures.

A few quantitative studies have been reported in the literature which indicate that the collection efficiency of the bed may be increased by: (1) electrostatic augmentation, and (2) cake filtration.

In this study we performed bench scale experiments to evaluate the increases in particle collection efficiency obtained by augmenting the GBF with electrostatic force and by establishing a filter cake. This report presents the experimental results.

SECTION 3

FIXED BED GRANULAR BED FILTER EXPERIMENTS

FIXED BED GRANULAR BED FILTER

The small scale fixed bed granular bed filter was made of 10.2 cm (4 in.) I.D. glass pipe. The filter was a bed packed with either -28 +35 mesh (420 μm to 595 μm diameter) sand, 1 mm diameter glass beads, or 1.6 mm diameter alumina spheres. A maximum gas flow rate of 0.44 m^3/min (15.5 CFM) was used.

Two types of particles were studied. They were monodisperse polystyrene latex (PSL) and redispersed power plant fly ash. The experimental setup for using PSL particles is shown in Figure 1. Filtered room air was used for the study and all flow rates were monitored with rotameters. Monodisperse polystyrene latex aerosol was generated using a Collison atomizer. The aerosol mist from the generator mixed with a stream of filtered dilution air and either passed through a Krypton 85 charge neutralizer or was charged by passing through a corona charging section.

Following the neutralizing section or the charging section, the aerosol was further diluted with filtered room air. It then flowed into the granular bed test section, which could either be polarized by imposing an electrostatic field across the bed in the direction of gas flow or could be grounded. The particle concentrations before and after the bed were measured with an optical counter. Pressure drop was monitored with calibrated gauges.

The experimental setup for using redispersed fly ash particles is shown in Figure 2. It is similar to the apparatus for using PSL particles except the Collison atomizer, charger and neutralizer were replaced with a fluidized bed particle generator.

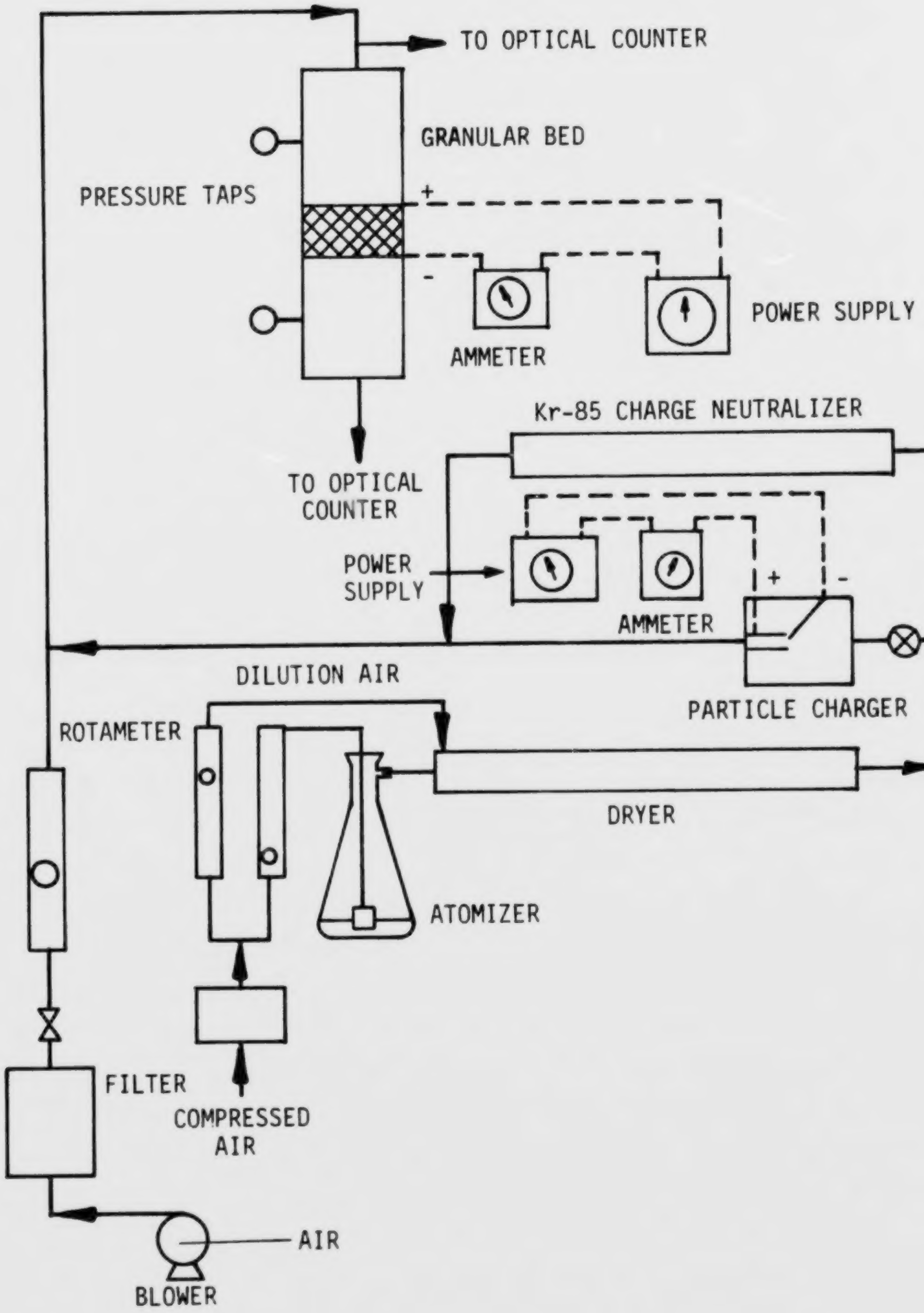
TO OPTICAL COUNTER
GRANULAR BED
PRESSURE TAPS
+
-
AMMETER
POWER SUPPLY
Kr-85 CHARGE NEUTRALIZER
TO OPTICAL COUNTER
POWER SUPPLY
AMMETER
+
-
PARTICLE CHARGER
DILUTION AIR
ROTAMETER
DRYER
ATOMIZER
FILTER
COMPRESSED AIR
AIR
BLOWER

Figure 1. Schematic diagram of the experimental apparatus with PSL dispenser.

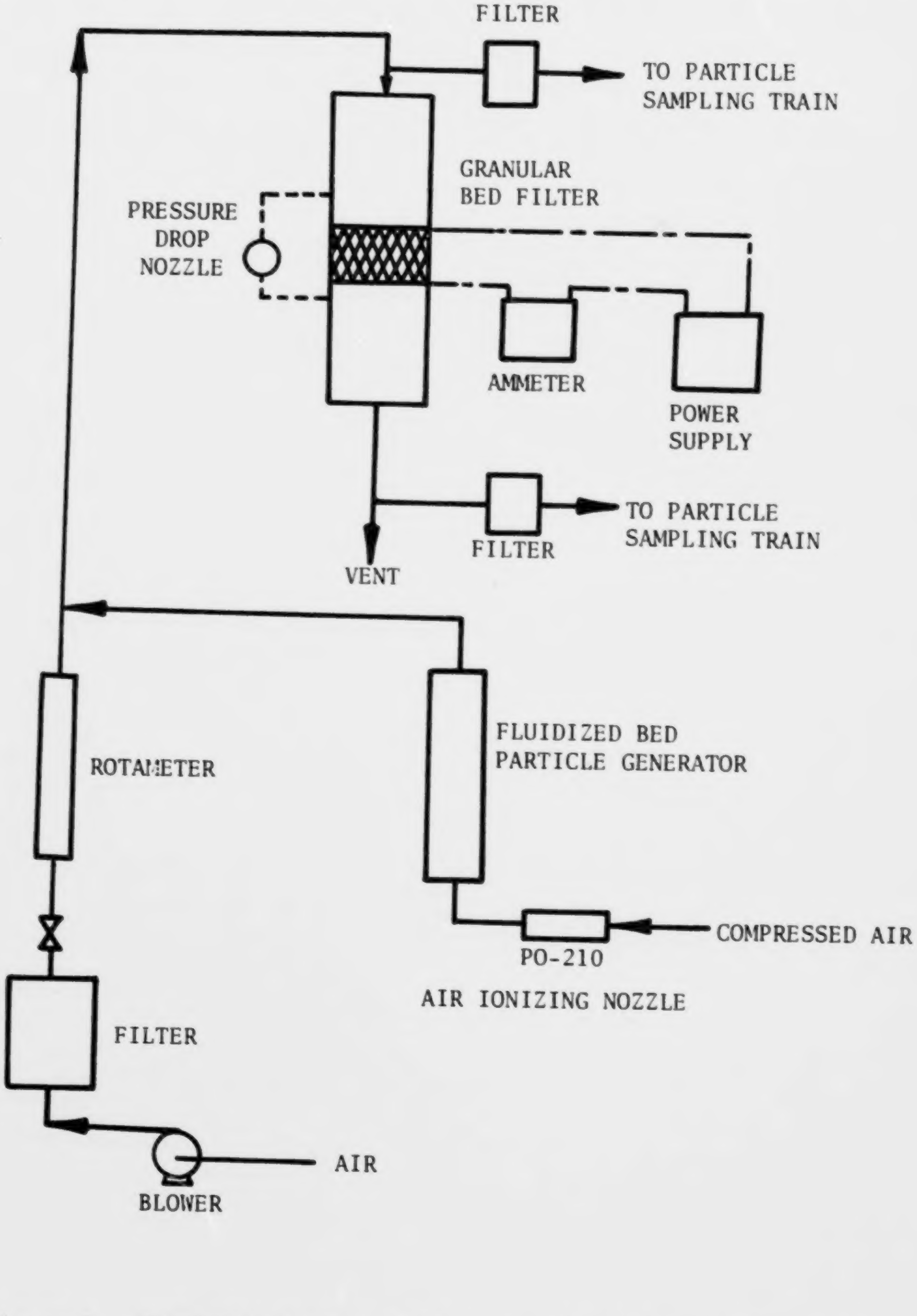
FILTER
TO PARTICLE SAMPLING TRAIN
GRANULAR BED FILTER
PRESSURE DROP NOZZLE
AMMETER
POWER SUPPLY
TO PARTICLE SAMPLING TRAIN
FILTER
VENT
ROTAMETER
FLUIDIZED BED PARTICLE GENERATOR
COMPRESSED AIR
PO-210
AIR IONIZING NOZZLE
FILTER
AIR
BLOWER

Figure 2. Schematic diagram of the experimental apparatus with fly ash generator.

COLLECTION EFFICIENCY OF A NEUTRAL CLEAN BED

Polystyrene Latex Particles

The particle penetration was measured for several bed materials and bed thicknesses. Gas phase pressure drop is plotted against superficial gas velocity in Figure 3. The data for neutralized 1.1 µm diameter polystyrene latex particles are presented in Figures A1 to A3 of Appendix "A".

As has been observed by other investigators, the particle penetration of a clean neutral bed decreases with increasing bed thickness, increasing superficial gas velocity, and decreasing granule diameter.

We (Yung et al., 1979) performed an extensive study of particle collection by clean granular bed filters and developed a mathematical model for particle collection by inertial impaction in a clean granular bed filter. The model is:

$$Pt_d = (1 - \eta)^{1.5Z/d_c} \qquad (1)$$

where: Pt_d = penetration for particle diameter "d_p", fraction
η = single impaction stage collection efficiency, fraction
Z = bed depth, cm
d_c = granule diameter, cm

The single stage collection efficiency was calculated from experimental data and can be approximated by the following empirical equation:

$$\eta = 10\, K_p^{3.23} \exp(0.27\, \ell n^2\, K_p) \qquad (2)$$

$$0.003 \leq K_p \leq 0.15$$

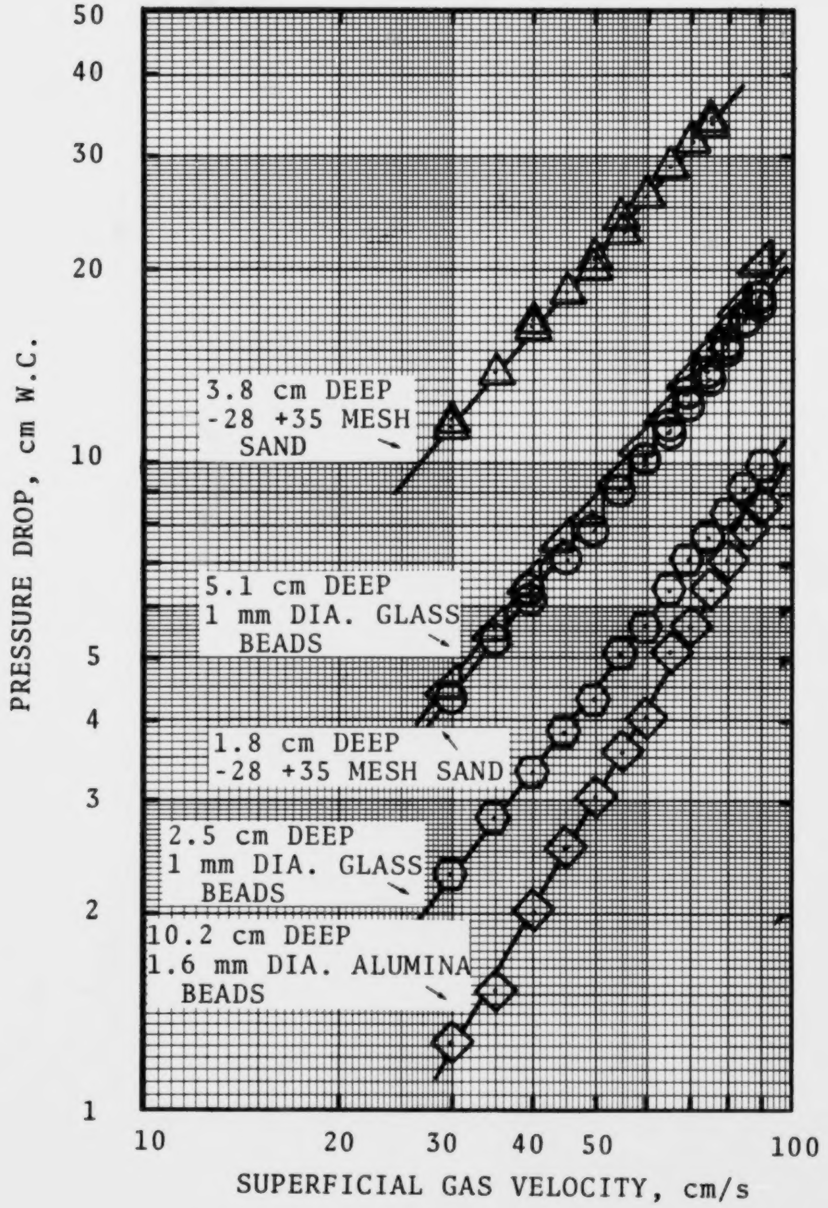

Figure 3. Experimental pressure drop of clean GBFs.

where: K_p = inertial impaction parameter, dimensionless

$$= \frac{C' d_p^2 \rho_p u_j}{9 \mu_G d_c} = \frac{3}{2} \frac{1-\varepsilon}{\varepsilon} \frac{C' d_p^2 \rho_p u_G}{9 \mu_G d_c}$$

C' = Cunningham slip correction factor, dimensionless
d_p = particle diameter, cm or μm
ρ_p = particle density, g/cm³
u_j = Jet velocity, cm/s
u_G = superficial gas velocity, cm/s
ε = bed porosity, fraction
d_c = granule diameter, cm
μ_G = gas viscosity, g-cm/s

Single stage collection efficiency based on equation (1) was calculated from data obtained in this study. Efficiencies computed this way are plotted against "K_p" in Figure 4 along with that reported by Yung et al. (1979). As can be seen, the two sets of data are in good agreement.

Experimentally determined penetrations of charged particles through neutral beds are plotted in Figures A-4 through A-6. Particle charging will decrease the penetration, as illustrated in Figure 5. For a 1.8 cm deep bed of -28 +35 mesh sand operated at u_G = 40 cm/s, the penetration decreased from 75% to 39% after charging only the particles.

Fly Ash Particles

Two runs were performed with redispersed fly ash particles. The aerosol was passed through the bed at a superficial gas velocity of 50 cm/s. The bed was packed with 1.5 mm diameter alumina spheres to a depth of 10.2 cm (4 in.).

Particle samples were taken isokinetically before and after the bed with filters. The particle size distributions were determined by analyzing the filtered samples with a Coulter Counter.

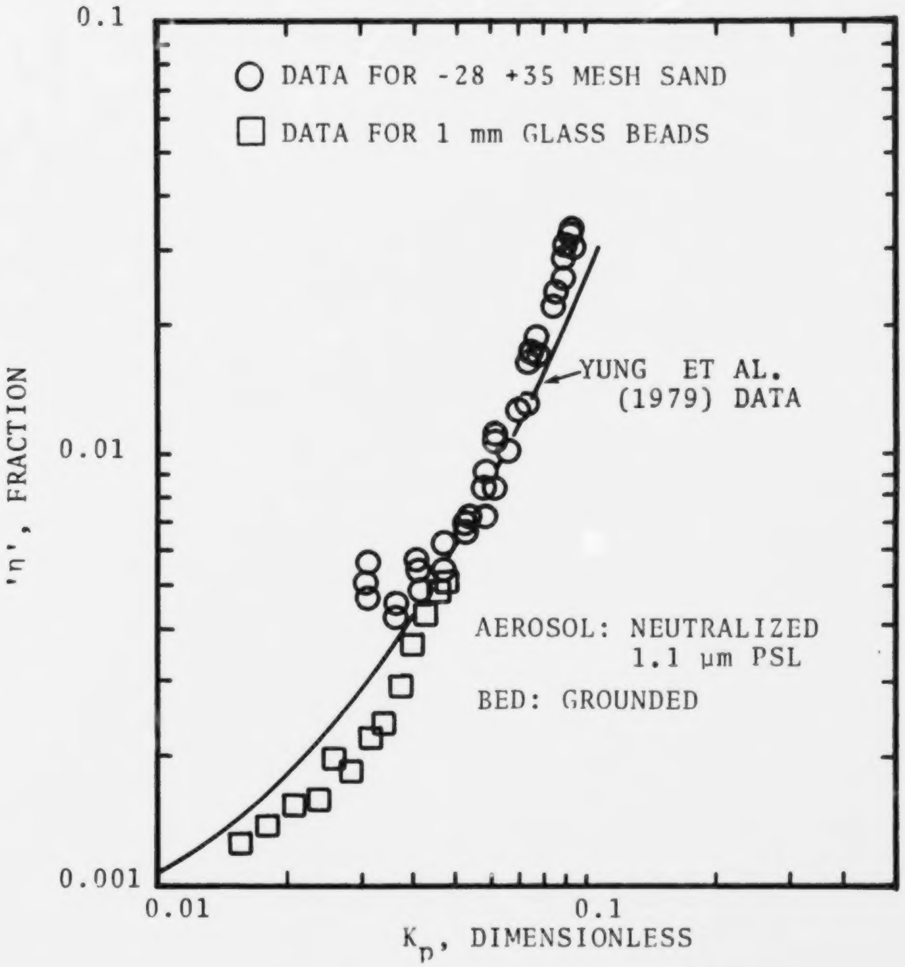

Figure 4. Impaction efficiency for round jet.

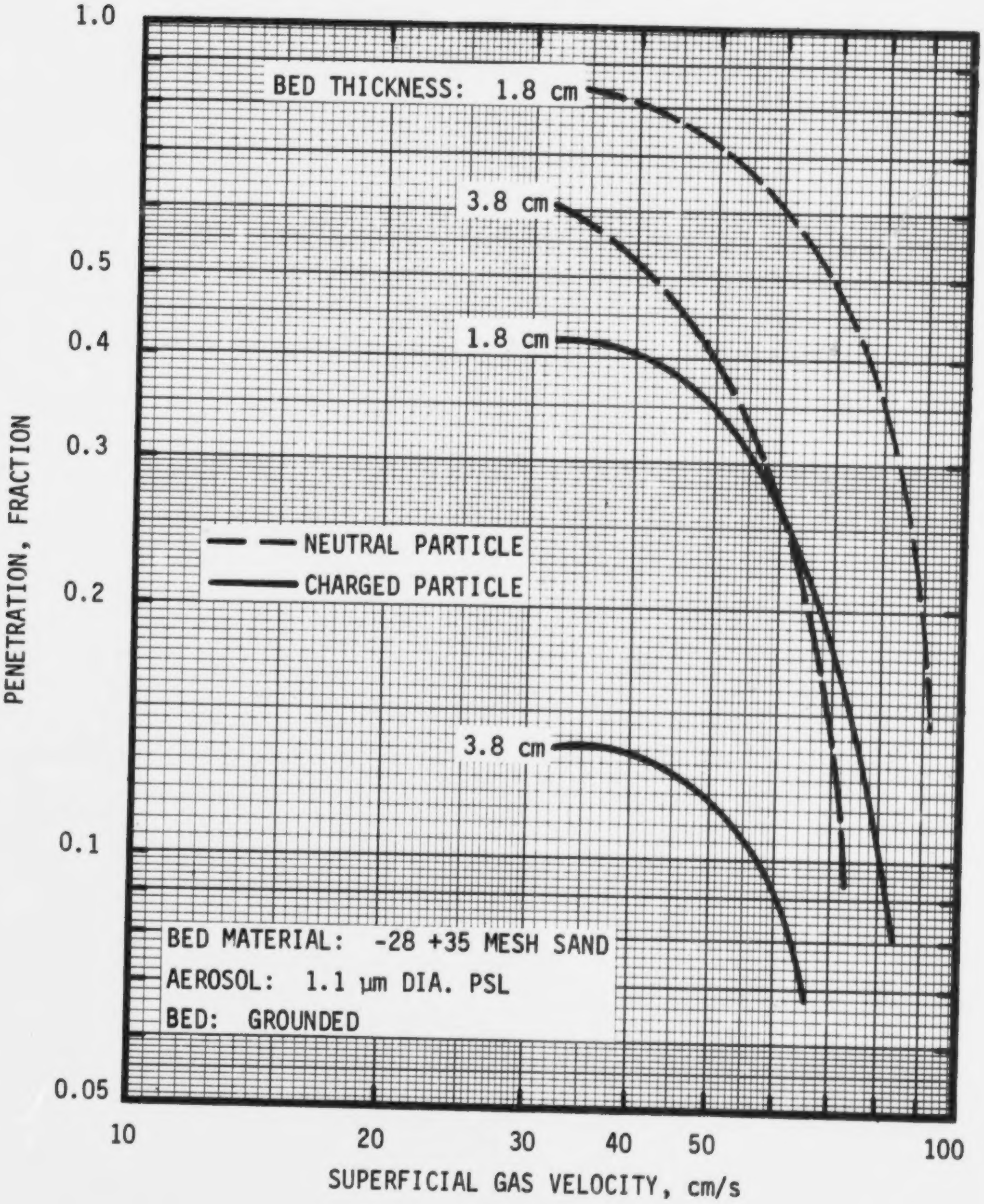

Figure 5. Effect of particle charging on penetration.

Grade penetration curves and the amount of particles collected by the bed were calculated from the filter data and Coulter Counter data.

The first run lasted 40 minutes. The inlet particle concentration was 2.45 g/DNm^3 (1.07 gr/SCF) and the outlet particle concentration was 0.018 g/DNm^3 (0.0075 gr/SCF). Thus, the overall penetration was 0.7%. The fly ash retention in the bed was calculated to be 0.31 g/cm^2 of bed cross section.

The second run lasted 105 minutes. The inlet and outlet particle concentrations were 1.4 g/DNm^3 (0.57 gr/SCF) and 0.11 g/DNm^3, respectively. The overall penetration was 8% and the particulate retention in the bed was 0.4 g/cm^3.

The difference in overall penetration was mainly due to the difference in inlet particle size distribution. Figure 6 shows the inlet and outlet particle size distributions for these two runs. For Run #1, the number median diameter, "d_{pN}" is 1.6 μm and the geometric standard deviation, "σ_g", is 1.6. For Run #2, d_{pN} = 0.8 μm and σ_g = 1.9.

The grade penetration curves for these two runs were close to each other as shown in Figure 7. The dashed line is the prediction based on equation (1). A particle density of 2.2 g/cm^3 was used in the calculations. The agreement between measurement and theory is good.

COLLECTION EFFICIENCY OF AN ELECTROSTATICALLY AUGMENTED BED

DC Augmented Bed

PSL Particles

The filtration efficiency can be enhanced by electrostatic augmentation. If the filtration medium is immersed in an electrostatic field, particles will be driven in a direction that tends to increase the probability of impact between particles and the filter medium.

Figures A-7 through A-10 in Appendix "A" show the experimental particle penetration of neutralized 1.1 μm diameter polystyrene latex particles through a clean DC augmented bed. Penetration

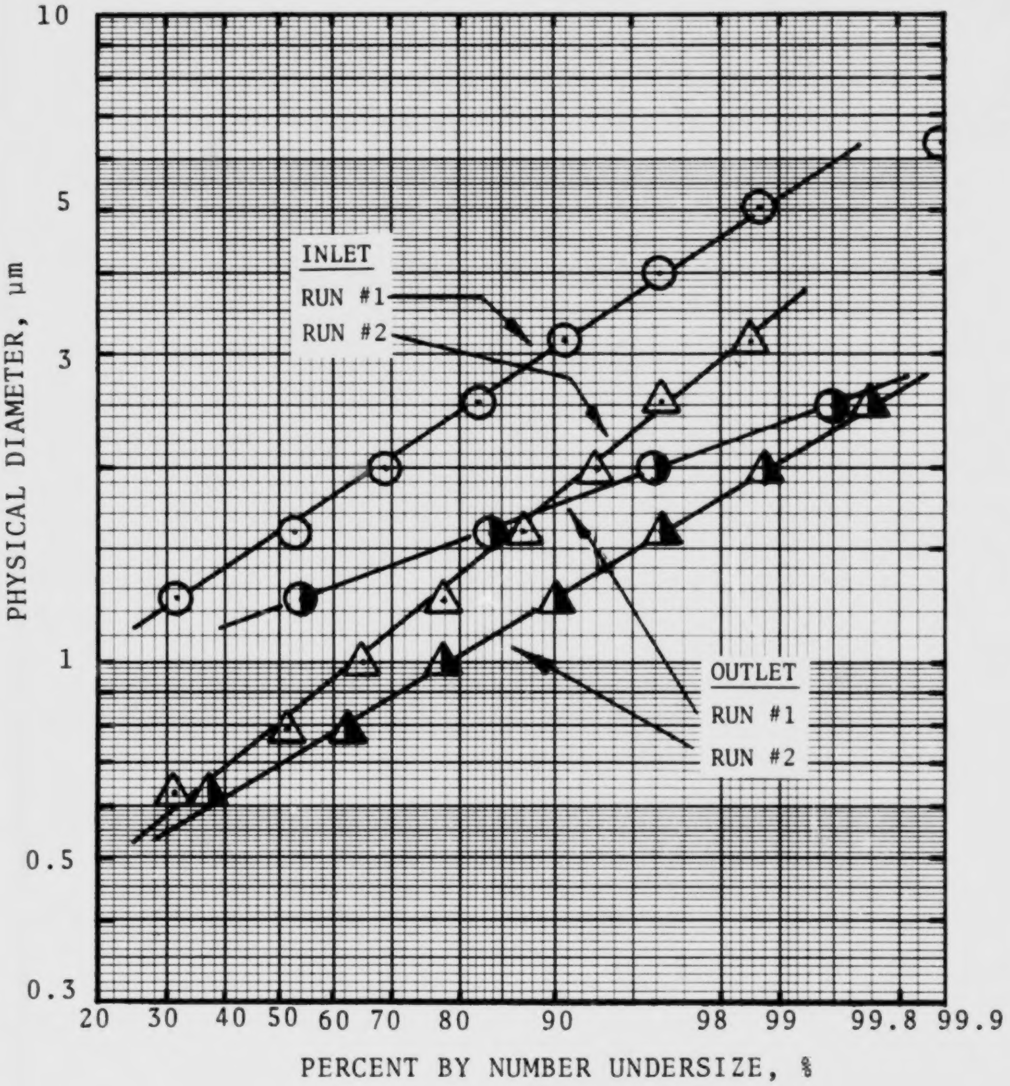

Figure 6. Redispersed fly ash particle size distribution.

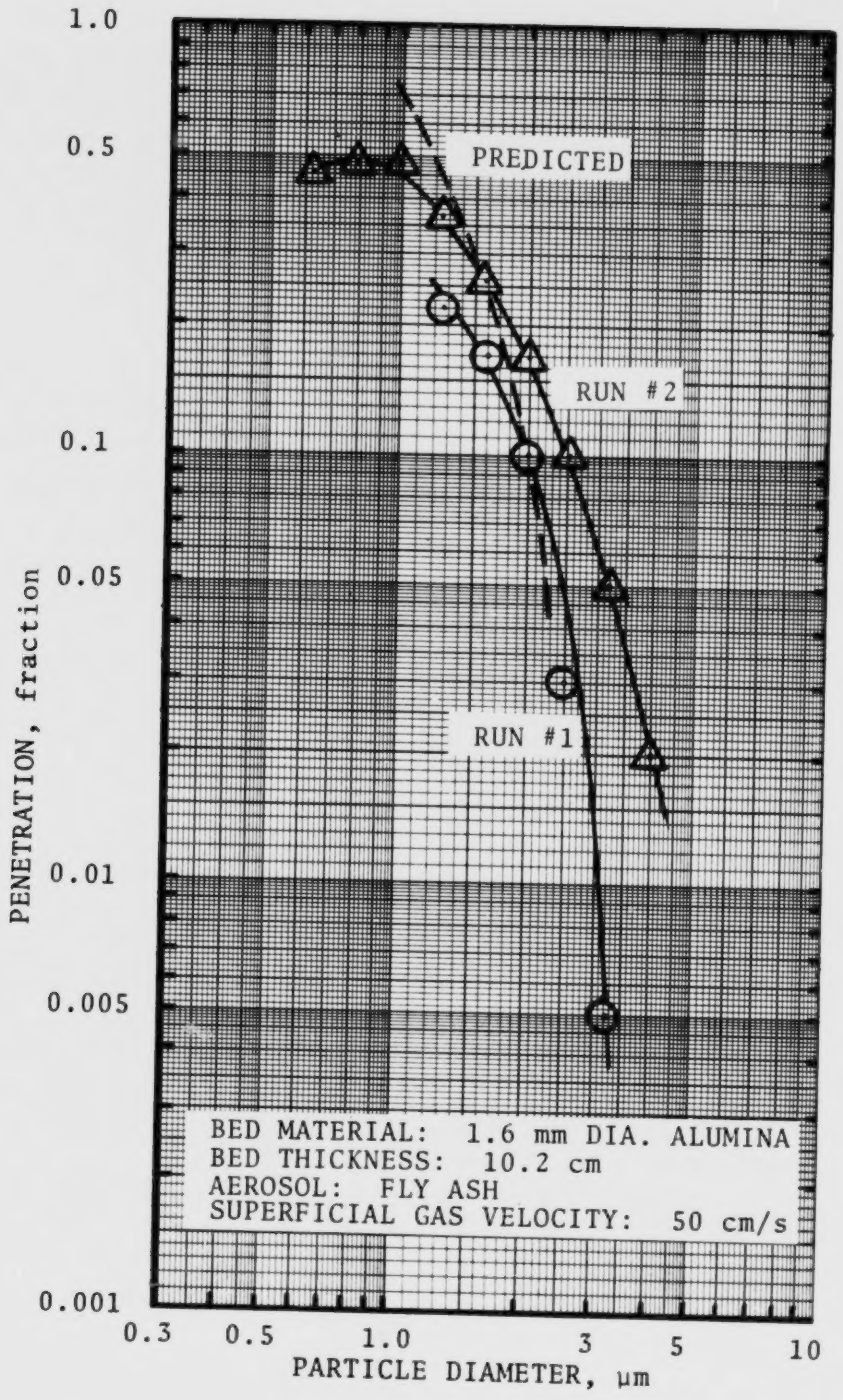

Figure 7. Experimental grade penetration of a fixed GBF.

of charged particles through a clean, DC polarized bed are shown in Figures A-11 through A-14.

By polarizing the bed, the particle collection efficiency was increased. The collection efficiency increased with increasing applied voltage across the bed. For a 1.8 cm deep bed packed with -28 +35 mesh sand, collection efficiency for 1 μm diameter particles at u_G = 40 cm/s increased from 25% to 90% (penetration decreased from 75% to 10%) when the applied voltage across the bed increased from 0 to 11.4 kV (from 0 to 6.3 kV/cm)

With the particles charged and the bed polarized, the GBF collection efficiency can be very high. The highest voltage across the bed in the charged particle/polarized bed experiment was 1.6 kV for the 1.8 cm deep bed of -28 +35 mesh sand. The collection efficiency for 1.1 μm diameter aerosol was 96% at u_G = 40 cm/s. The applied voltage across the bed could be higher but the experimental measurements were limited by the sensitivity of the optical counter. At higher applied voltage the particle concentration at the GBF outlet was too low for the counter to measure accurately.

Polarizing the bed and/or charging the particles did not change the pressure drop across a clean bed.

Figure 8 shows the voltage and current relationship across the bed. Since water is a semi-conductor, the current flow varies with moisture content in the bed and with the humidity of gas passing through the bed. Data shown in Figure 8, were taken when the relative humidity of the ambient air was 60%. As can be seen from Figure 8, the current flow is almost independent of the superficial gas velocity at a constant voltage across the bed.

Figure 9 shows a cross plot of the data. Particle penetration for 1.1 μm diameter particle is plotted against field strength for beds operated at a superficial gas velocity of 40 cm/s. The pressure drop across the beds was 6.4 cm W.C.

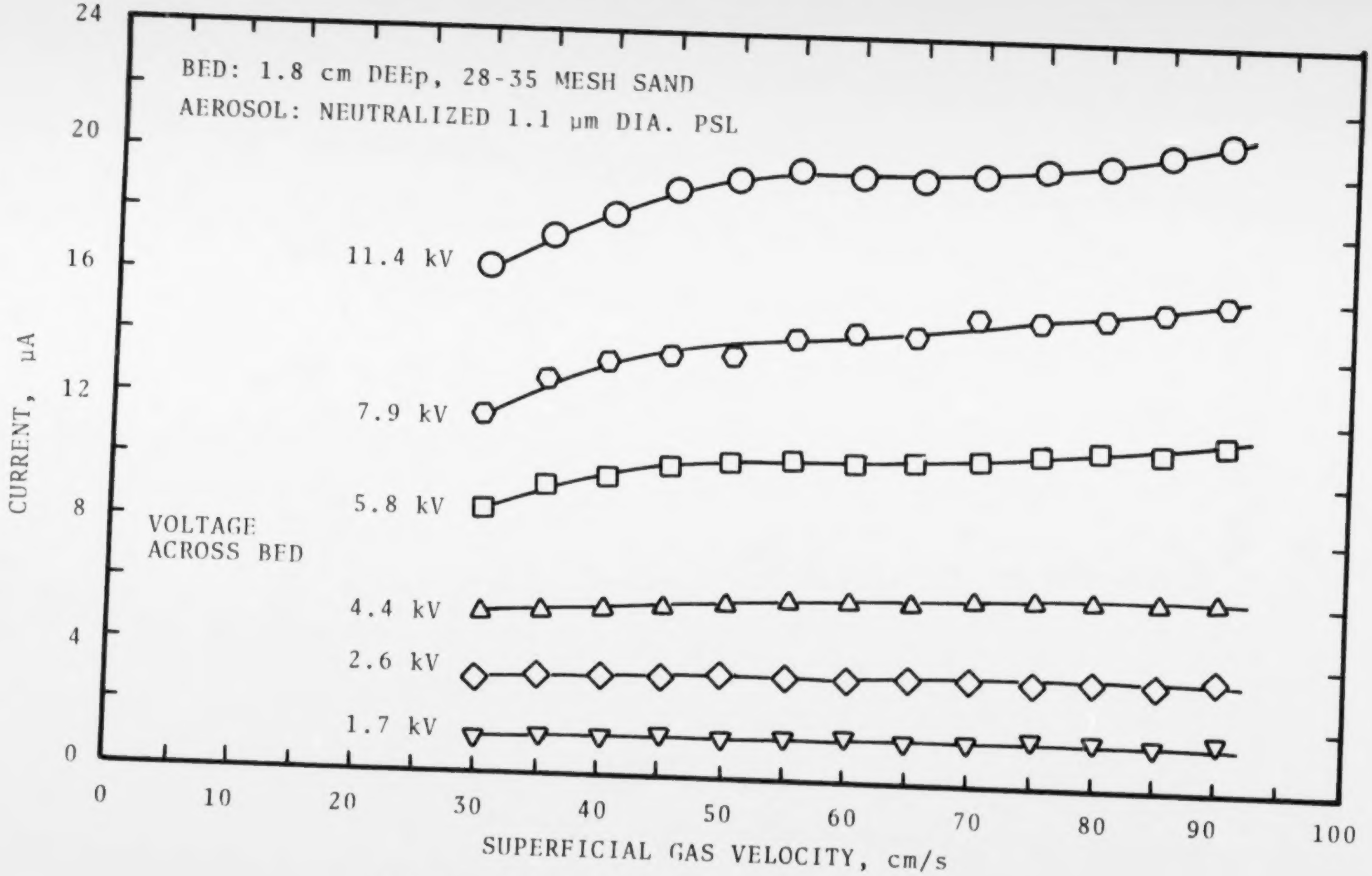

Figure 8. Experimental voltage-current relation.

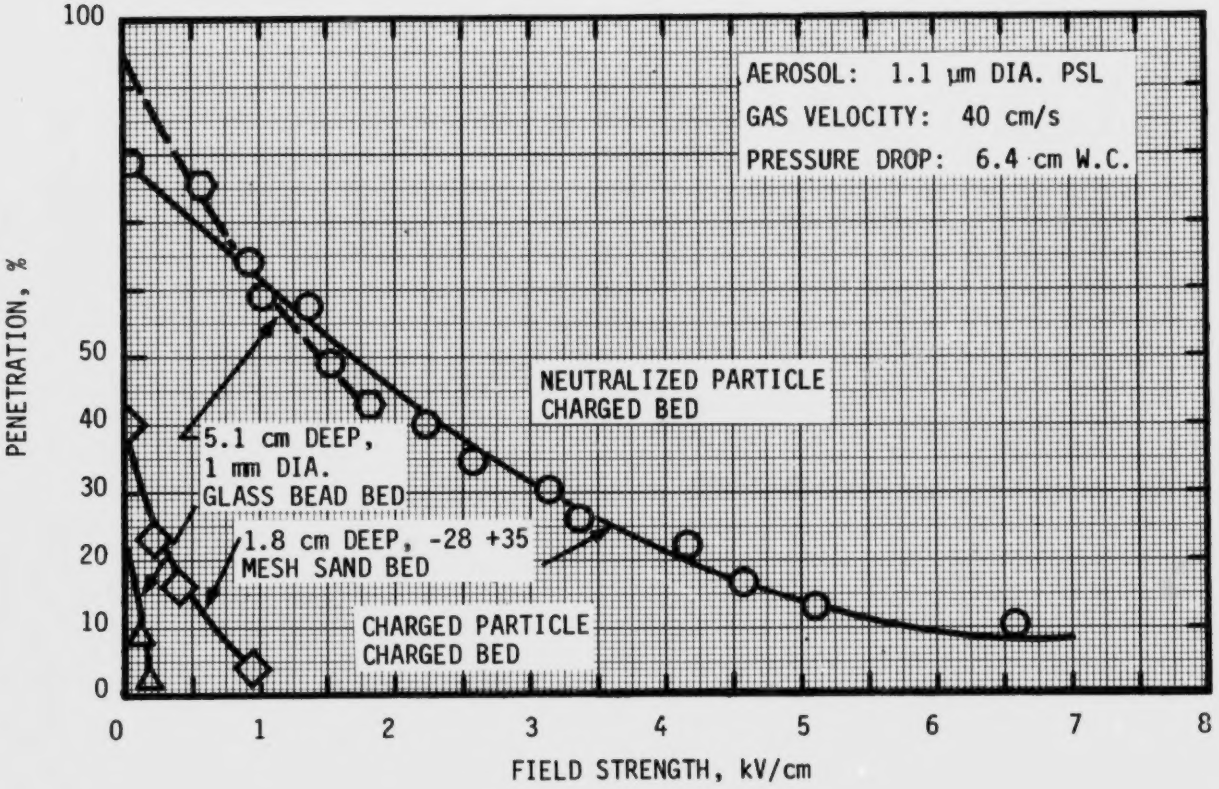

Figure 9. Effect of field strength on particle penetration.

The pressure drops across 1.8 cm deep bed of -28 +35 mesh (500 μm diameter) sand and 5.1 cm deep bed of 1 mm diameter glass beads were identical. When both the bed and particles were uncharged, the sand bed gave higher collection efficiency as revealed by comparing Figure A-1 with Figure A-2. However, when the beds were charged, the collection efficiencies of the sand bed and the glass bed were about the same, at the same field strength (Figure 9). Thus, for an industrial GBF with polarized beds, deeper beds of larger granules could be used in place of shallow beds of fine granules. The use of larger granules can reduce the possibility of plugging of the retaining grids by dust since larger opening retaining grids could be used.

The use of larger granules and deeper bed does have a drawback. It requires a higher applied voltage to obtain the same field strength.

Fly Ash Particles

One run was done with fly ash particles. The grade penetration curve for a DC polarized bed is shown in Figure 10 along with that for a neutral bed. As with PSL particles, the collection efficiency was greatly improved by polarizing the bed with an external field. The improvement is greater for submicron particles than larger particles.

AC Polarized Bed

A few runs were performed to determine the feasibility of using AC to polarize the bed. Figure 11 shows the data for the penetration of neutralized 1.1 μm diameter particles through an AC polarized bed, 10.2 cm deep of 1.6 mm diameter alumina spheres. Data for neutral bed and for DC polarized bed are also shown.

Polarizing the bed with AC did slightly improve the collection efficiency of the bed for 1.1 μm diameter particles. However, the improvement appeared to be less than DC polarization with the same field strength. In addition, the power consumption

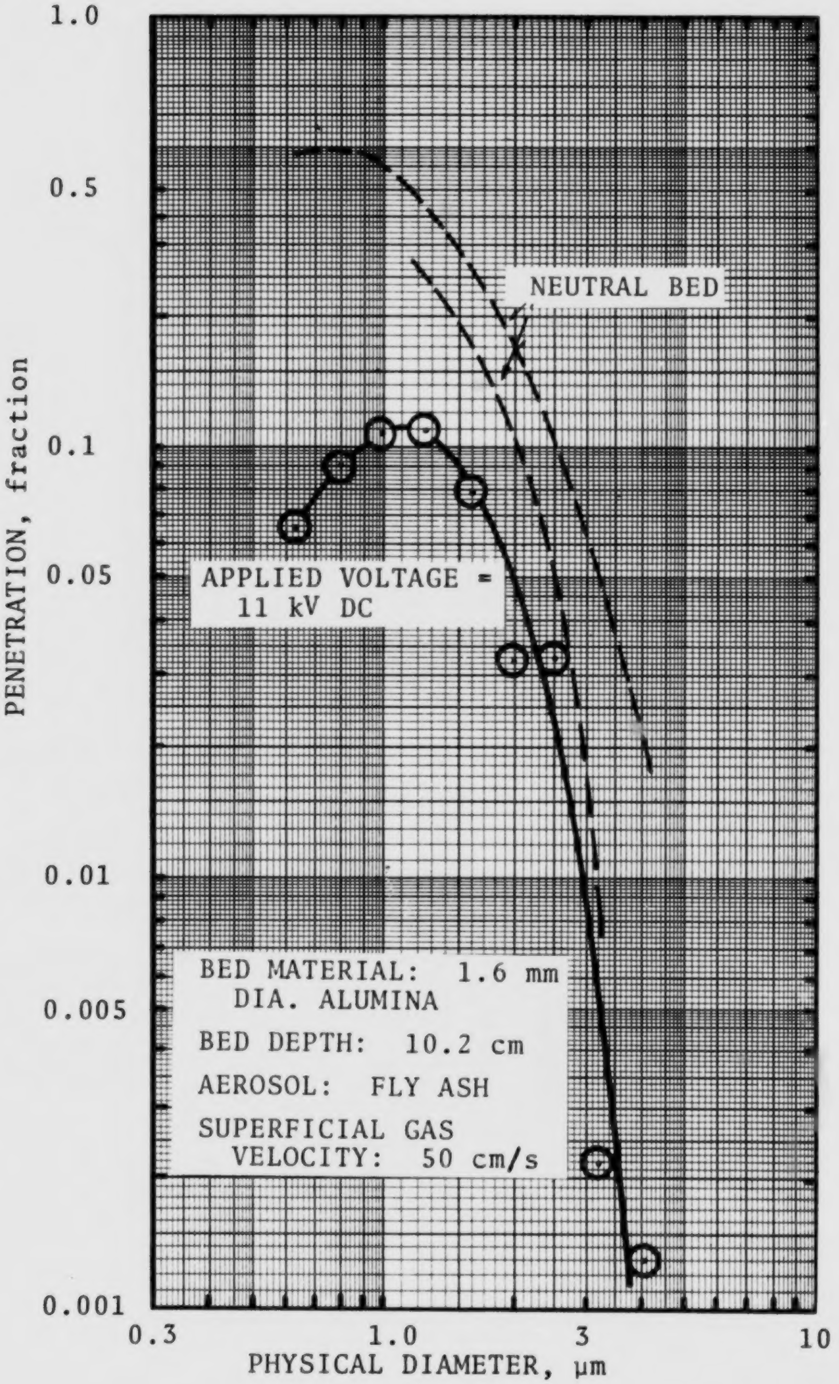

Figure 10. Experimental grade penetration of a charged GBF.

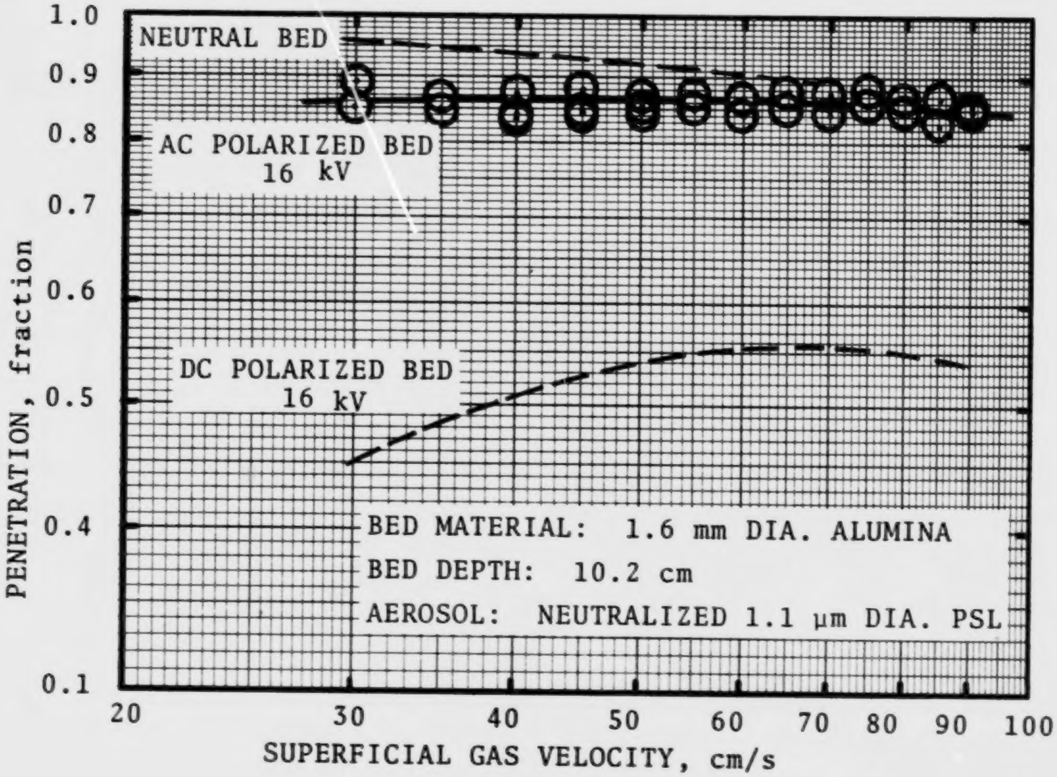

Figure 11. Experimental particle penetration of a clean AC polarized GBF.

with AC polarization was about ten times higher than with DC polarization (for DC polarization, I = 1 μA; for AC polarization, I = 10 μA).

CAKE FILTRATION

The collection efficiency of the granular bed will be higher if there is a filter cake. The increase will depend on the cake structure and the amount of dust retained in the bed. If it is an internal cake, the pores will be smaller than the clean bed. Smaller pores result in a higher jet velocity, a higher impaction parameter, and a higher collection efficiency.

If the cake is a surface cake, the predominant particle collection mechanism is sieving. The collection efficiency of the bed will depend only on the pore size in the cake and will be independent of the bed thickness and granule diameter.

Experiments were performed to determine the effect of filter cake on efficiency. The bed was first loaded with dust by passing redispersed fly ash through the bed at a superficial gas velocity of 50 cm/s. The amount of dust retained in the bed was calculated from the inlet and outlet particle concentrations (calculated from simultaneous inlet and outlet filter sample) and the time the dust was passed through the bed.

After the bed was loaded with fly ash, a monodisperse polystyrene latex aerosol of 1.1 μm diameter was generated and passed through the dirty bed. Inlet and outlet particle concentrations were measured with an optical particle counter.

Experiments were done for the following conditions:

1. Neutral particle and neutral dirty bed,
2. Neutral particle and DC polarized dirty bed,
3. Charged particle and neutral dirty bed,
4. Charged particle and DC polarized dirty bed,
5. Neutral particle and AC polarized dirty bed, and
6. Charged particle and AC polarized dirty bed.

Experimental data are plotted in Figures A-15 through A-20 in Appendix "A".

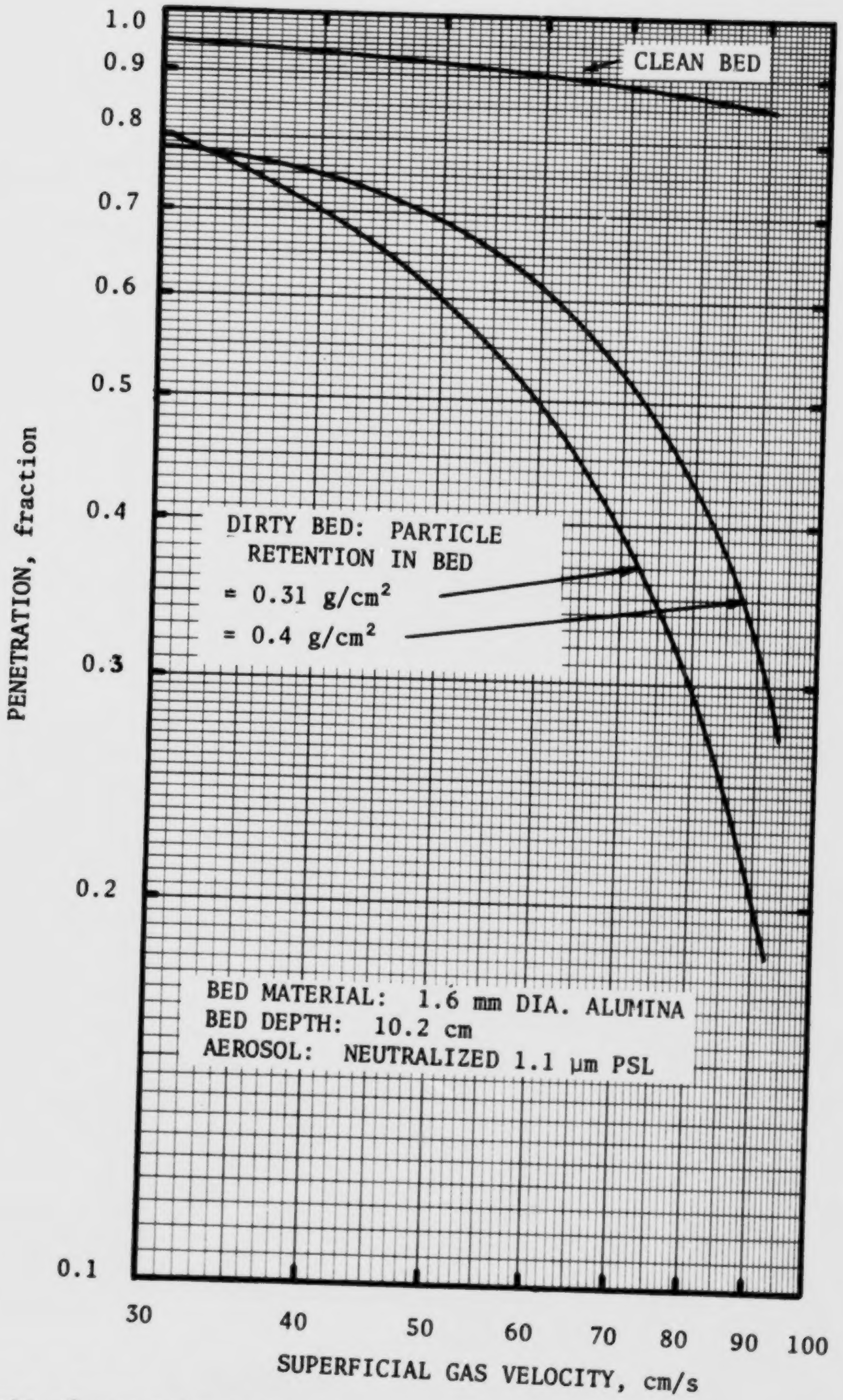

Figure 12. Effects of particle loading in bed on penetration of a fixed GBF.

Figure 12 shows the effect of filter cake on efficiency. As expected, the presence of filter cake increased the collection efficiency of the bed. The collection efficiency of the bed with a particle retention of 0.31 g/cm^2 is higher than the bed with a particle retention of 0.40 g/cm^2. This suggests that collection efficiency not only depends on the amount of particles retained in the bed but also on the cake structure. In both dirty beds, the filter cakes existed as internal cake. No surface cake was visible. In the bed with a particulate deposit of 0.31 g/cm^2, the cake concentrated near the surface. In the bed with a particle deposit of 0.4 g/cm^3, the particles had penetrated all the way through the bed.

Figure 13 shows pressure drop data. Dirty beds have a higher pressure drop than the clean bed. The bed with a particle deposit of 0.31 g/cm^2 had a higher efficiency than the bed with 0.4 g/cm^2; however, its pressure drop was also higher.

Data for electrostatically augmented dirty beds are summarized in Figures 14 and 15. As in the case with the clean beds, penetration decreases with increasing applied voltage across the bed, and DC polarization is more effective than AC polarization.

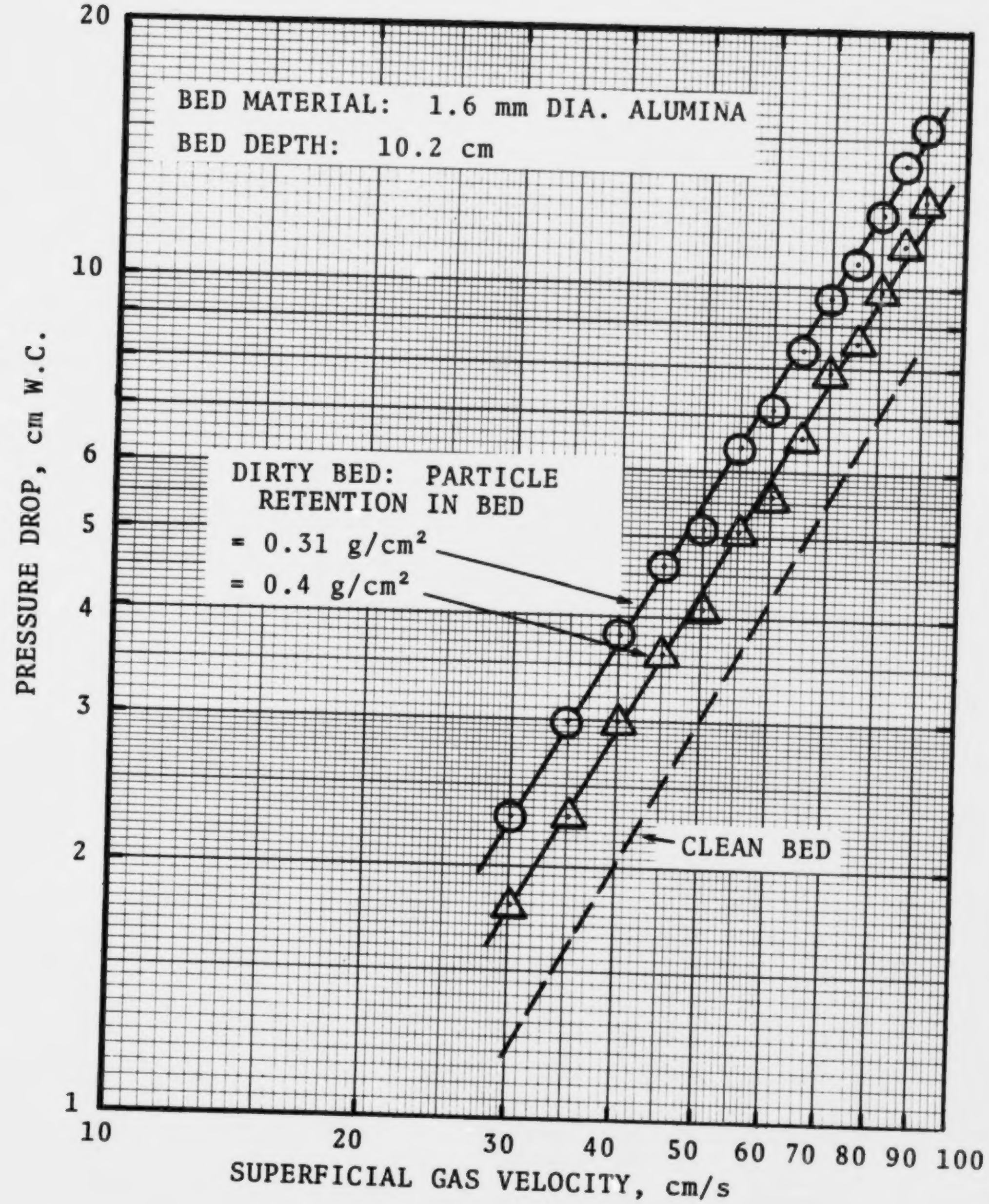

Figure 13. Experimental pressure drop of a dirty GBF.

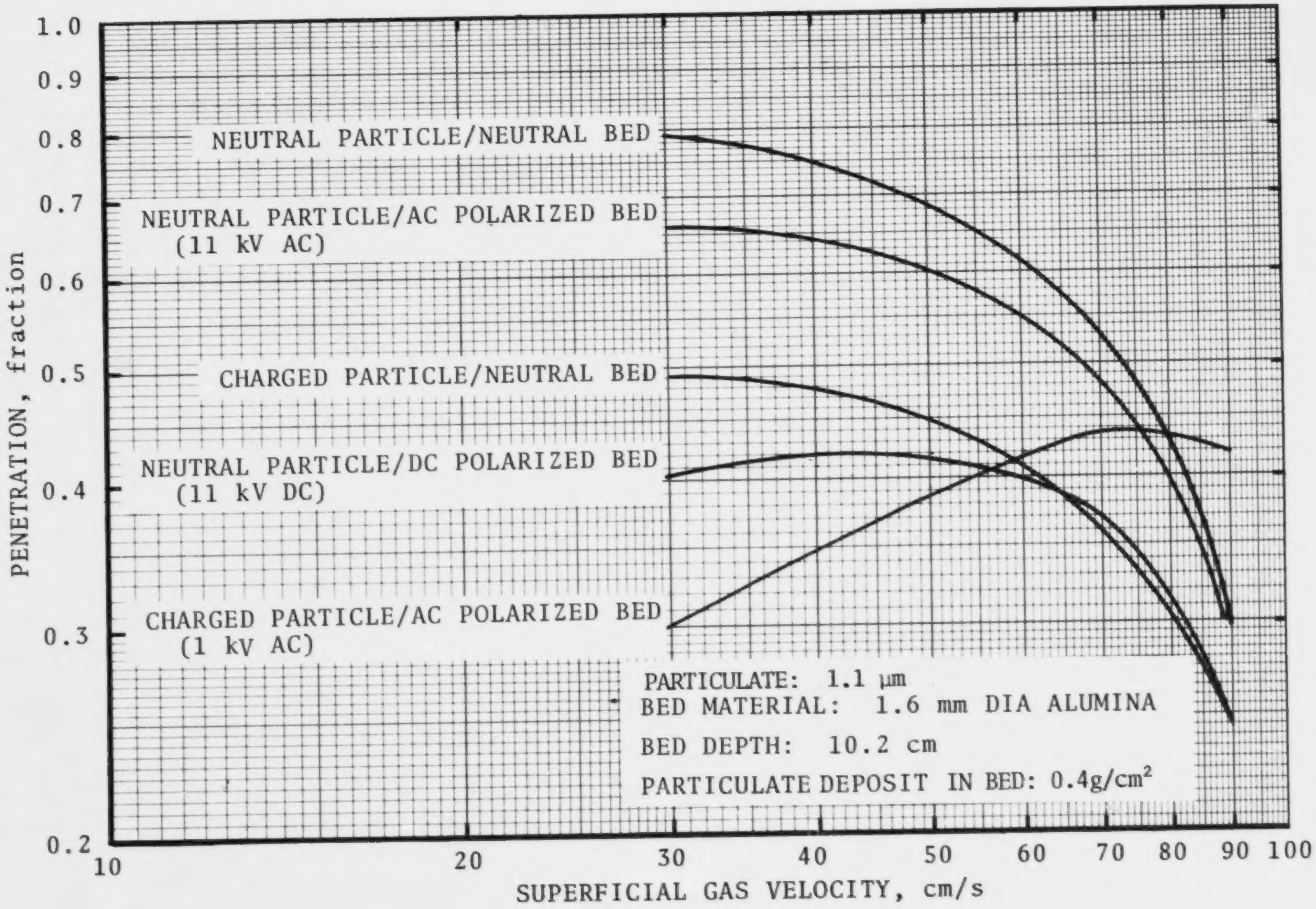

Figure 14. Experimental penetration of a dirty GBF.

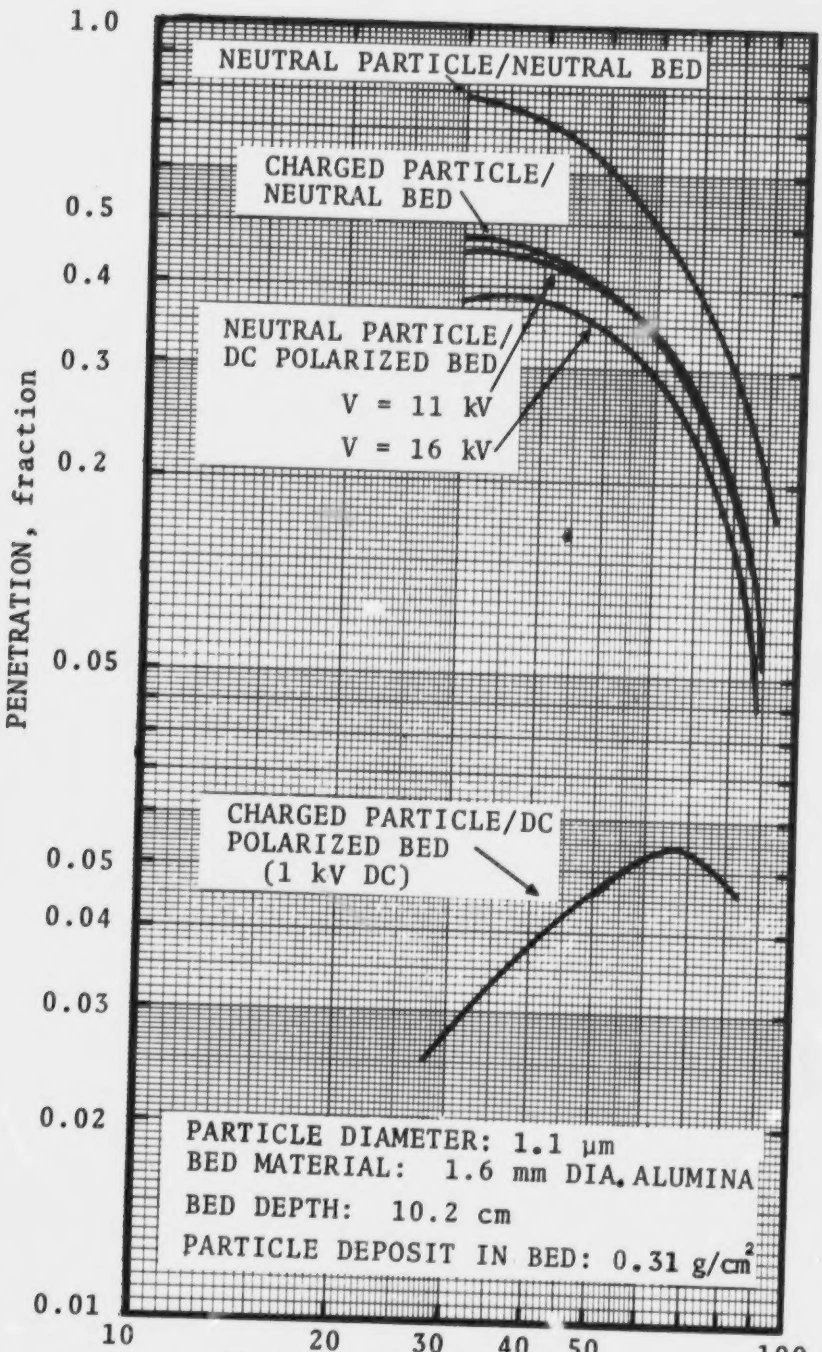

Figure 15. Experimental penetration of a dirty GBF.

SECTION 4

MOVING BED GRANULAR BED FILTER EXPERIMENTS

EXPERIMENTAL SETUP

Figure 16 shows the experimental setup for the moving bed granular bed filter. It mainly consisted of a blower and a granular bed filter test section. The system was operated under forced draft condition.

The GBF test section consisted of a particle charger and a single downflowing vertical panel of granules which were held in place by means of two retaining grids. The panel was 20.3 cm wide, 91 cm long, and 15 cm thick (8" x 36" x 6"). The front retaining grid was a steel plate perforated with horizontal slots. The slotted portion of the plate was 45 cm long (18 in.). Each slot was 3.2 mm wide and 22 mm long (1/8 in x 7/8 in.). Spacing between slots was 3.2 mm (1.8 in.). Louvers were used for the back retaining grid.

The bed was packed with 1.6 mm diameter alumina spheres. During operation, the granules were continuously removed from the bed at the bottom with an ejector and were returned to the overhead hopper manually. The bed could be polarized by connecting one of the retaining grids to a high voltage power supply and by grounding the other retaining grid.

The particles were charged by corona wires. Wire diameter was 0.18 mm (0.007 in.). Ground electrodes were made of 1.25 cm diameter (0.5 in.) aluminum rods. Wire/rod spacing was 3.8 cm (1.5 in.).

One power supply was used both to charge the particle and to polarize the bed. The applied voltage for all runs was 20 kV DC. This is equivalent to a field strength of 1.31 kV/cm in the bed and 5.26 kV/cm in the particle charger.

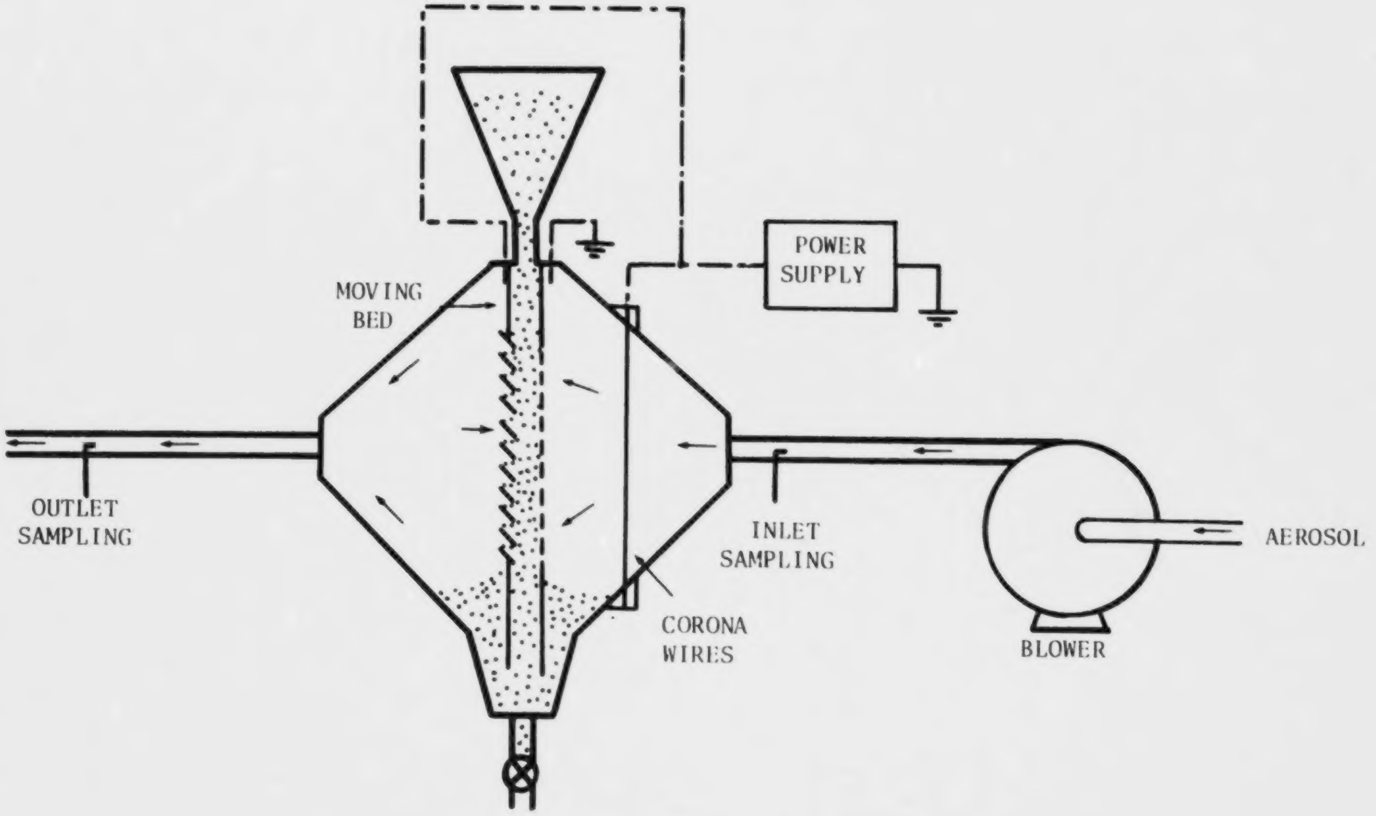
MOVING BED
POWER SUPPLY
OUTLET SAMPLING
INLET SAMPLING
AEROSOL
CORONA WIRES
BLOWER

Figure 16. Moving bed GBF (34.3 m^3/min).

DATA

Room air and redispersed fly ash particles were used for all experiments. The fly ash particles were fed into the blower inlet. Particle size distribution and concentration were measured simultaneously at the granular bed filter inlet and outlet ducts using cascade impactors. Grade penetration was calculated from impactor data for all runs. Static pressures were measured with pressure gauges at the inlet and outlet sampling points. Pressure drop is equal to the difference and therefore includes the entrance and exit losses.

A total of twenty-one runs were done. Test conditions included:

1. Neutral bed/uncharged particle
2. Polarized bed/uncharged particle
3. Neutral bed/charged particle
4. Polarized bed/charged particle.

The superficial gas velocity through the bed varied between 45 and 60 cm/s. The ratio "M" of granule mass recirculated to gas mass flow varied between 0.5 and 1.5.

Test conditions and particle data are summarized in Table 1. Cascade impactor data are listed in Appendix "B". Grade penetration curves are given in Appendix "C".

DATA ANALYSIS

Figure 17 shows the measured particle penetration for various operating conditions. As with the case of the fixed granular bed filter, polarizing the bed or charging the particles resulted in a significant improvement in performance. Simultaneous bed polarization and particle charging gave very efficient collection in excess of 98% for all particle sizes measured.

Large quantities of particles are collected by the outlet probe. Since the particles collected by the probe are large, they may originate from reentrainment. The grinding of the granules due to the relative motion of the filter granules can

TABLE 1. TEST CONDITIONS AND PARTICLE DATA

Run No.	u_G cm/s	M kg/kg	ΔP cm W.C.	E_b kV/cm	E_p kV/cm	d_{pg}, μmA Inlet	d_{pg}, μmA Outlet	σ_g Inlet	σ_g Outlet	C, mg/DNm³ Inlet	C, mg/DNm³ Outlet	$\overline{Pt}$, %
1	45	1.02	5.6	0	0	17.0	3.5	5.9	2.3	752.1	115.2	15.3
2	45	0.99	5.6	0	0	9.0	3.0	3.3	2.3	530.3	97.1	18.3
3	45	0.98	5.6	1.31	0	8.0	60.0	3.5	50.0	802.3	38.9	4.8
4	45	0.91	5.6	1.31	0	12.0	10.0	5.2	12.2	1,449.0	69.3	4.8
5	45	1.13	5.6	1.31	5.26	4.0	21.0	3.1	14.0	1,082.0	38.1	3.5
6	45	1.00	5.6	1.31	5.26	3.4	15.0	3.1	10.0	1,446.0	32.3	2.2
7	45	1.05	5.6	0	5.26	6.0	5.0	3.0	4.5	1,311.0	75.8	5.8
8	45	1.07	5.6	0	5.26	3.8	6.4	3.5	5.8	1,111.0	81.0	7.3
9	51	1.05	6.6	0	0	5.2	3.0	2.5	2.5	444.9	54.1	12.2
10*	51	1.00	6.4	0	0	6.0	4.0	3.3	3.6	497.6	188.4	37.9
11	46	1.16	5.8	1.31	0	13.0	7.4	5.7	21.1	387.6	43.6	11.2
12	52	0.58	7.1	0	0	7.0	4.0	2.9	3.2	463.1	44.3	9.6
13	52	0.63	7.1	0	0	38.0	10.0	5.4	7.4	1,171.0	38.6	3.3
14	57	1.06	7.9	1.31	0	8.2	14.0	3.2	5.5	1,067.0	61.1	5.7
15	51	0.51	7.1	1.31	0	10.0	20.0	3.4	3.3	1,102.2	53.0	4.8
16	46	0.72	5.8	0	0	7.2	3.0	2.9	5.8	751.2	115.2	15.3
17	45	0.59	5.9	0	0	6.0	3.2	2.9	3.2	530.3	99.1	18.3
18	57	1.55	6.7	1.31	0	9.0	23.0	3.3	7.0	461.0	47.6	10.3
19	57	0.85	8.1	1.31	0	6.0	40.0	2.9	10.0	547.5	34.6	6.3
20	45	1.06	5.6	1.31	5.26	6.0	25.0	2.3	17.3	446.7	49.0	11.0
21	45	1.06	5.6	1.31	5.26	6.5	35.0	2.8	23.3	684.1	39.5	5.8

*Note: Dirty granules

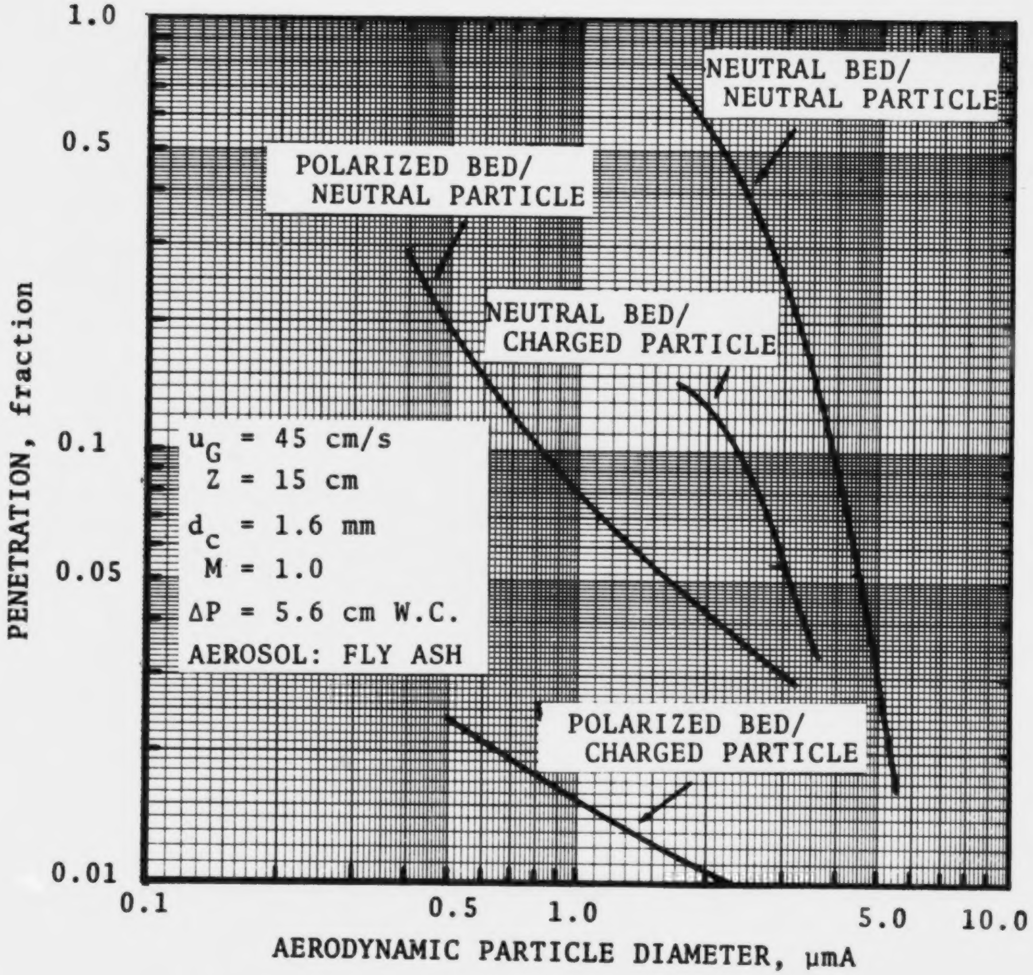

Figure 17. Measured particle penetration for various opening conditions of a GBF.

dislodge the collected particles and allow them to be reentrained into the gas stream. The reentrainment rate depends on the granule recirculation rate and the filtration gas velocity. At higher recirculation rates, collected particles are easier to dislodge.

Electrically augmenting the bed and/or particles did not minimize reentrainment.

Figures 18 and 19 show the effect of granule recirculation rate on particle penetration. Lower recirculation rate results in lower particle penetration and higher pressure drop. This could be a result of a smaller bed porosity for a bed with a lower recirculation rate. According to Ergun's equation for pressure drop across a packed bed and Equation (1), smaller bed porosity leads to higher pressure drop and particle collection efficiency.

Beds with lower recirculation rate also result in less attrition of retaining grids and granules and less dislodging and reentraining of the collected particles. Therefore, the granule recirculation should be kept as slow as possible. However, it should not be so slow that the collected particles will saturate the bed. The drag force exerted on the collected particles by the gas flow will gradually force the collected particles through from the dirty to the clean side of the filter. As the deposit extends through the bed, the bed can become saturated with dust and reentrainment may result causing the collection efficiency to decrease.

The final selection of the granule recirculation rate depends on the gas velocity, inlet particle concentration, bed depth, bed height and granule size.

Figure 20 shows the effect of granule cleanliness on penetration. The dirty granules had been circulated through the bed twice without cleaning. As expected, dirty granules result in higher penetration. This occurs presumably because particles are reentrained from the downstream side of the bed.

Figure 21 shows the comparison of measured penetration for a fixed and a moving granular bed filter. The fixed bed data were reported earlier in Section 3. As can be seen, a fixed

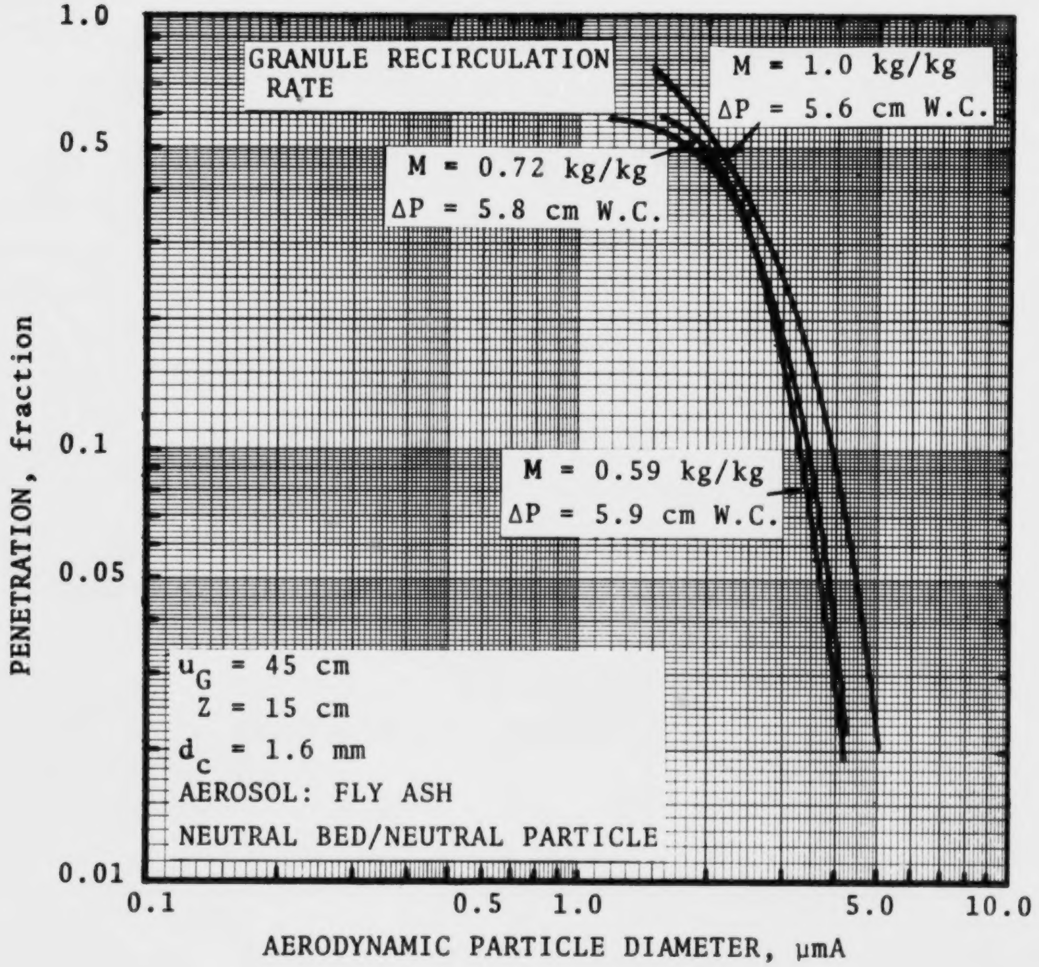

Figure 18. Effect of granule recirculation rate on penetration.

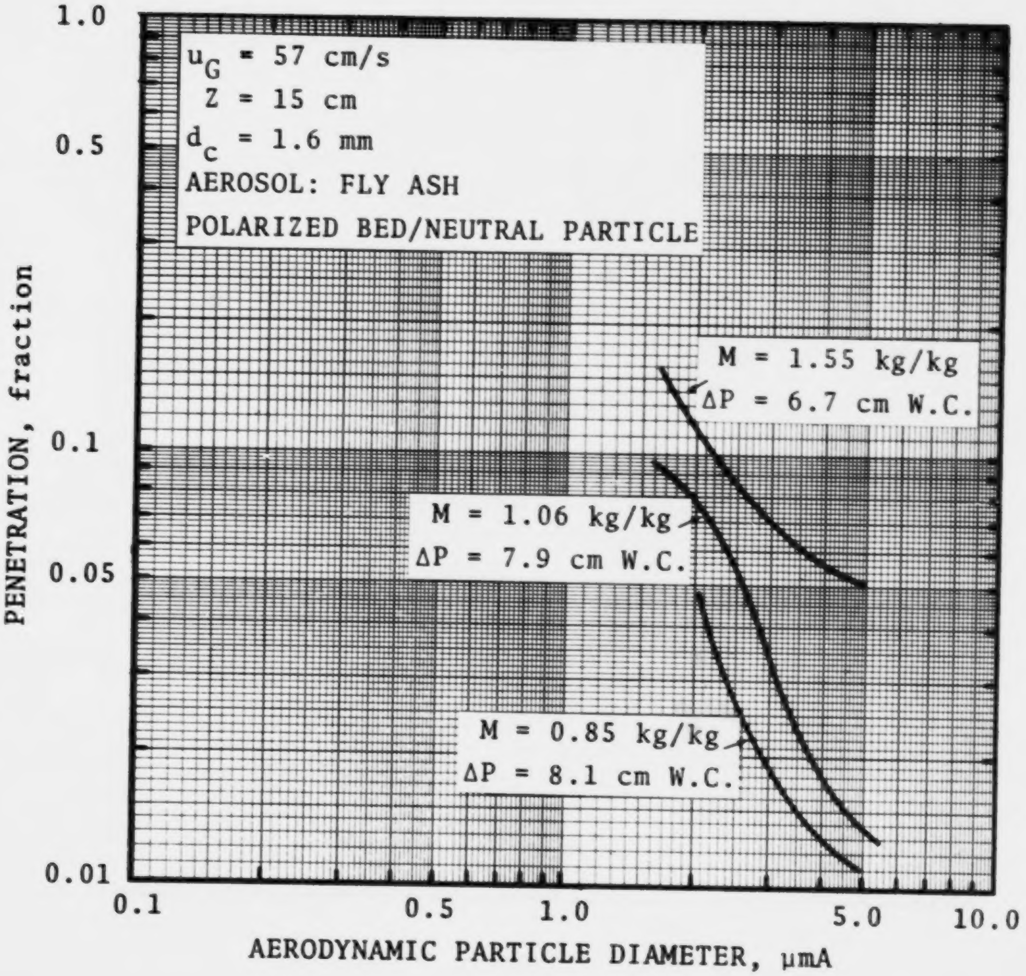

Figure 19. Effect of granule recirculation rate on penetration.

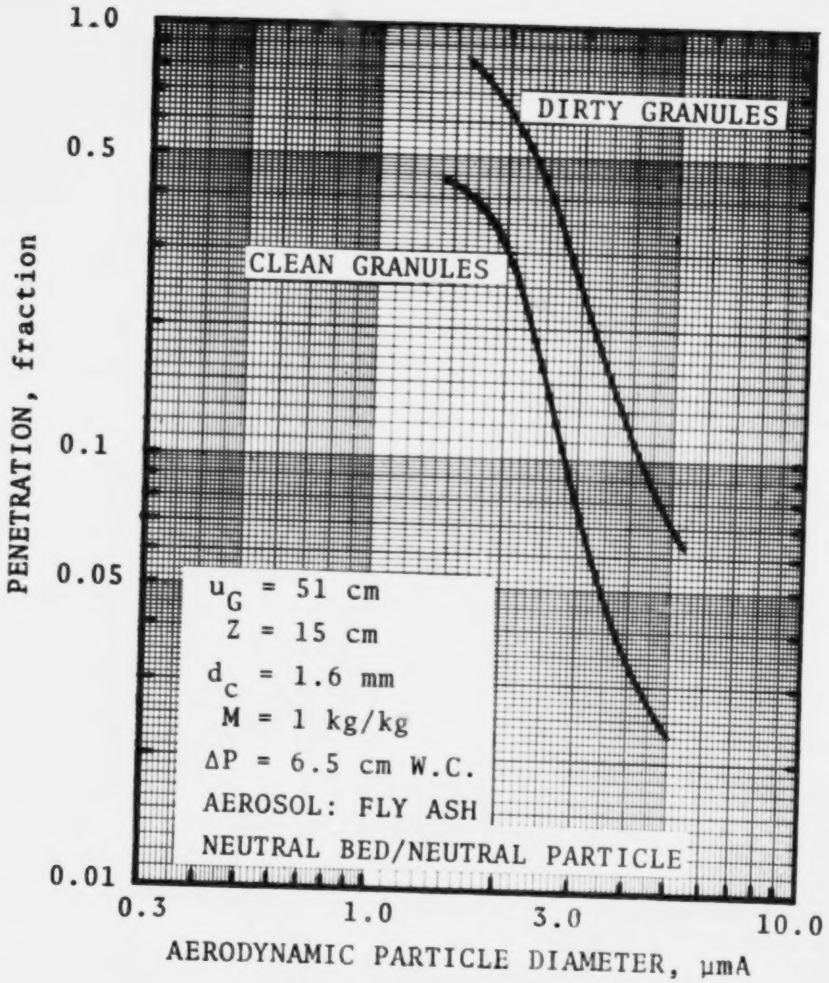

Figure 20. Effect of granule cleanliness on penetration.

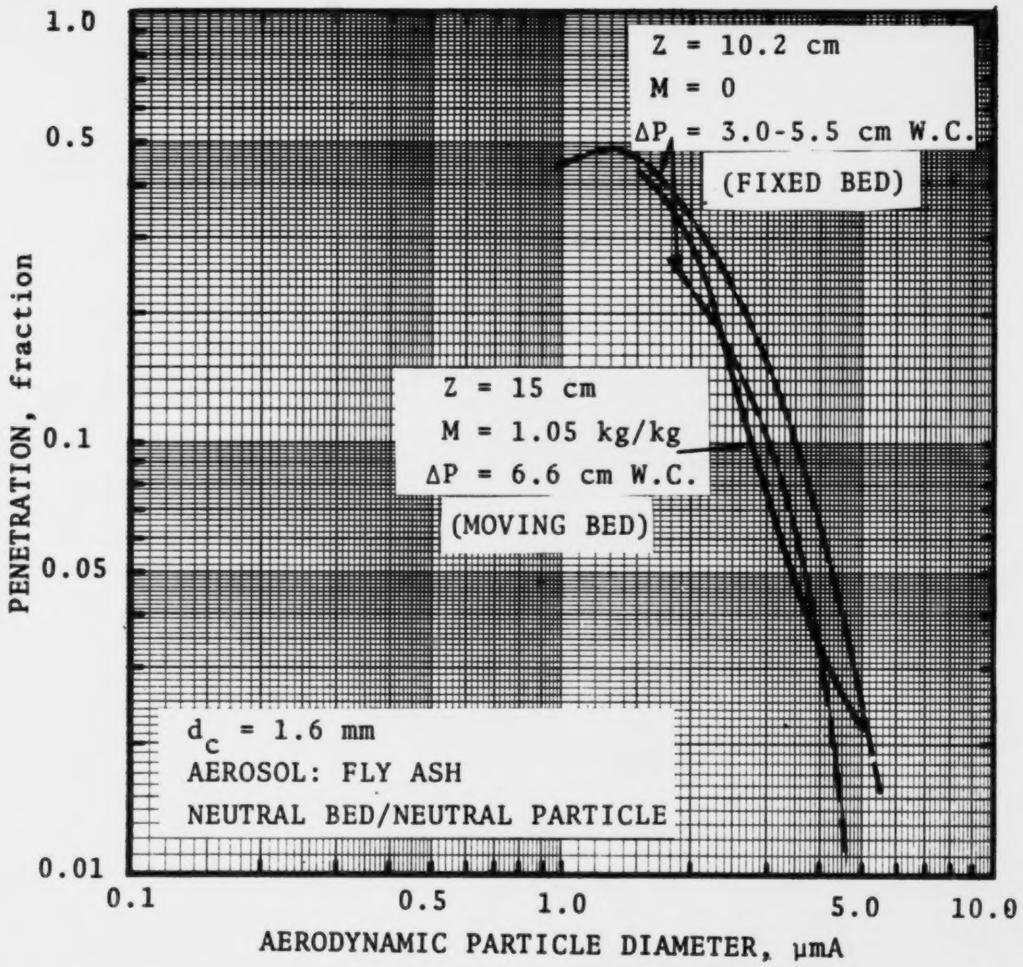

Figure 21. Measured penetrations of a fixed bed and a moving GBF.

bed with a bed depth of 10.2 cm has the same capability as a moving bed with a bed depth of 15 cm and a granule recirculation rate of 1 kg/kg.

Effects of gas velocity on penetration are shown in Figures 22 and 23. As with fixed bed, higher gas velocity gives lower penetration.

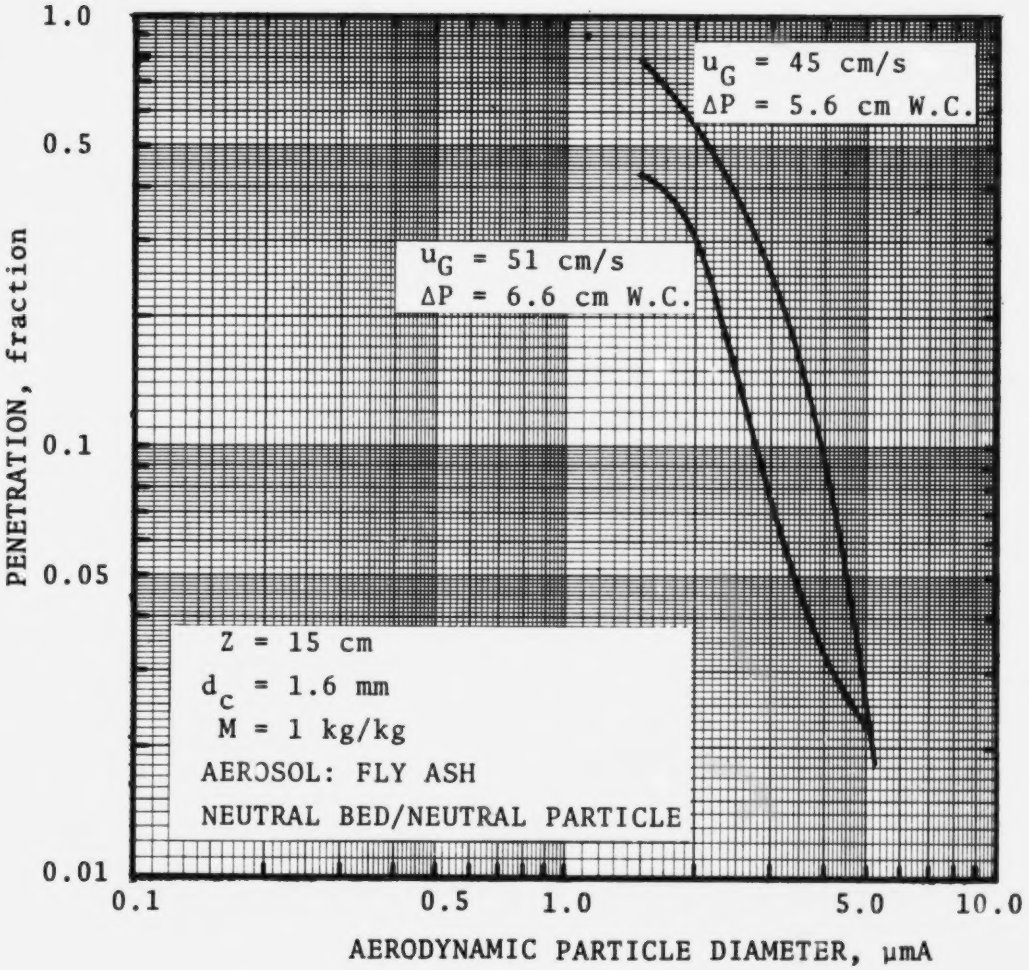

Figure 22. Effect of gas velocity on penetration.

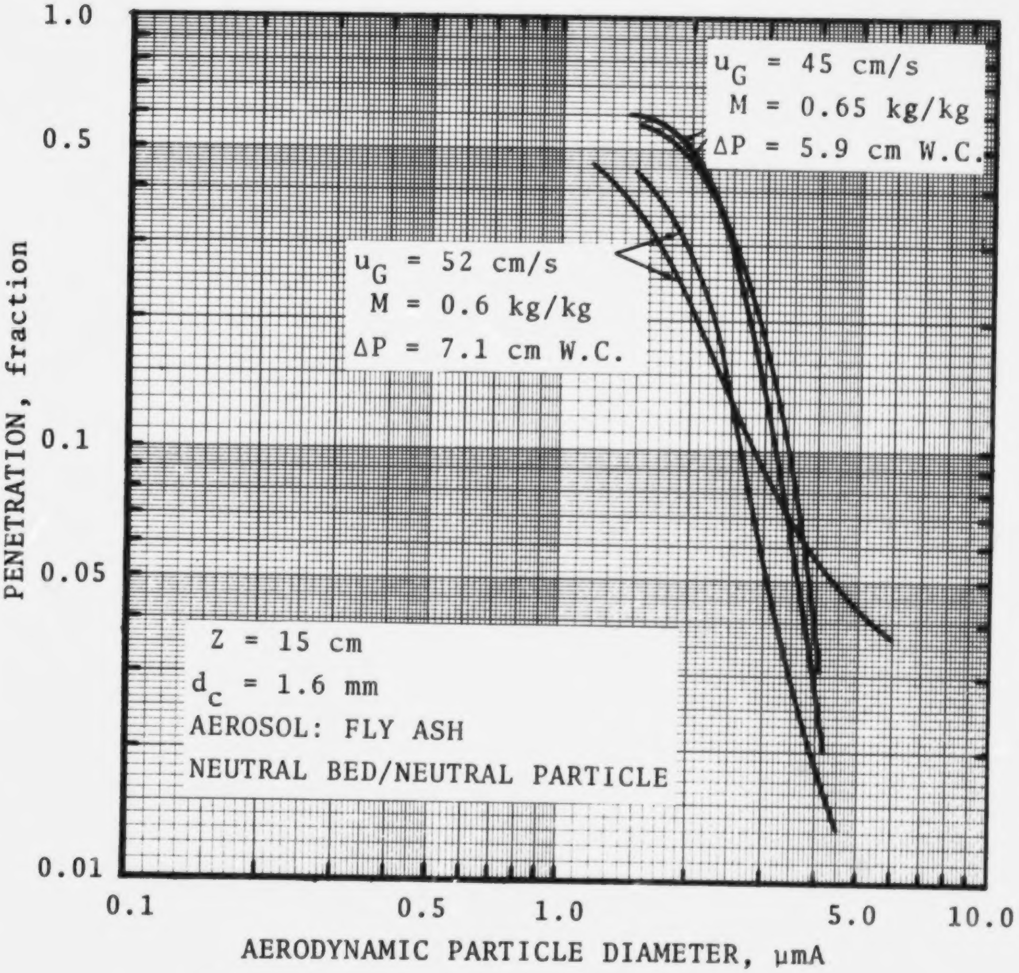

Figure 23. Effect of gas velocity on penetration.

SECTION 5

EVALUATION OF ELECTRICAL AUGMENTATION OF GRANULAR BED FILTERS

The use of granular bed filters for HTP applications is limited by the particulate and gaseous pollutant removal efficiencies and operating difficulties. Particulate cleanup requirements for HTP processes vary depending on the intended use of the gas. If it is to be vented, the gas must be cleaned sufficiently to meet the emission standards. The recently promulgated new source performance standard for coal-fired boilers is 13 mg/MJ (0.03 lb/10^6 BTU).

If the hot gas is to be expanded through a gas turbine, then the gas must meet the turbine requirement for cleanliness. A gas containing dust particles can severely erode and corrode turbine blades and other internal blades can impair the aerodynamic performance of the turbine.

Turbine requirements are not well established at this time. Westinghouse (1974) suggested that a mass loading less than 0.37 g/Nm^3 (0.15 gr/SCF) for particles smaller than 2 μm in diameter and less than 0.0023 g/Nm^3 (0.001 gr/SCF) for particles larger than 2 μm. Sverdrup and Archer (1977) estimated that to protect the turbine, the particulate concentration should be no more than 0.005 g/Nm^3 (0.002 gr/SCF) and there should be no particles larger than 6 μm in diameter.

By using the particle size distribution and concentration reported by Hoke et al. (1977, 1978), Yung et al. (1979) showed through theoretical calculation that the collection efficiency of a granular bed filter appears to be insufficient to meet the new emissions regulations for particulates. Depending on the amount of submicron particles a turbine can tolerate, performance may still be satisfactory for protecting gas turbines.

The experimental results of the present study and that of Self et al. (1979) show that the collection efficiency of a granular bed filter can be dramatically enhanced by electrical augmentation. By charging the particles and polarizing the bed to a field of a few kV/cm, the bed could achieve a collection efficiency of more than 98% for all particle sizes.

These tests were done under ambient conditions. Calvert and Parker (1977) stated that high temperature and pressure particle collection is more difficult than at low temperatures when other parameters remain the same. However, a higher electric field could be applied to the bed at high temperature. Higher electric field will lead to a higher collection efficiency.

Hoke (1977) reported that the particles from the secondary cyclone of the Exxon PFBC (pressurized fluidized bed coal combustor) miniplant has a mass median diameter of 3.5 μm and a geometric standard deviation of 2.9. The mass concentration varies, but could be as high as 2.5 g/Nm³ (1 gr/SCF). By assuming the electrified GBF has the same fractional penetration at HTP as that at low temperature and pressure, the overall collection efficiency of the GBF was calculated to be more than 99.5%. Therefore, the particle emissions would be 0.013 g/Nm³ (0.005 gr/SCF) and this would be in compliance with the particulate emission standards.

Quantitative data on the costs of HTP granular bed filters are not available. The estimated capital costs of an electrified GBF is expected to be slightly higher than that of a non-aided GBF. The added costs are mainly due to the high voltage power supply, electrical insulation and connection systems.

Although electrified granular bed filters have the capability for controlling fine particles at high temperature and pressure, they are far from a proven, state-of-the-art technology. There are many operational problems and uncertainties which need to be resolved before HTP electrified GBFs can be considered sufficiently reliable for commercial application.

SECTION 6

FUTURE RESEARCH RECOMMENDATIONS

It has been shown that by electrostatically augmenting the bed and/or particles, the collection efficiency of the granular bed filter improved significantly. It has the potential to meet the most stringent cleanup requirements under ambient conditions. It is expected that the same statement will hold for high temperature and high pressure conditions where higher electric fields can be imposed on the beds.

However, there are many operational problems and uncertainties which need to be resolved before high temperature and high pressure granular bed filters can be considered sufficiently reliable and economical for commercial application. Future research and development work is needed in the following areas:

1. Bed cleaning methods and ways to reduce the cost of granule regeneration and recirculation.
2. Electrode configuration and high temperature and high pressure electrode insulation.
3. How to reduce particle seepage through the bed during cleaning or filtration.
4. How to reduce attrition of granules causing particle reentrainment.
5. How to reduce temperature losses and pressure drop across the bed.

Most of these can be studied in the laboratory and the most promising combination can be tested on a pilot-plant scale. A detailed program to demonstrate the feasibility of using electrostatic augmentation to improve granular bed filters for particle collection at high temperature is described below. We recommend a study of the electrostatically augmented granular bed filter on a pilot plant scale of about 14.2 Am^3/min (500 ACFM). To duplicate actual industrial application, fresh test dust should be produced instead of regenerated dust. Since granular bed filters will be used in advanced energy processes, it is desirable to test the electrostatically augmented granular bed filter on these processes. A good approach would be to use an actual fluidized bed combustor (atmospheric or pressurized).

The granular bed filter should be designed in such a way that it is easy to change from one configuration to another. Bed cleaning can be achieved either by fluidization or by continuously withdrawing granules and dust from the bed.

To aid the design of the pilot plant, some small-scale experimental work should be conducted concurrently. In outline, the objectives consist of the following tasks:

1. Conduct small-scale experiments to obtain design information.
2. Design the pilot plant.
3. Fabricate, install, and start up the pilot plant.
4. Prepare a detailed test plan describing,
    a. The proposed test matrix.
    b. The measurement techniques to be used.
    c. The data handling methods.
5. Conduct test programs.
6. Analyze data, conduct engineering and cost analyses of various configurations.
7. Based on the above analyses, design and estimate the cost of a granular bed filter system for high temperature and high pressure applications.
8. Recommend a test program to demonstrate a full-scale granular bed filter system on a high temperature and high pressure source.

REFERENCES

Calvert, S. and R. Parker, "Effects of Temperature and Pressure on Particle Collection Mechanisms: Theoretical Review," EPA 600/7-77-002, January 1977.

Hoke, R.C., et al., "Studies of the Pressurized Fluidized-Bed Coal Combustion Process," EPA 600/7-77-107, September 1977.

Hoke, R.C., et al., "Miniplant Studies of Pressurized Fluidized Bed Coal Combustion: Third Annual Report," EPA 600/7-78-069, April 1978.

Self, S.A., R.H. Cross, and R.H. Eustis, "Electrical Augmentation of Granular Bed Filter," HTGL Report No. 112, Department of Mechanical Engineering, Stanford University, March 1979.

Sverdrup, E.F. and D.H. Archer, "The Tolerance of Large Gas Turbines to Rocks, Dusts, and Chemical Corrodants," presented at the EPA/ERDA Symposium on High Temperature and Pressure Particulate Control, Washington, D.C., September 1977.

Westinghouse Electric Corporation, "Clean Power Generation from Coal," O.C.R., 84, NTIS No. PB 234-188, April 1974.

Yung, S.C., R. Patterson, R. Parker and S. Calvert, "Evaluation of Granular Bed Filters for High Temperature/High Pressure Particulate Control," EPA 600/7-79-020, January 1979.

APPENDIX A

FIXED BED GBF EXPERIMENTAL DATA

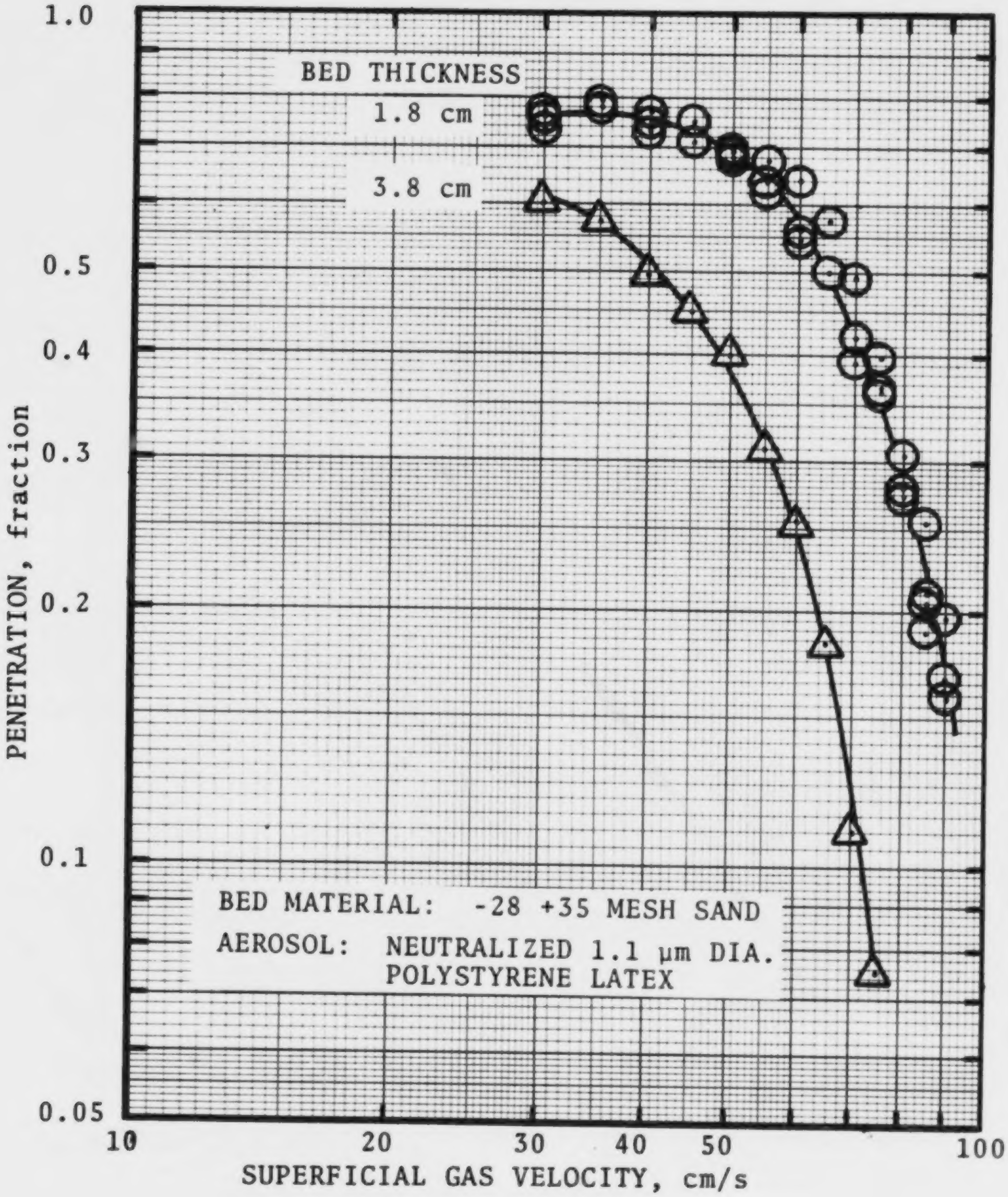

Figure A-1 Experimental particle penetration of a clean, grounded GBF.

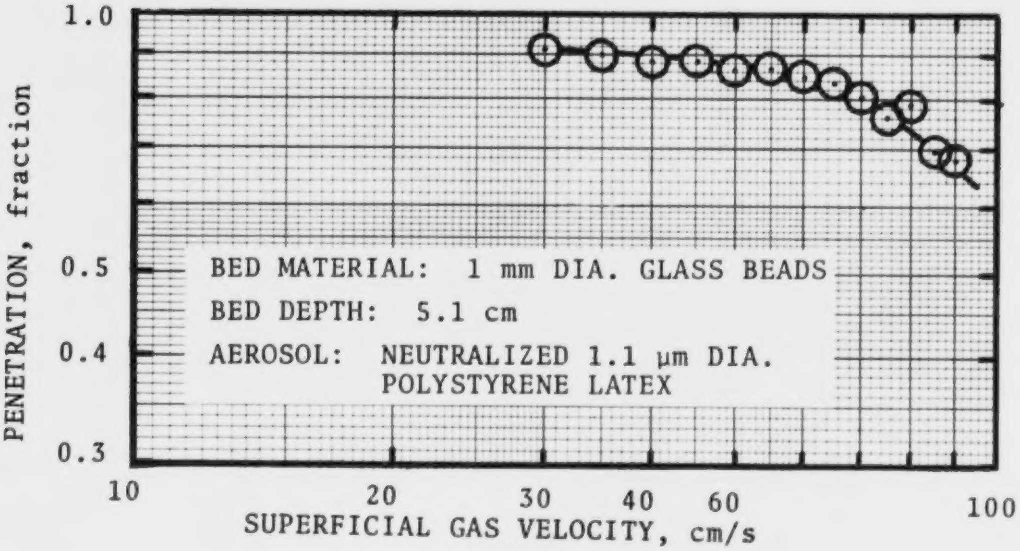

Figure A-2. Experimental particle penetration of a clean, grounded GBF.

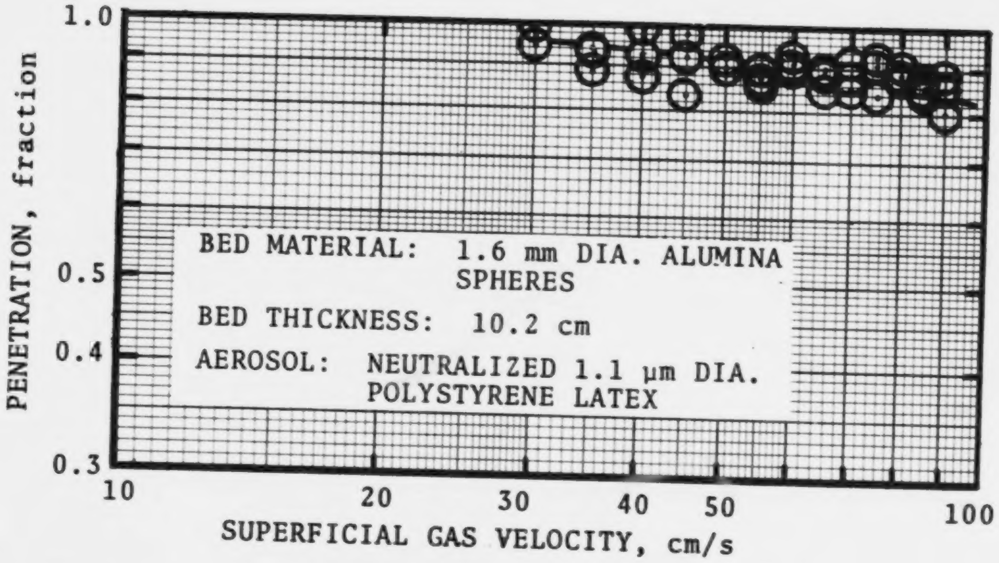

Figure A-3. Experimental particle penetration of a clean, neutralized GBF.

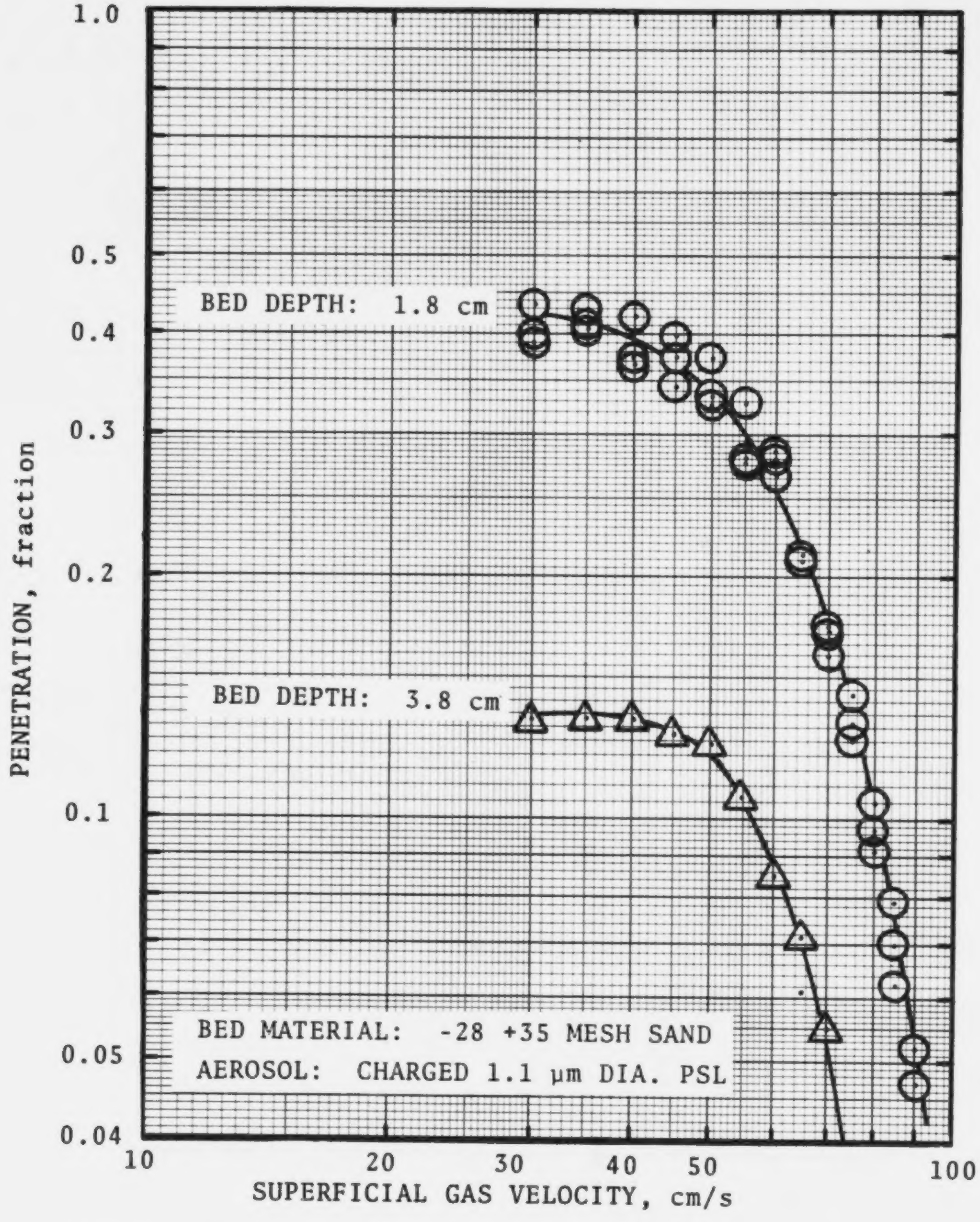

Figure A-4. Experimental charged particle penetration through neutral, clean GBF.

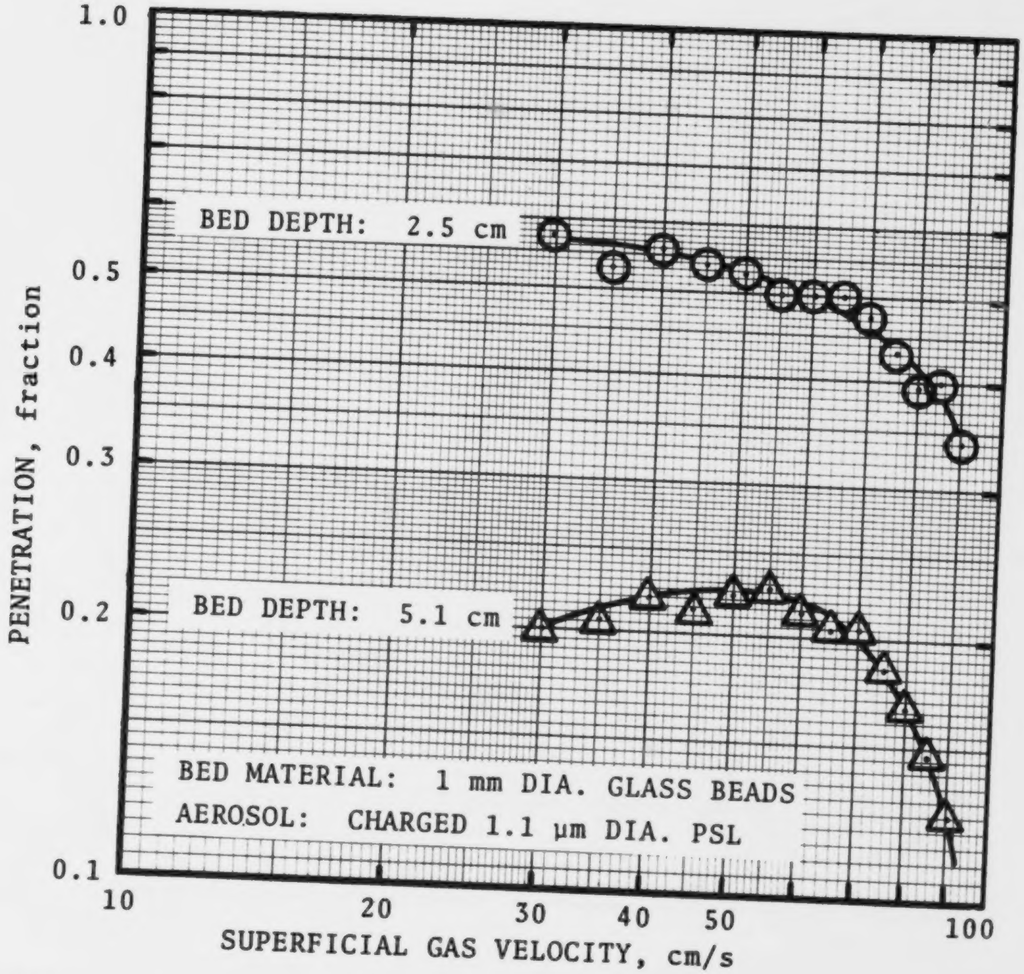

Figure A-5. Experimental charged particle penetration through neutral, clean GBF.

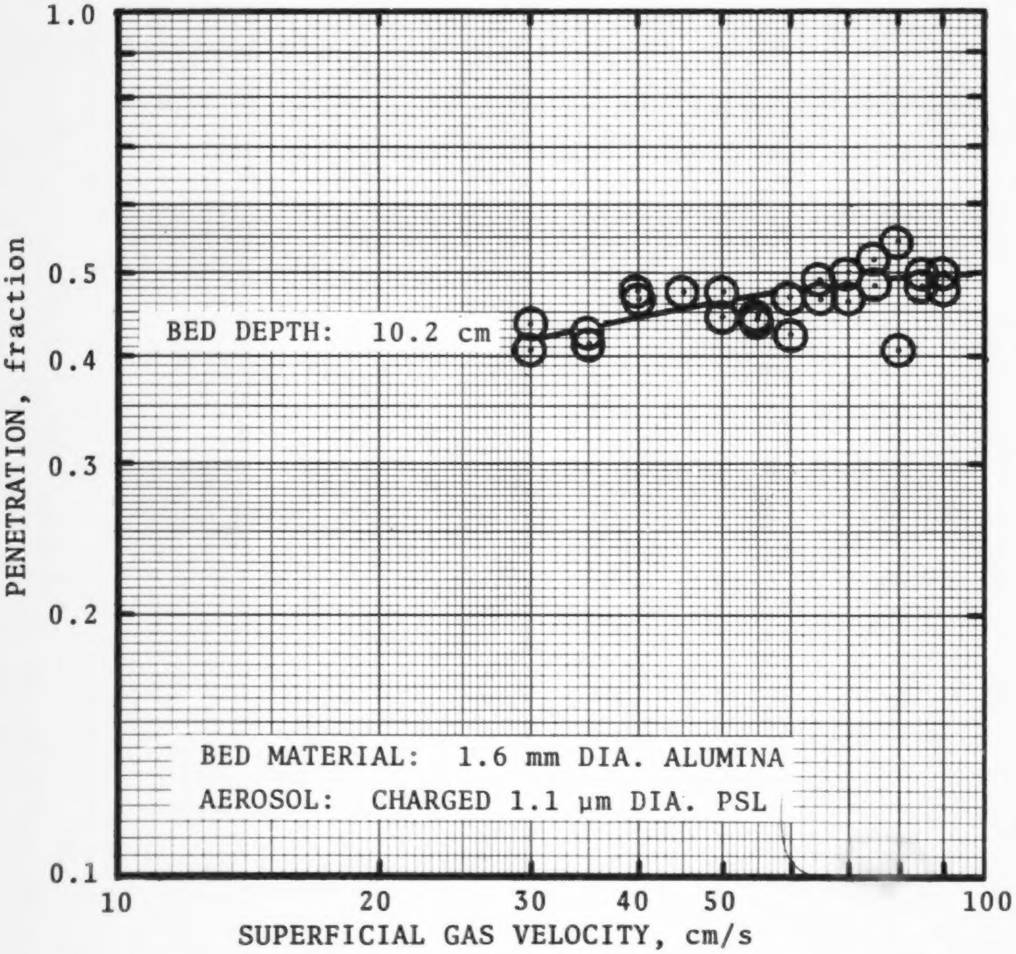

Figure A-6. Experimental charged particle penetration through a neutral, clean GBF.

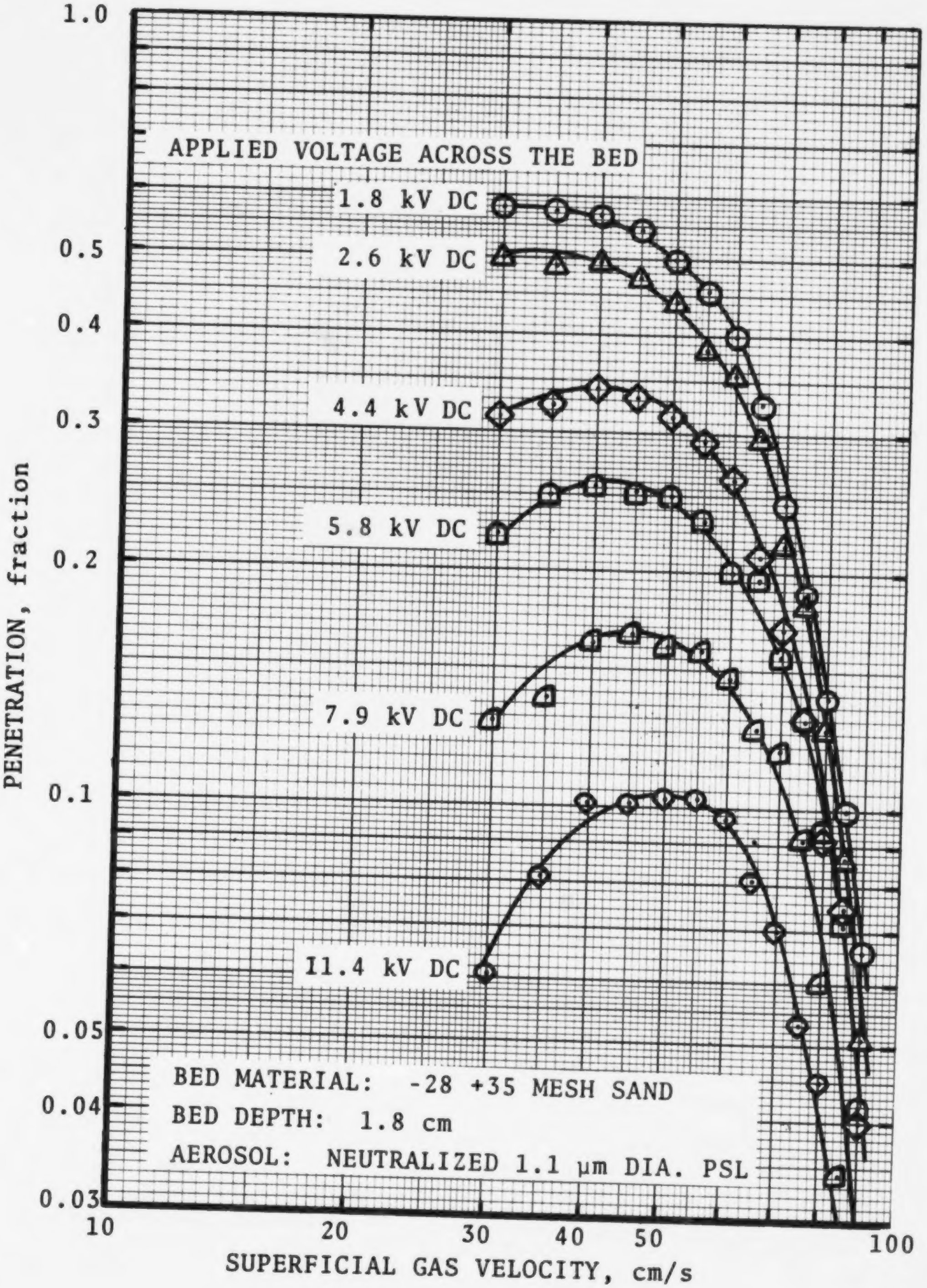

Figure A-7. Experimental particle penetration of a clean, DC polarized GBF.

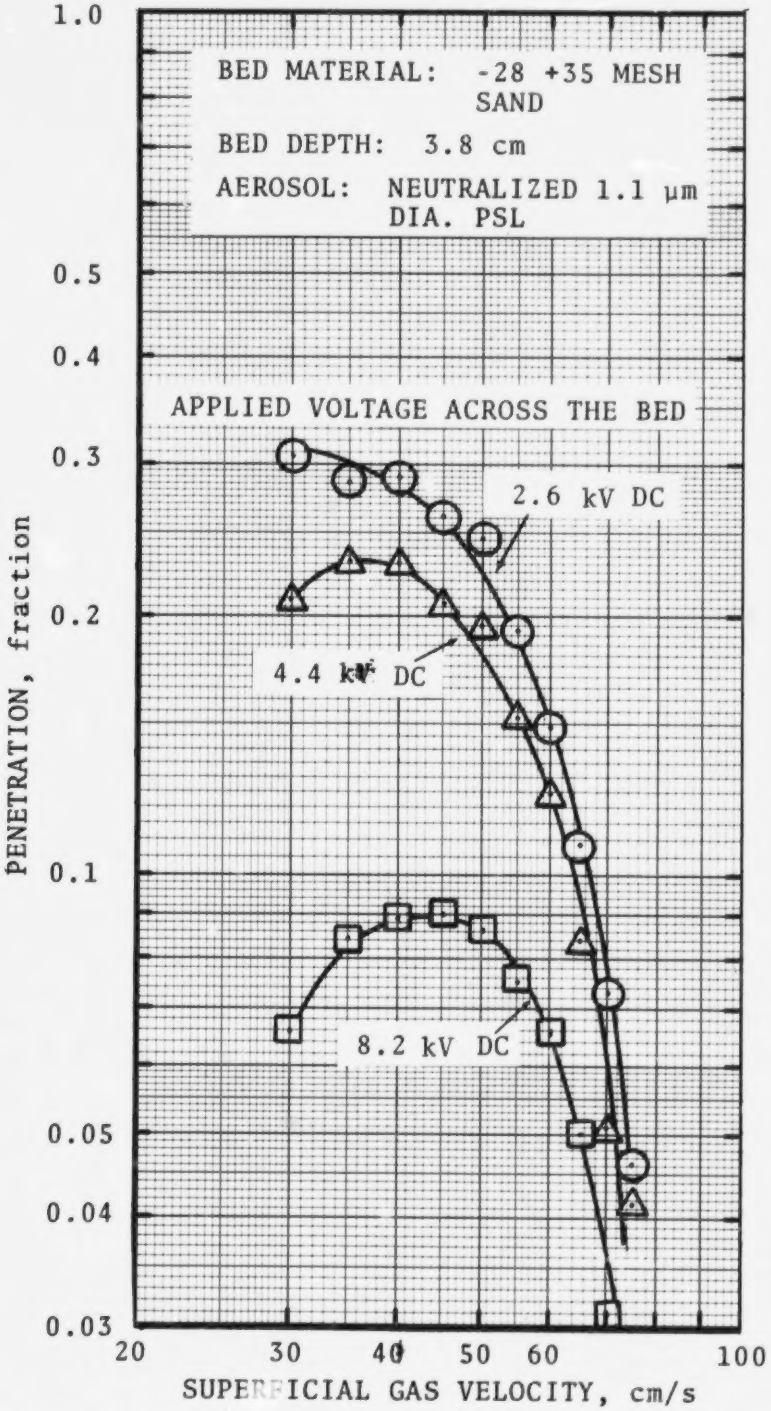

Figure A-8. Experimental particle penetration of a clean, DC polarized GBF.

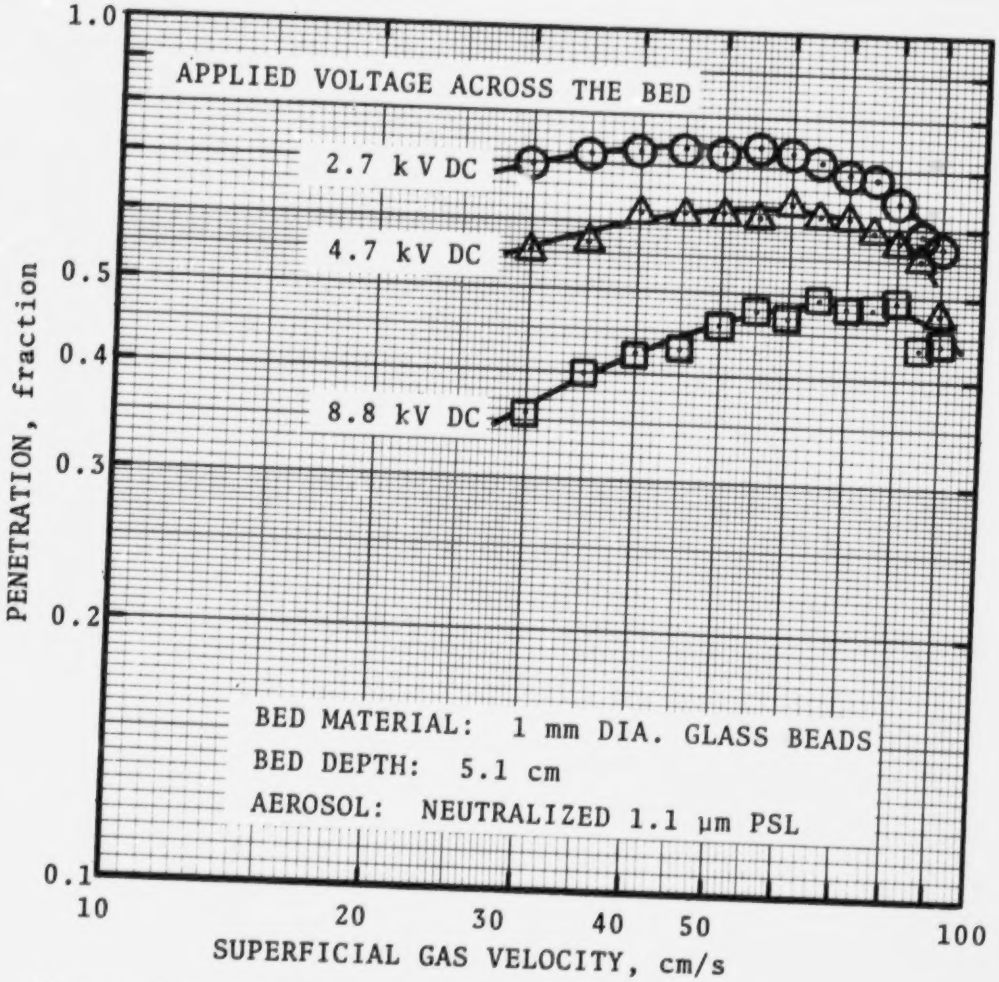

Figure A-9. Experimental particle penetration of a DC polarized, clean GBF.

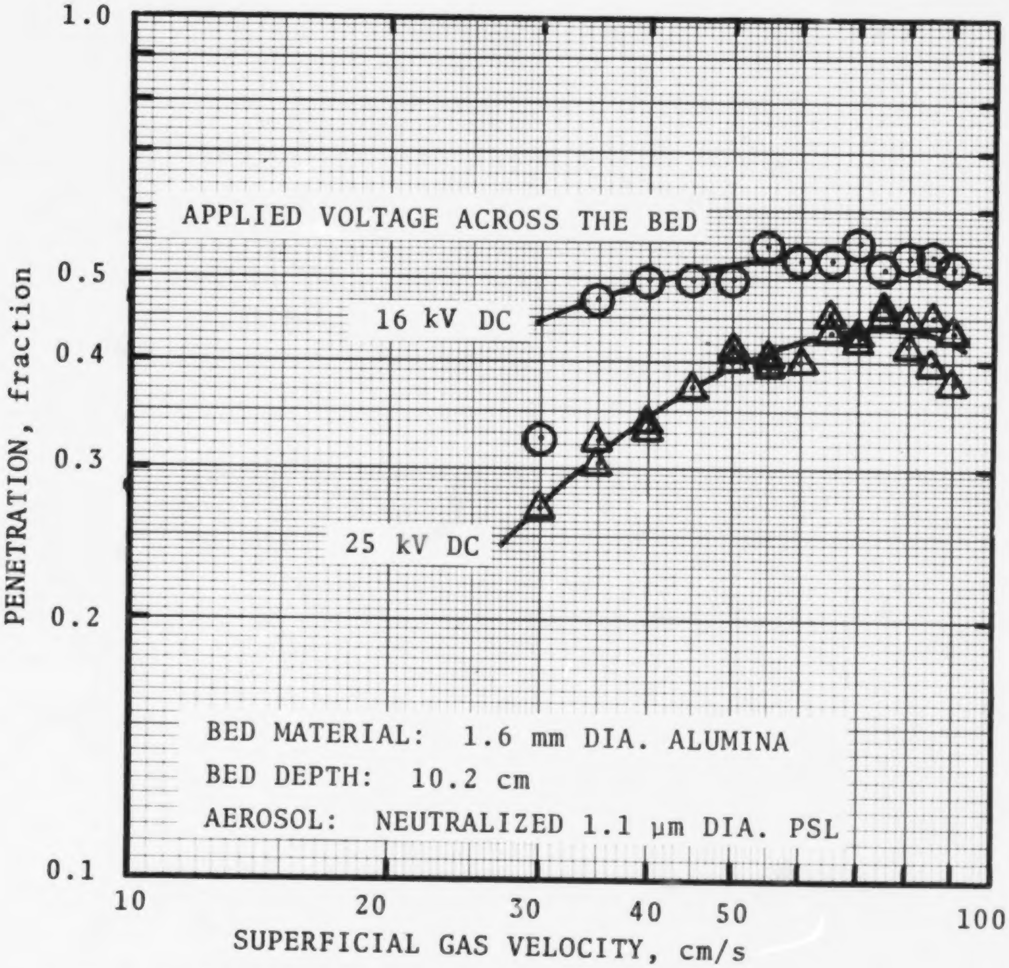

Figure A-10. Experimental particle penetration of a clean, DC polarized GBF.

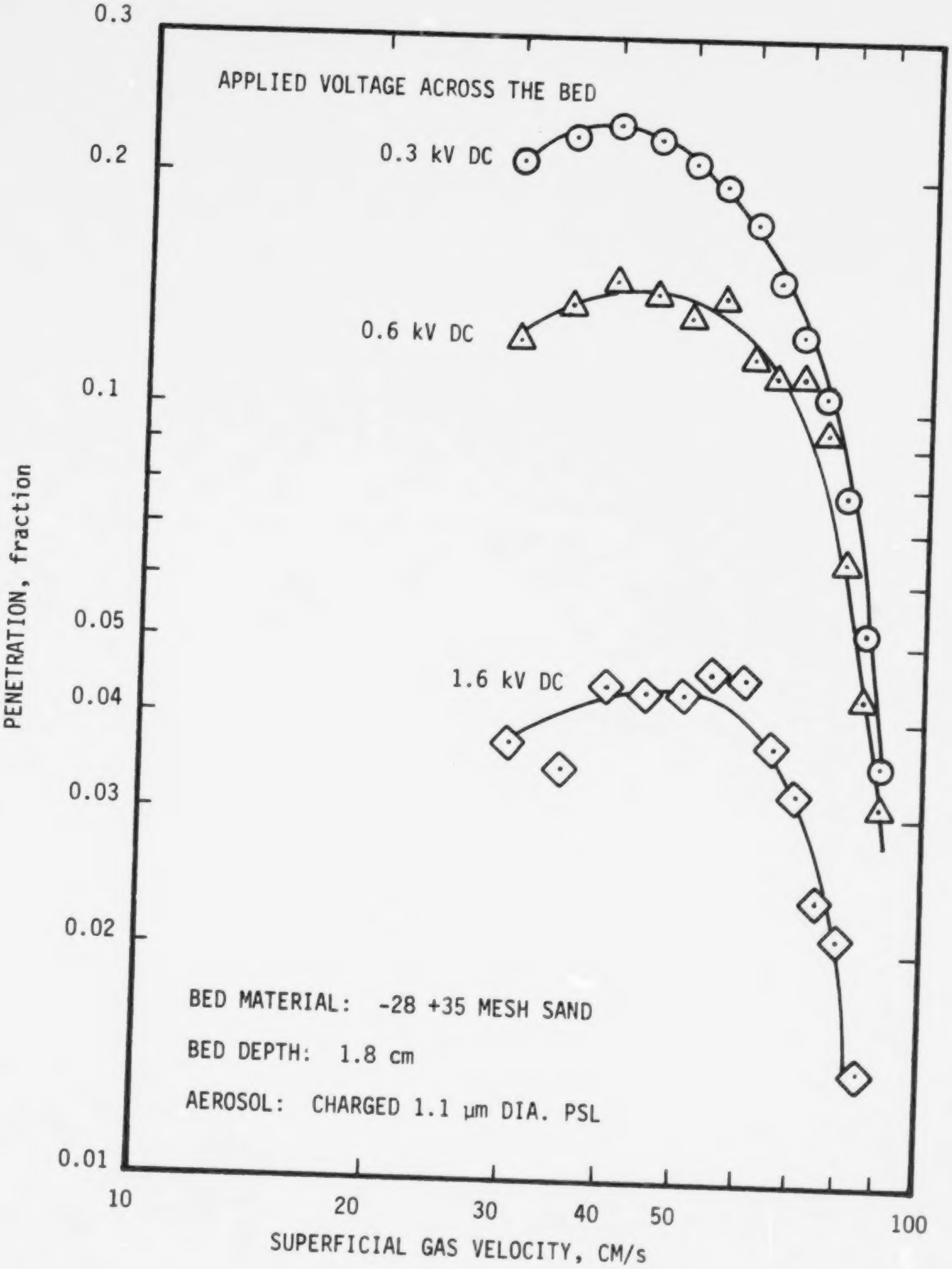

Figure A-11. Experimental charged particle penetration through a clean DC polarized GBF.

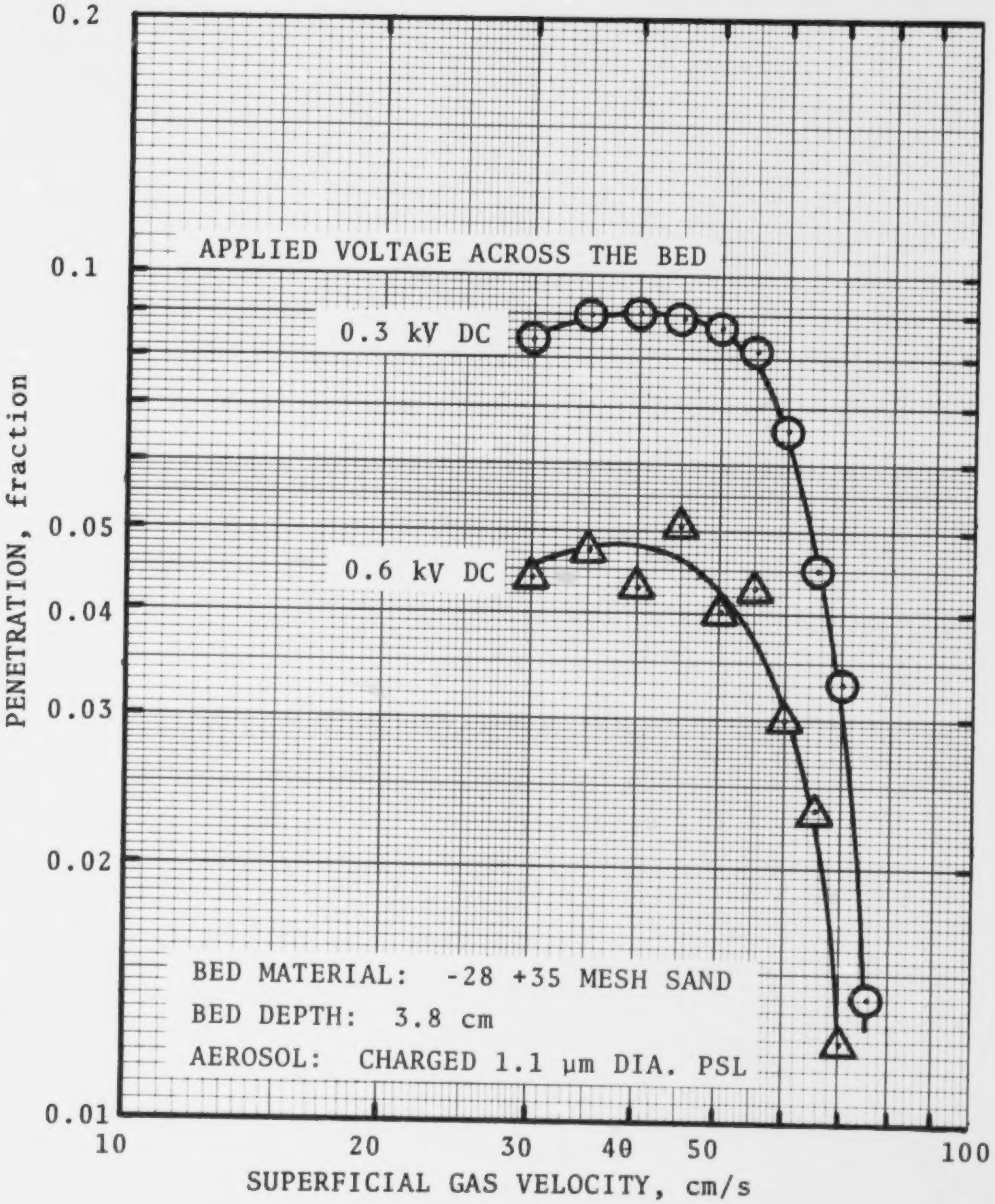

Figure A-12. Experimental charged particle penetration through a clean, DC polarized GBF.

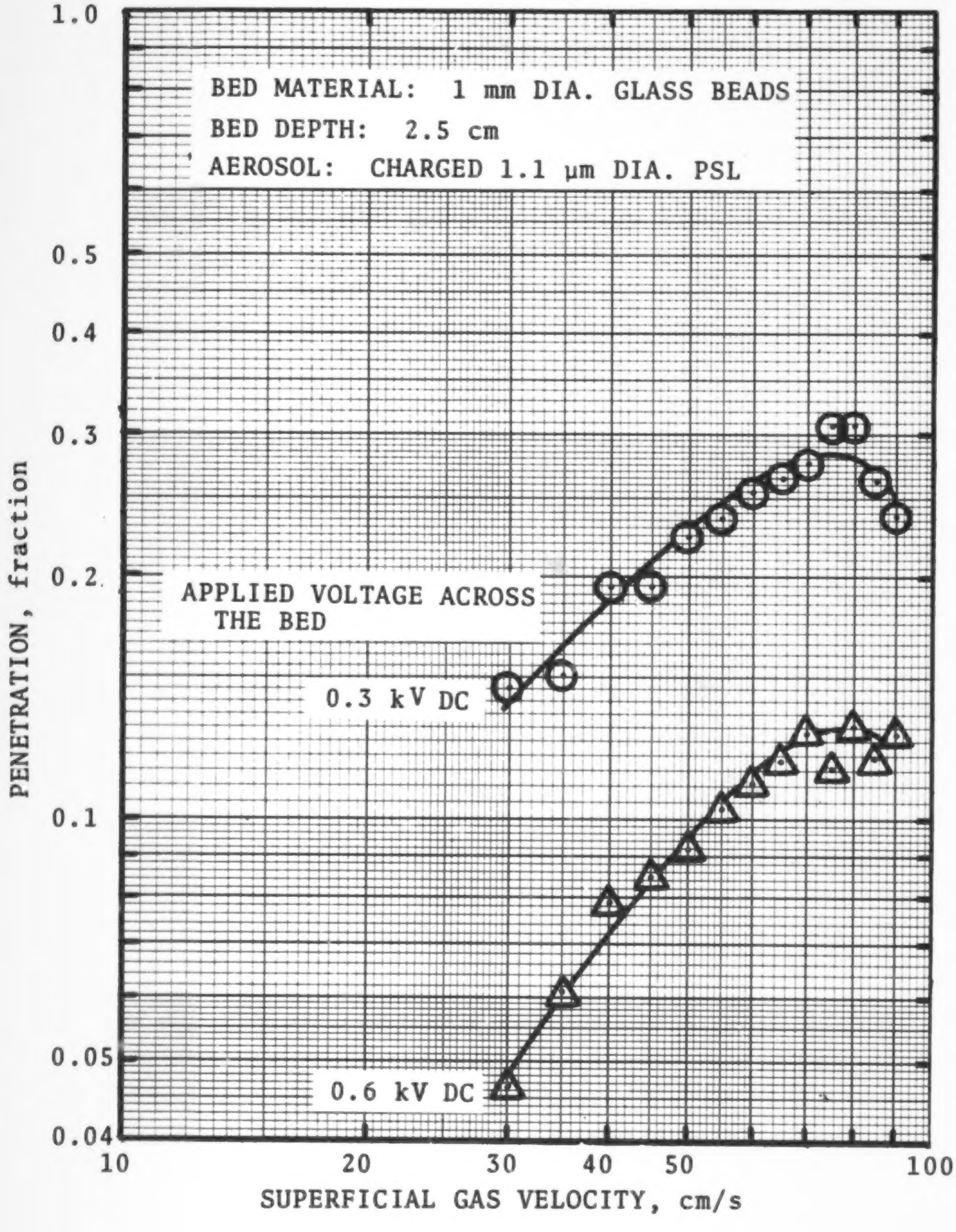

Figure A-13. Experimental charged particle penetration through a clean, DC polarized GBF.

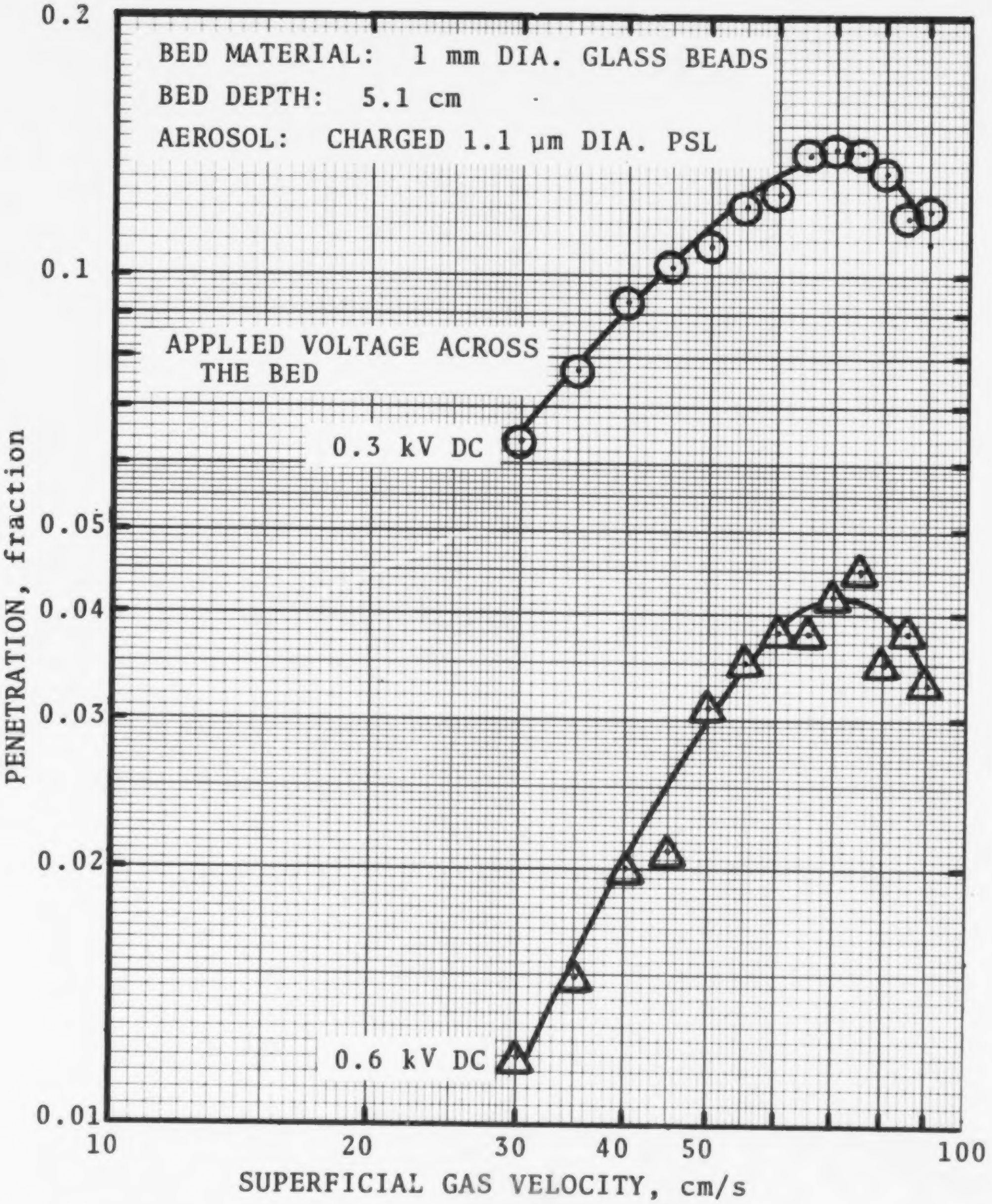

Figure A-14. Experimental charged particle penetration through a clean, DC polarized GBF.

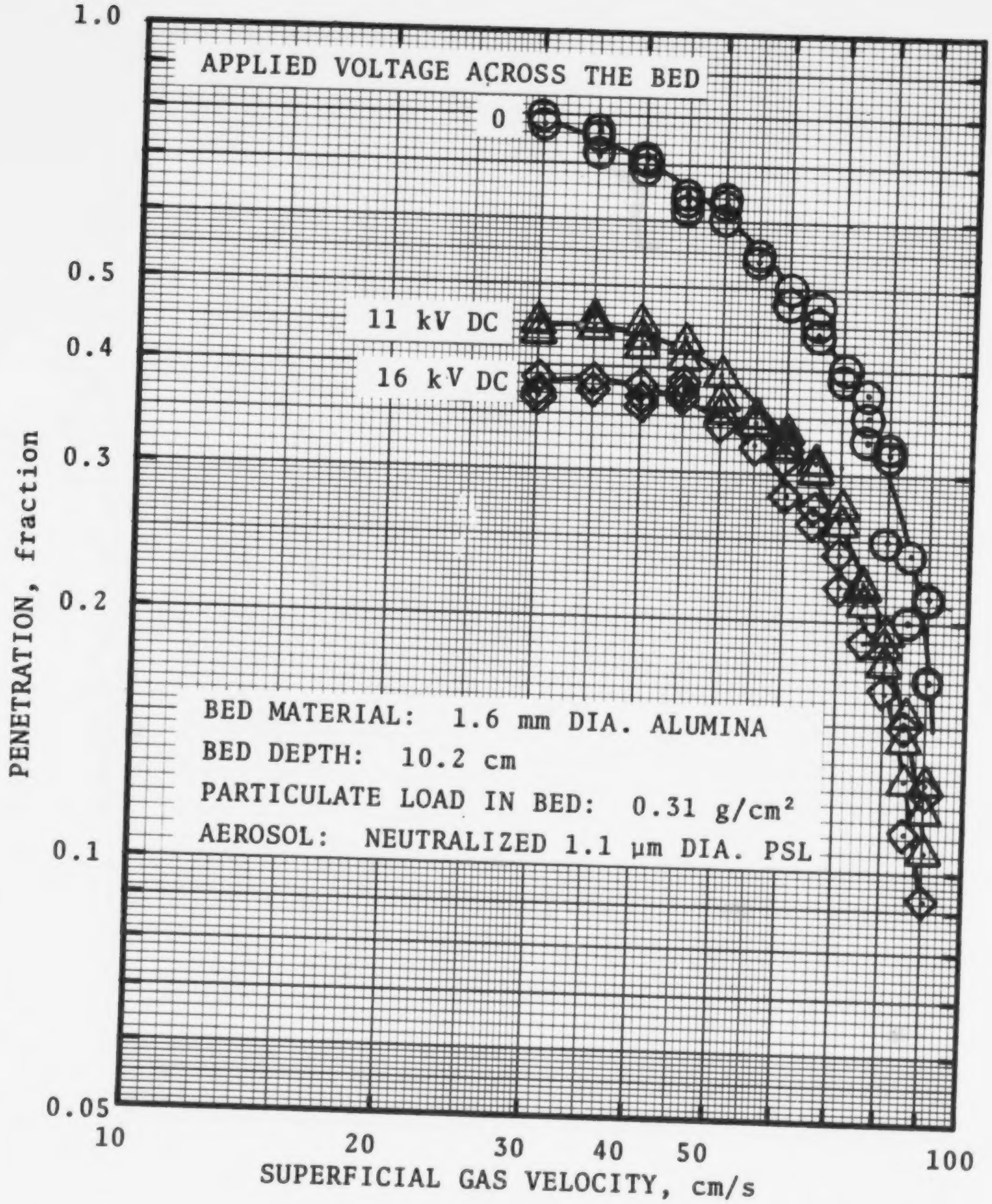

Figure A-15. Experimental particle penetration of a dirty GBF.

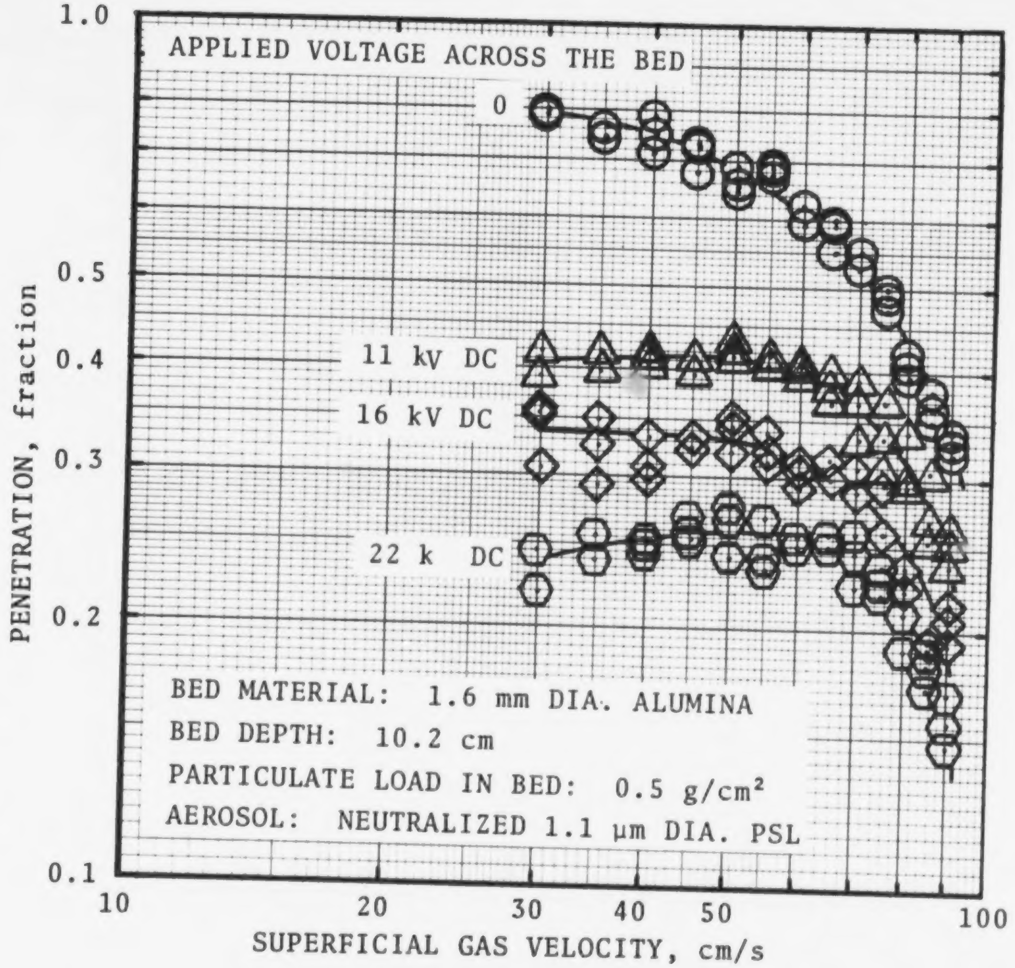

Figure A-16. Experimental penetration of a dirty, charged GBF.

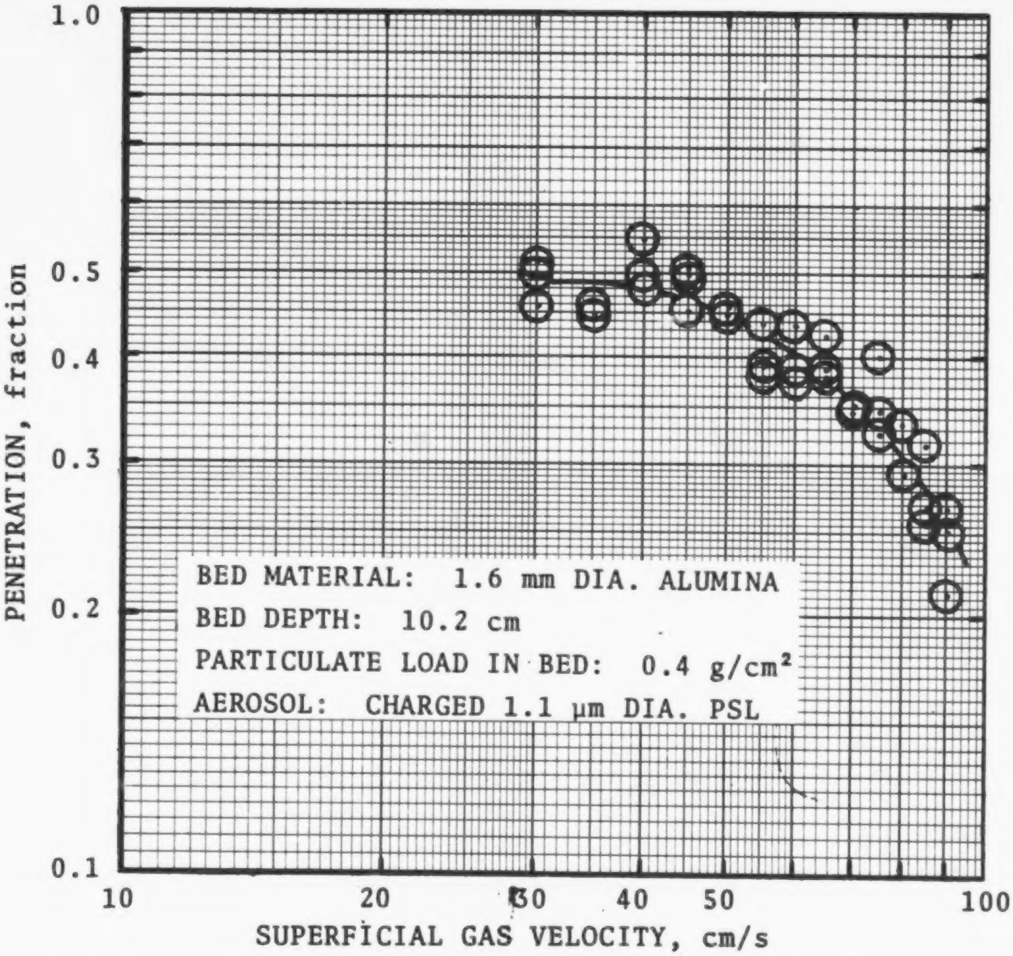

Figure A-17. Experimental penetration of a dirty, grounded fixed GBF.

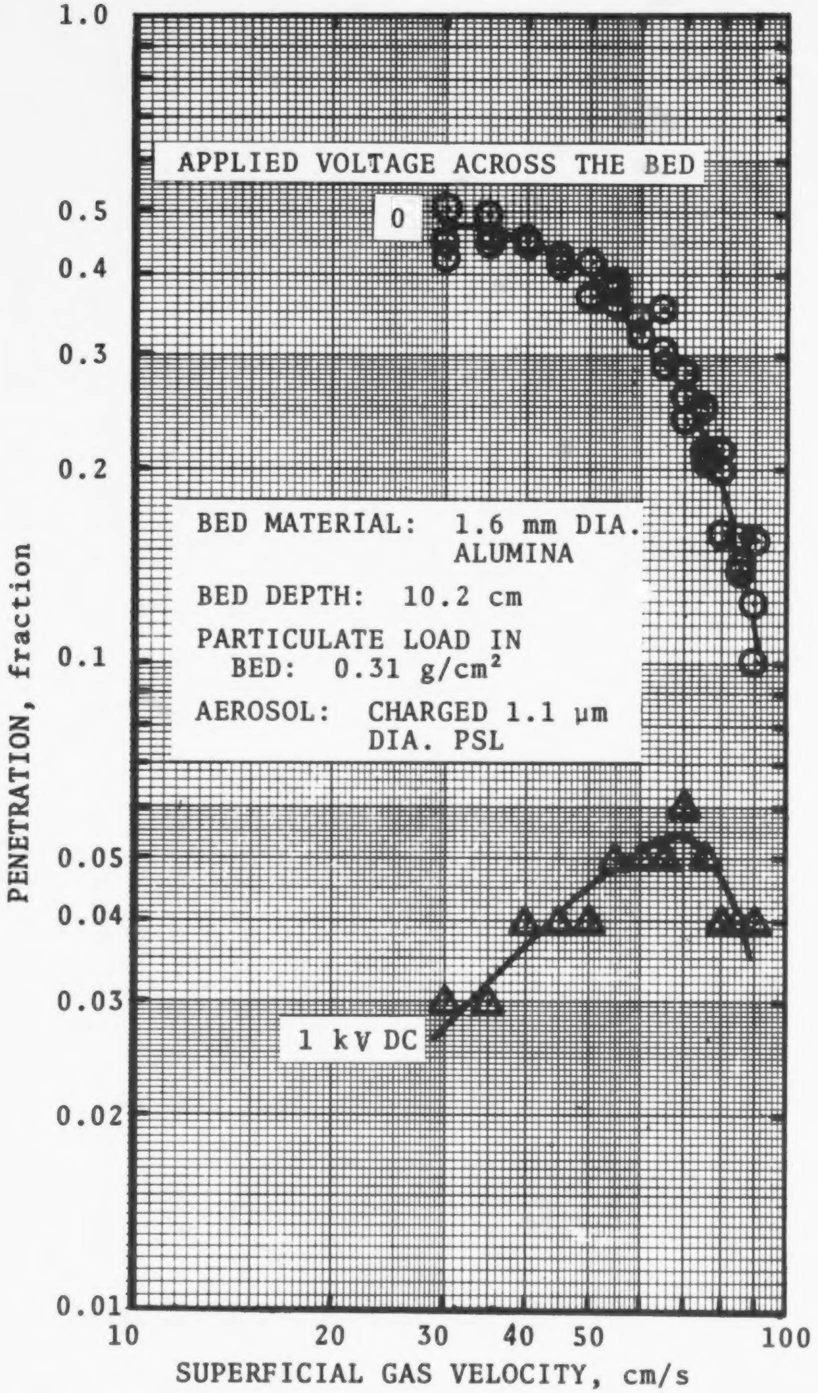

Figure A-18. Experimental penetration of a dirty GBF.

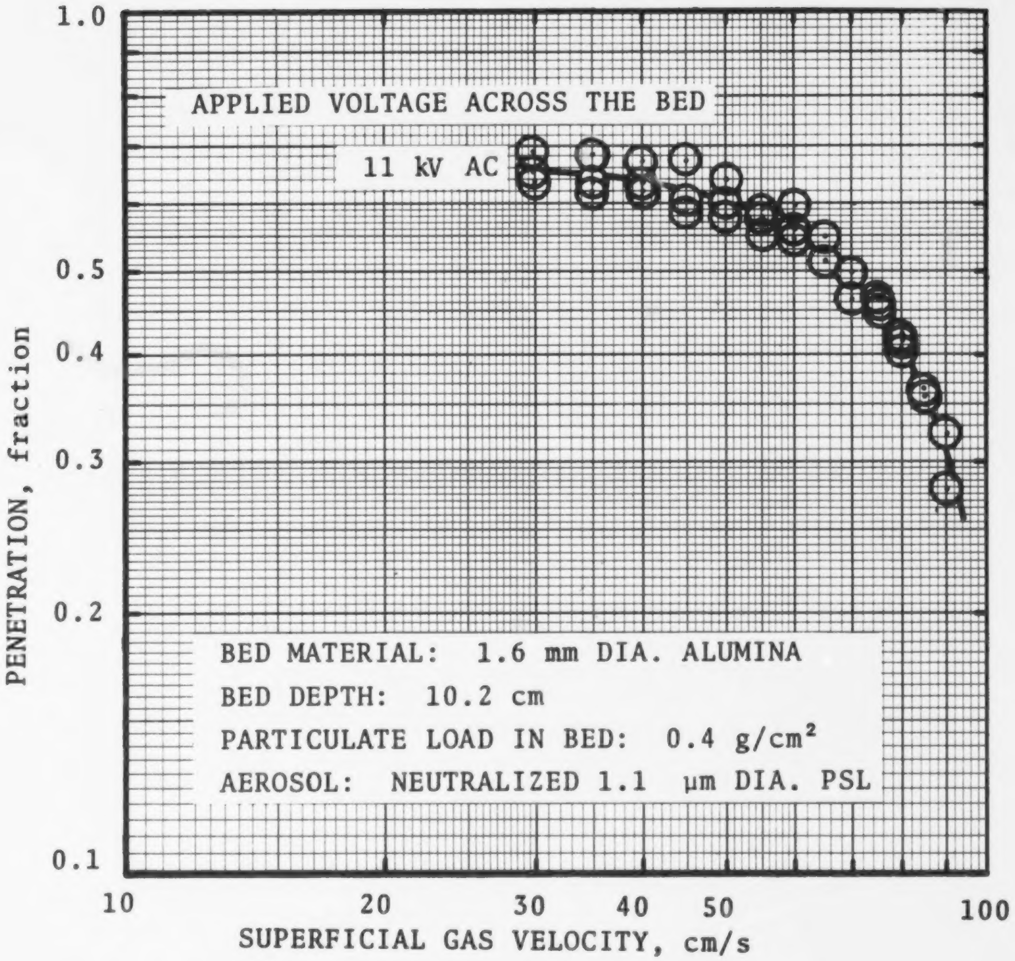

Figure A-19. Experimental penetration of an AC charged, dirty, fixed GBF.

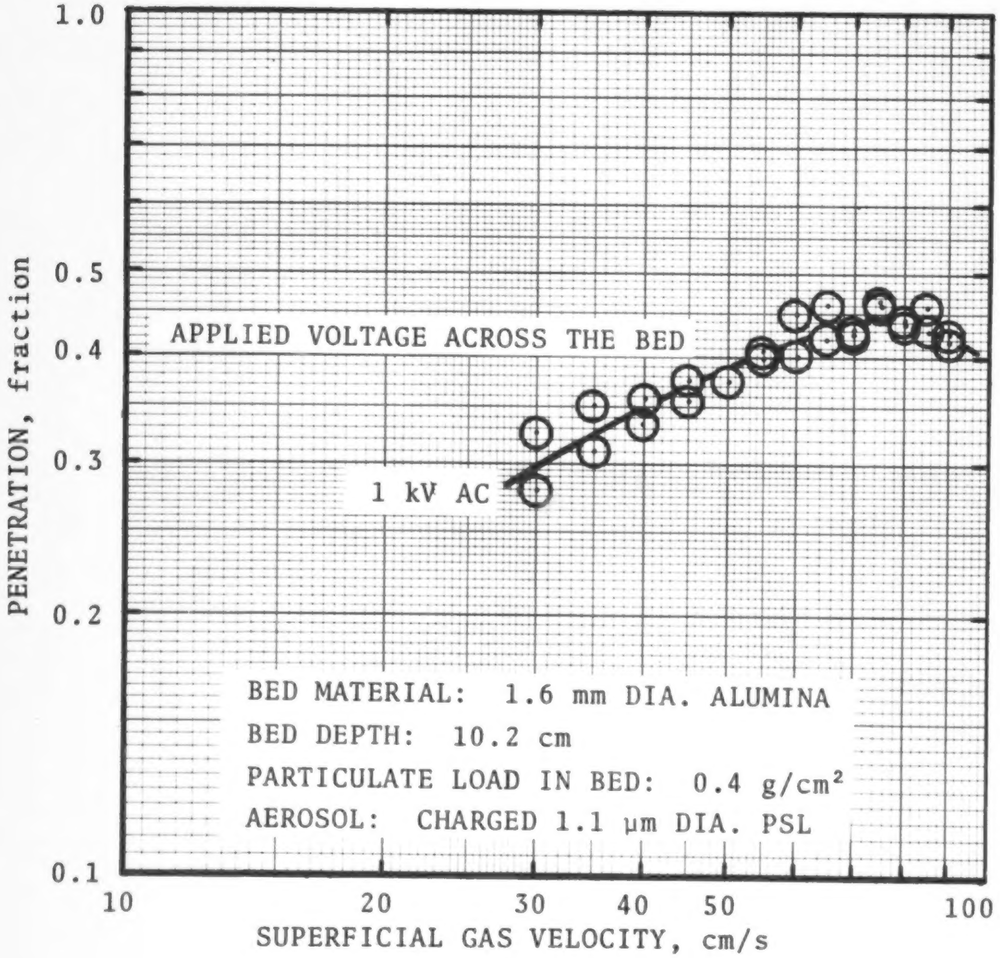

Figure A-20. Experimental penetration of an AC charged, dirty, fixed GBF.

APPENDIX B

CASCADE IMPACTOR PARTICLE DATA

TABLE B-1. CASCADE IMPACTOR DATA FOR RUN #1

Stage No.	Inlet			Outlet		
	Cum. Mass (mg)	Cum. Particle Concentration (mg/DNm³)	Particle Diameter (μmA)	Cum. Mass (mg)	Cum. Particle Concentration (mg/DNm³)	Particle Diameter (μmA)
Probe	136.4	753.6		17.3	104.8	
1	91.9	507.7	27.9	13.4	81.2	29.2
2	84.4	466.3	12.2	13.2	80.0	12.8
3	78.0	430.9	4.7	12.7	76.9	4.9
4	44.3	244.8	2.4	11.7	70.9	2.5
5	19.3	106.6	1.4	8.9	53.9	1.5
6	6.8	37.6	0.8	2.9	17.6	0.8
7	1.9	10.5	0.4	0.2	1.2	0.5
Filter	0.3	1.7		0	0	

TABLE B-2. CASCADE IMPACTOR DATA FOR RUN #2

Stage No.	Inlet			Outlet		
	Cum. Mass (mg)	Cum. Particle Concentration (mg/DNm³)	Particle Diameter (μmA)	Cum. Mass (mg)	Cum. Particle Concentration (mg/DNm³)	Particle Diameter (μmA)
Probe	77.8	492.4		22.6	96.6	
1	52.1	329.7	30.0	16.2	69.2	24.6
2	51.5	325.9	13.2	15.9	68.0	10.8
3	48.3	305.7	5.1	15.6	66.7	4.2
4	30.3	191.8	2.6	14.8	63.3	2.1
5	11.9	75.3	1.5	9.4	40.2	1.3
6	3.4	21.5	0.9	3.2	13.7	0.7
7	1.0	6.3	0.4	1.3	5.6	0.4
Filter	0.3	1.9		0.6	2.6	

TABLE B-3. CASCADE IMPACTOR DATA FOR RUN #3

Stage No.	Inlet			Outlet		
	Cum. Mass (mg)	Cum. Particle Concentration (mg/DNm³)	Particle Diameter (μmA)	Cum. Mass (mg)	Cum. Particle Concentration (mg/DNm³)	Particle Diameter (μmA)
Probe	173.3	802.3		12.1	38.9	
1	123.4	571.3	25.6	3.9	12.5	24.6
2	115.3	533.8	11.2	3.9	12.5	10.8
3	103.2	477.8	4.3	3.9	12.5	4.2
4	60.7	281.0	2.2	3.7	11.9	2.1
5	27.9	129.2	1.3	2.3	7.4	1.3
6	10.2	47.2	0.7	1.1	3.5	0.7
7	1.9	8.8	0.4	0.8	2.6	0.4
Filter	0.7	3.2		0.1	0.3	

TABLE B-4. CASCADE IMPACTOR DATA FOR RUN #4

Stage No.	Inlet			Outlet		
	Cum. Mass (mg)	Cum. Particle Concentration (mg/DNm³)	Particle Diameter (μmA)	Cum. Mass (mg)	Cum. Particle Concentration (mg/DNm³)	Particle Diameter (μmA)
Probe	234.8	1449.0		21.6	69.3	
1	163.8	1010.8	34.1	14.0	44.9	24.5
2	144.6	892.4	15.0	12.6	40.4	10.7
3	129.5	799.2	5.8	11.1	35.6	4.2
4	79.5	490.6	2.9	8.5	27.3	2.1
5	49.2	303.6	1.7	6.1	19.6	1.3
6	25.6	158.0	1.0	4.0	12.8	0.7
7	9.1	56.2	0.5	2.5	8.0	0.4
Filter	2.8	17.3		1.3	4.2	

TABLE B-5. CASCADE IMPACTOR DATA FOR RUN #5

Stage No.	Inlet			Outlet		
	Cum. Mass (mg)	Cum. Particle Concentration (mg/DNm³)	Particle Diameter (μmA)	Cum. Mass (mg)	Cum. Particle Concentration (mg/DNm³)	Particle Diameter (μmA)
Probe	180.7	1,082.0		12.0	38.1	
1	148.3	888.0	33.6	5.1	16.2	24.4
2	142.4	852.7	14.7	5.0	15.9	10.7
3	137.5	823.3	5.7	4.7	14.9	4.1
4	109.8	657.5	2.9	3.2	10.2	2.1
5	71.9	430.5	1.7	2.1	6.7	1.2
6	38.1	228.1	1.0	1.3	4.1	0.7
7	14.8	88.6	0.5	0.6	1.9	0.4
Filter	2.9	17.4		0.2	0.6	

TABLE B-6. CASCADE IMPACTOR DATA FOR RUN #6

Stage No.	Inlet			Outlet		
	Cum. Mass (mg)	Cum. Particle Concentration (mg/DNm³)	Particle Diameter (μmA)	Cum. Mass (mg)	Cum. Particle Concentration (mg/DNm³)	Particle Diameter (μmA)
Probe	164.8	1446.0		15.2	32.3	
1	133.9	1174.9	49.6	7.6	16.2	24.5
2	129.0	1131.9	4.3	7.2	15.3	10.7
3	98.5	864.3	2.5	6.5	13.8	4.2
4	65.4	573.8	1.4	4.4	9.4	2.1
5	33.2	291.3	0.7	3.0	6.4	1.3
6	8.0	70.2	0.5	1.9	4.0	0.7
7	2.1	18.4	0.3	0.9	1.9	0.4
Filter	0.8	7.0		0.3	0.6	

TABLE B-7. CASCADE IMPACTOR DATA FOR RUN #7

	Inlet			Outlet		
Stage No.	Cum. Mass (mg)	Cum. Particle Concentration (mg/DNm³)	Particle Diameter (μmA)	Cum. Mass (mg)	Cum. Particle Concentration (mg/DNm³)	Particle Diameter (μmA)
Probe	158.6	1311.0		33.8	75.8	
1	114.5	946.5	48.4	24.3	54.5	25.0
2	106.6	881.2	4.2	24.1	54.0	11.0
3	58.3	481.9	2.4	23.4	52.5	4.2
4	33.5	276.9	1.4	18.4	41.3	2.1
5	12.3	101.7	0.7	11.0	24.7	1.3
6	3.2	26.5	0.5	3.0	6.7	0.7
7	0.6	5.0	0.3	0.6	1.3	0.4
Filter	0.2	1.7		0.3	0.7	

TABLE B-8. CASCADE IMPACTOR DATA FOR RUN #8

	Inlet			Outlet		
Stage No.	Cum. Mass (mg)	Cum. Particle Concentration (mg/DNm³)	Particle Diameter (μmA)	Cum. Mass (mg)	Cum. Particle Concentration (mg/DNm³)	Particle Diameter (μmA)
Probe	178.9	1111.0		25.5	81.0	
1	135.3	840.2	34.2	17.6	55.9	24.4
2	132.3	821.6	15.0	17.0	54.0	10.7
3	127.6	792.4	5.8	16.2	51.5	4.1
4	123.4	766.3	2.9	12.3	39.1	2.1
5	77.5	481.3	1.7	7.6	24.1	1.2
6	45.5	282.6	1.0	2.0	6.4	0.7
7	19.0	118.0	0.5	0.4	1.3	0.4
Filter	4.1	25.5		0.2	0.6	

TABLE B-9. CASCADE IMPACTOR DATA FOR RUN #9

Stage No.	Inlet			Outlet		
	Cum. Mass (mg)	Cum. Particle Concentration (mg/DNm^3)	Particle Diameter (μmA)	Cum. Mass (mg)	Cum. Particle Concentration (mg/DNm^3)	Particle Diameter (μmA)
Probe	65.4	444.9		9.3	54.1	
1	56.7	385.7	25.4	7.7	44.8	28.7
2	55.9	380.3	11.1	7.7	44.8	12.6
3	52.2	355.1	4.3	7.7	44.8	4.9
4	31.0	210.9	2.2	6.8	39.6	2.4
5	9.5	64.6	1.3	5.1	29.7	1.5
6	1.8	12.2	0.7	1.4	8.1	0.8
7	0	0	0.4	0.3	1.7	0.5
Filter	0	0		0.1	0.6	

TABLE B-10. CASCADE IMPACTOR DATA FOR RUN #10

Stage No.	Inlet			Outlet		
	Cum. Mass (mg)	Cum. Particle Concentration (mg/DNm^3)	Particle Diameter (μmA)	Cum. Mass (mg)	Cum. Particle Concentration (mg/DNm^3)	Particle Diameter (μmA)
Probe	83.6	497.6		32.4	188.4	
1	65.0	386.9	26.2	23.5	136.6	28.8
2	62.8	373.8	11.5	21.9	127.3	12.6
3	58.4	347.8	4.4	20.5	119.2	4.9
4	37.4	222.6	2.3	18.4	107.0	2.4
5	16.3	97.0	1.3	14.5	84.3	1.5
6	6.9	41.1	0.7	7.0	40.7	0.8
7	3.3	19.6	0.4	3.3	19.2	0.5
Filter	1.6	9.5		1.5	8.7	

TABLE B-11. CASCADE IMPACTOR DATA FOR RUN #11

Stage No.	Inlet			Outlet		
	Cum. Mass (mg)	Cum. Particle Concentration (mg/DNm³)	Particle Diameter (µmA)	Cum. Mass (mg)	Cum. Particle Concentration (mg/DNm³)	Particle Diameter (µmA)
Probe	43.8	387.6		4.8	43.6	
1	31.7	280.5	28.9	4.0	36.5	29.2
2	30.4	269.0	12.7	3.3	30.1	12.8
3	27.8	246.0	4.9	2.6	23.7	5.0
4	12.5	110.6	2.5	2.2	20.1	2.5
5	9.1	80.5	1.5	2.0	18.3	1.5
6	3.2	28.3	0.8	1.3	11.9	0.8
7	1.4	12.4	0.4	1.0	9.1	0.5
Filter	1.1	9.7		0.9	8.2	

TABLE B-12. CASCADE IMPACTOR DATA FOR RUN #12

Stage No.	Inlet			Outlet		
	Cum. Mass (mg)	Cum. Particle Concentration (mg/DNm³)	Particle Diameter (µmA)	Cum. Mass (mg)	Cum. Particle Concentration (mg/DNm³)	Particle Diameter (µmA)
Probe	74.1	463.1		8.2	44.3	
1	57.4	358.7	24.5	7.0	37.8	27.8
2	53.2	332.5	10.7	6.7	36.2	12.2
3	48.2	301.2	4.2	6.5	35.1	4.7
4	27.0	168.7	2.1	5.4	29.2	2.4
5	9.1	56.9	1.2	3.9	21.1	1.4
6	1.9	11.9	0.7	1.0	5.4	0.8
7	0.5	3.1	0.3	0	0	0.5
Filter	0.2	1.2		0	0	

TABLE B-13. CASCADE IMPACTOR DATA FOR RUN #13

Stage No.	Inlet			Outlet		
	Cum. Mass (mg)	Cum. Particle Concentration (mg/DNm^3)	Particle Diameter (μmA)	Cum. Mass (mg)	Cum. Particle Concentration (mg/DNm^3)	Particle Diameter (μmA)
Probe	188.5	1171.0		7.3	38.6	
1	89.5	556.0	24.4	4.2	22.2	27.5
2	70.2	436.1	10.7	4.0	21.2	12.0
3	50.3	312.5	4.1	3.9	20.6	4.7
4	24.1	149.7	2.1	3.4	18.0	2.3
5	8.0	49.7	1.2	2.3	12.2	1.4
6	2.2	13.7	0.7	0.3	1.6	0.8
7	0.9	5.6	0.3	0	0	0.5
Filter	0.4	2.5		0	0	

TABLE B-14. CASCADE IMPACTOR DATA FOR RUN #14

Stage No.	Inlet			Outlet		
	Cum. Mass (mg)	Cum. Particle Concentration (mg/DNm^3)	Particle Diameter (μmA)	Cum. Mass (mg)	Cum. Particle Concentration (mg/DNm^3)	Particle Diameter (μmA)
Probe	73.3	461.0		9.1	47.6	
1	50.5	317.6	24.3	5.5	28.8	27.1
2	47.3	297.5	10.6	4.8	25.1	11.9
3	42.7	268.5	4.2	4.2	22.0	4.6
4	23.9	150.3	2.1	2.5	13.1	2.3
5	7.9	49.7	1.2	1.3	6.8	1.4
6	2.2	13.8	0.7	0.4	2.1	0.8
7	0.6	3.8	0.3	0.2	1.0	0.5
Filter	0.3	1.9		0	0	

TABLE B-15. CASCADE IMPACTOR DATA FOR RUN #15.

Stage No.	Inlet			Outlet		
	Cum. Mass (mg)	Cum. Particle Concentration (mg/DNm^3)	Particle Diameter (μmA)	Cum. Mass (mg)	Cum. Particle Concentration (mg/DNm^3)	Particle Diameter (μmA)
Probe	205.0	1102.2		9.7	53.0	
1	155.3	835.0	22.5	3.0	16.4	27.7
2	149.9	806.0	9.9	2.6	14.2	12.1
3	101.3	544.6	3.8	2.1	11.5	4.7
4	46.5	250.0	1.9	1.5	8.2	2.3
5	11.5	61.8	1.1	0.9	4.9	1.4
6	2.2	11.8	0.6	0.1	0.6	0.8
7	0	0	0.3	0		0.5
Filter	0	0		0		

TABLE B-16. CASCADE IMPACTOR DATA FOR RUN #16

Stage No.	Inlet			Outlet		
	Cum. Mass (mg)	Cum. Particle Concentration (mg/DNm^3)	Particle Diameter (μmA)	Cum. Mass (mg)	Cum. Particle Concentration (mg/DNm^3)	Particle Diameter (μmA)
Probe	130.7	751.2		18.9	115.2	
1	98.6	566.7	28.6	16.2	98.7	29.3
2	90.1	517.8	12.5	15.2	92.6	12.8
3	82.7	475.2	4.8	14.8	90.2	5.0
4	47.0	270.1	2.4	13.7	83.5	2.5
5	20.1	115.5	1.4	11.2	68.3	1.5
6	6.9	39.7	0.8	5.5	33.5	0.8
7	1.5	8.6	0.4	2.3	14.0	0.5
Filter	0.5	2.9		1.4	8.5	

TABLE B-17. CASCADE IMPACTOR DATA FOR RUN #17

Stage No.	Inlet			Outlet		
	Cum. Mass (mg)	Cum. Particle Concentration (mg/DNm^3)	Particle Diameter (μmA)	Cum. Mass (mg)	Cum. Particle Concentration (mg/DNm^3)	Particle Diameter (μmA)
Probe	76.9	530.3		16.7	97.1	
1	60.3	415.8	25.7	11.4	66.3	28.8
2	59.7	411.7	11.3	11.4	66.3	12.6
3	56.9	392.4	4.4	11.4	66.3	4.9
4	32.4	223.4	2.2	11.0	64.0	2.4
5	12.9	89.0	1.3	8.6	50.0	1.5
6	3.8	26.2	0.7	2.6	15.1	0.8
7	1.5	10.3	0.4	0.2	1.2	0.5
Filter	0.7	4.8		0	0	

TABLE B-18. CASCADE IMPACTOR DATA FOR RUN #18

Stage No.	Inlet			Outlet		
	Cum. Mass (mg)	Cum. Particle Concentration (mg/DNm^3)	Particle Diameter (μmA)	Cum. Mass (mg)	Cum. Particle Concentration (mg/DNm^3)	Particle Diameter (μmA)
Probe	144.1	1067.0		11.3	61.1	
1	97.6	722.7	26.7	5.7	30.8	27.8
2	95.1	704.2	11.7	4.8	26.0	12.2
3	84.7	627.2	4.5	4.2	22.7	4.7
4	44.8	331.7	2.3	2.6	14.1	2.3
5	15.6	115.5	1.3	1.6	8.7	1.4
6	3.5	25.9	0.8	0.4	2.2	0.8
7	0.3	2.2	0.4	0.1	0.5	0.5
Filter	0.1	0.7		0	0	

TABLE B-19. CASCADE IMPACTOR DATA FOR RUN #19.

	Inlet			Outlet		
Stage No.	Cum. Mass (mg)	Cum. Particle Concentration (mg/DNm^3)	Particle Diameter (μmA)	Cum. Mass (mg)	Cum. Particle Concentration (mg/DNm^3)	Particle Diameter (μmA)
Probe	86.5	547.5		6.5	34.6	
1	66.6	421.5	24.5	2.1	11.2	27.4
2	65.2	412.7	10.7	1.9	10.1	12.0
3	61.3	388.0	4.2	1.9	10.1	4.6
4	36.5	231.0	2.1	1.3	6.9	2.3
5	12.6	79.8	1.2	0.8	4.3	1.4
6	2.8	17.7	0.7	0.2	1.1	0.8
7	0.5	3.2	0.3	0.1	0.5	0.5
Filter	0.4	2.5		0.1	0.5	

TABLE B-20. CASCADE IMPACTOR DATA FOR RUN #20.

	Inlet			Outlet		
Stage No.	Cum. Mass (mg)	Cum. Particle Concentration (mg/DNm^3)	Particle Diameter (μmA)	Cum. Mass (mg)	Cum. Particle Concentration (mg/DNm^3)	Particle Diameter (μmA)
Probe	88.9	446.7		7.7	49.0	
1	71.0	356.8	21.8	1.0	6.4	24.5
2	70.5	354.2	9.6	0.7	4.5	10.7
3	64.3	323.1	3.7	0.6	3.8	4.2
4	31.7	159.3	1.9	0.4	2.5	2.1
5	7.8	39.2	1.1	0.2	1.3	1.3
6	1.0	5.0	0.6	0.1	0.6	0.7
7	0.3	1.5	0.3	0	0	0.4
Filter	0	0		0	0	

TABLE B-21. CASCADE IMPACTOR DATA FOR RUN #21

Stage No.	Inlet			Outlet		
	Cum. Mass (mg)	Cum. Particle Concentration (mg/DNm^3)	Particle Diameter (μmA)	Cum. Mass (mg)	Cum. Particle Concentration (mg/DNm^3)	Particle Diameter (μmA)
Probe	86.2	684.1		5.8	39.5	
1	64.9	515.1	27.4	1.0	6.8	31.0
2	63.8	506.3	12.0	0.8	5.4	13.6
3	61.2	485.7	4.7	0.8	5.4	5.3
4	38.0	301.6	2.4	0.5	3.4	2.6
5	14.1	111.9	1.4	0.3	2.0	1.6
6	3.6	28.6	0.8	0	0	0.9
7	0.6	4.8	0.4	0	0	0.6
Filter	0.2	1.6		0	0	

APPENDIX C

EXPERIMENTAL GRADE PENETRATION CURVES OF THE MOVING BED GRANULAR BED FILTER

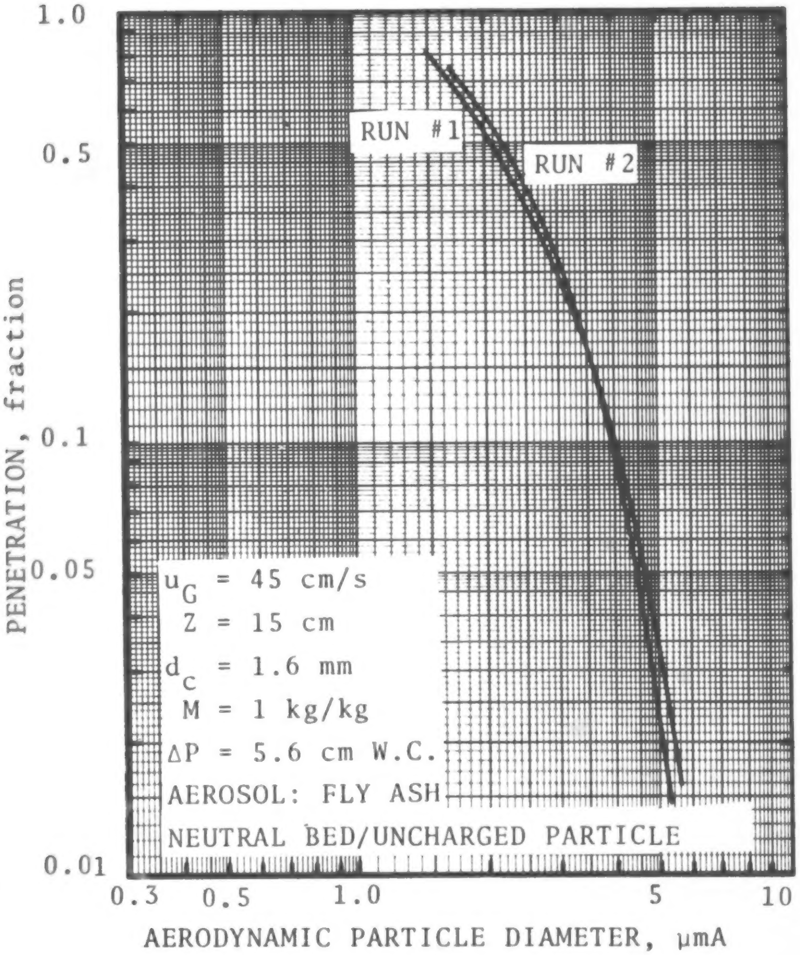

Figure C-1. Experimental grade penetration curves of the moving GBF.

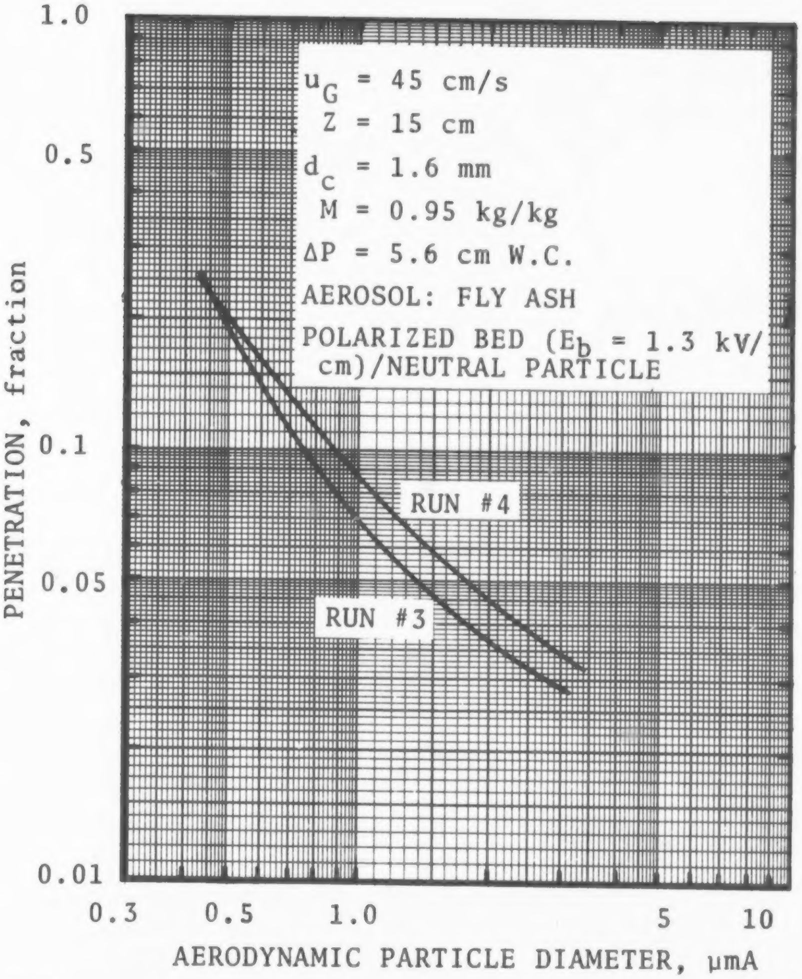

Figure C-2. Experimental grade penetration curves of the moving GBF.

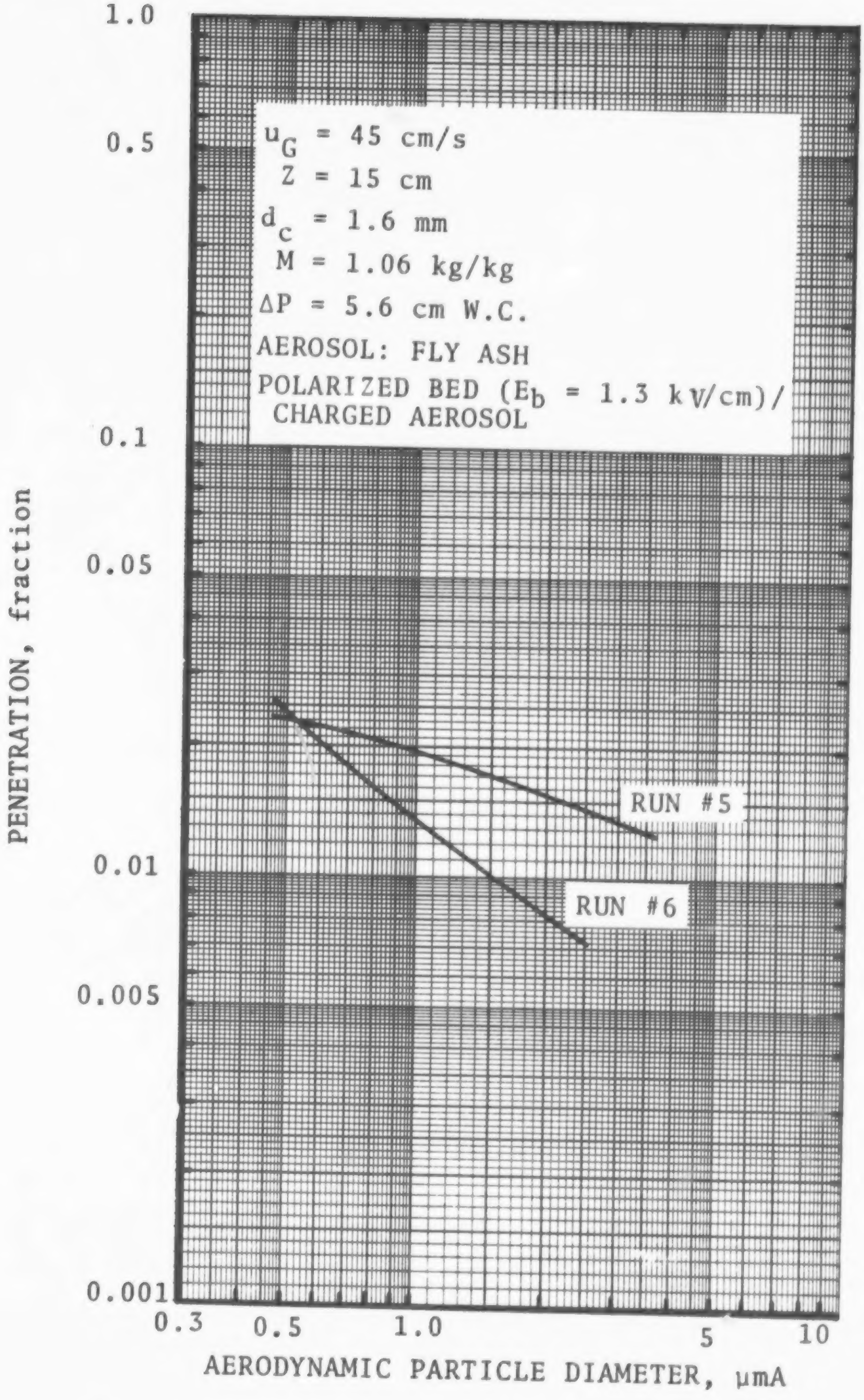

Figure C-3. Experimental grade penetration curves of the moving GBF.

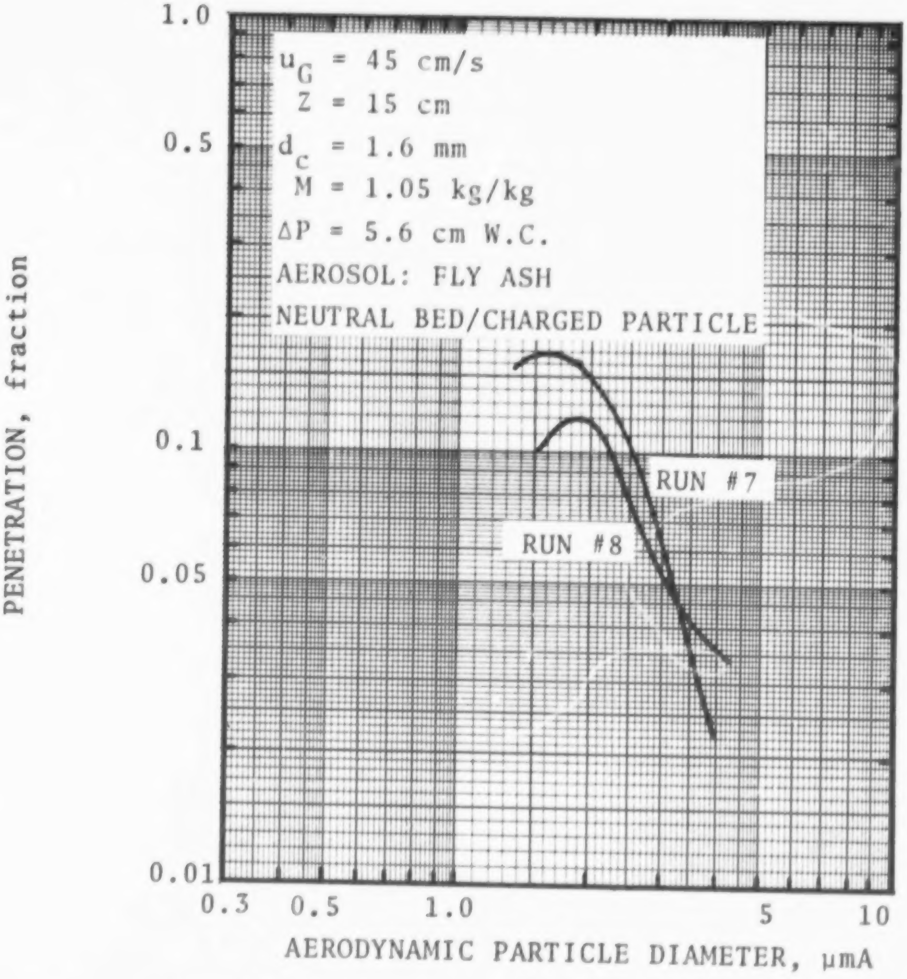

Figure C-4. Experimental grade penetration curves of the moving GBF.

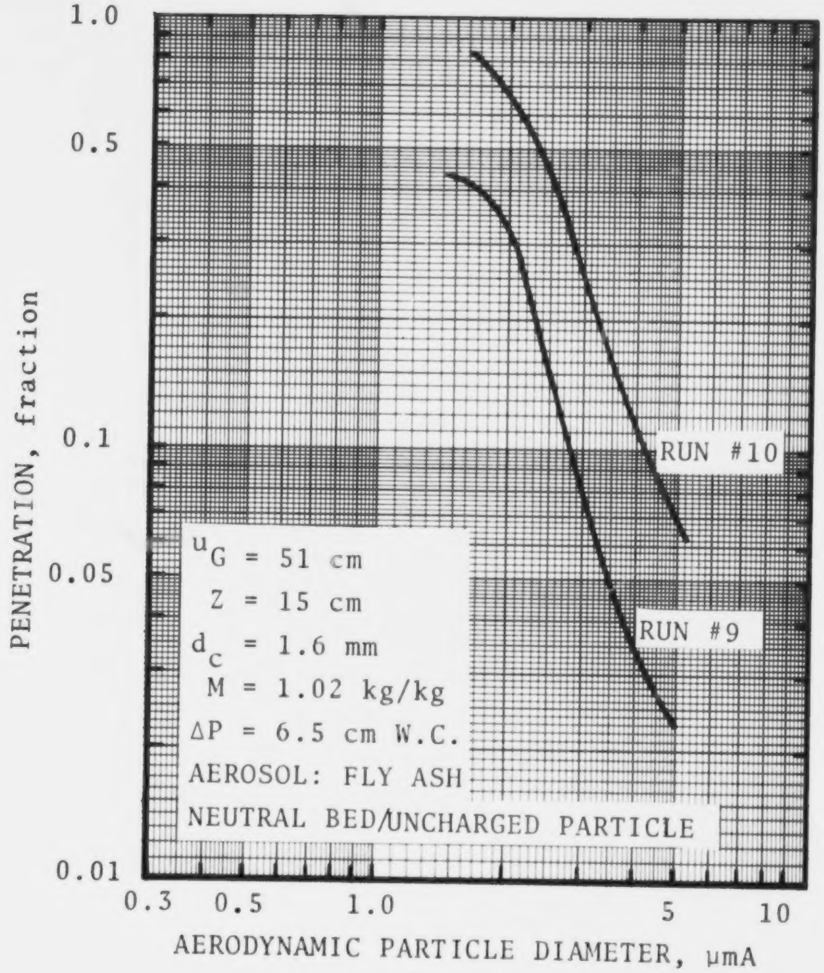

Figure C-5. Experimental grade penetration curves of the moving GBF.

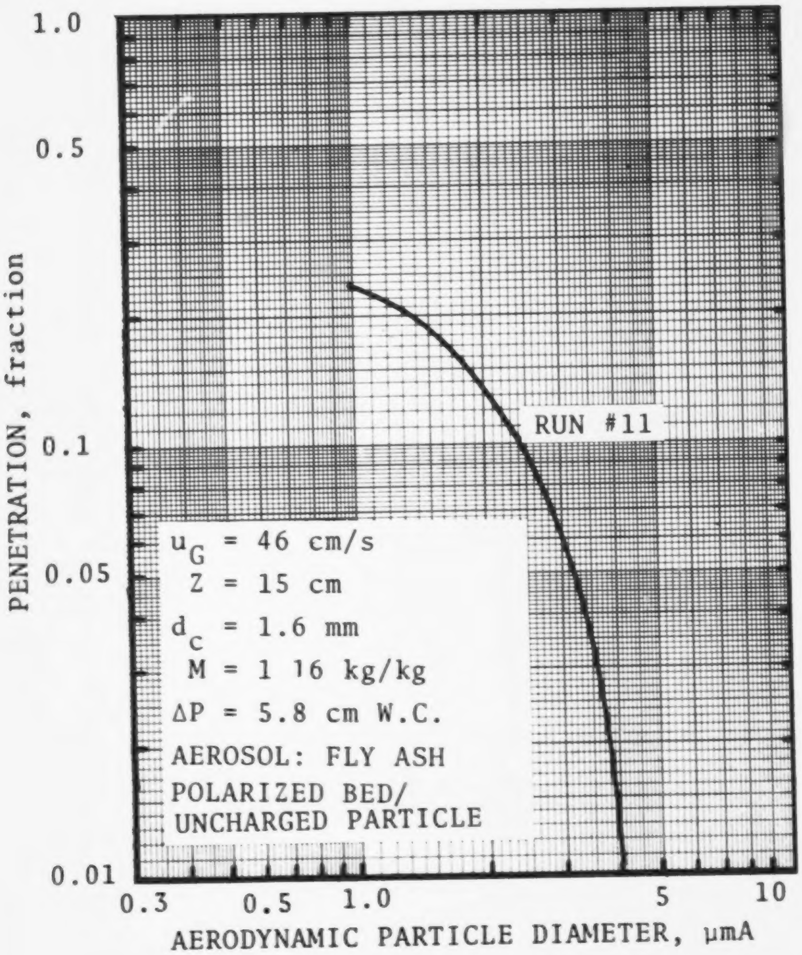

Figure C-6. Experimental grade penetration curves of the moving GBF.

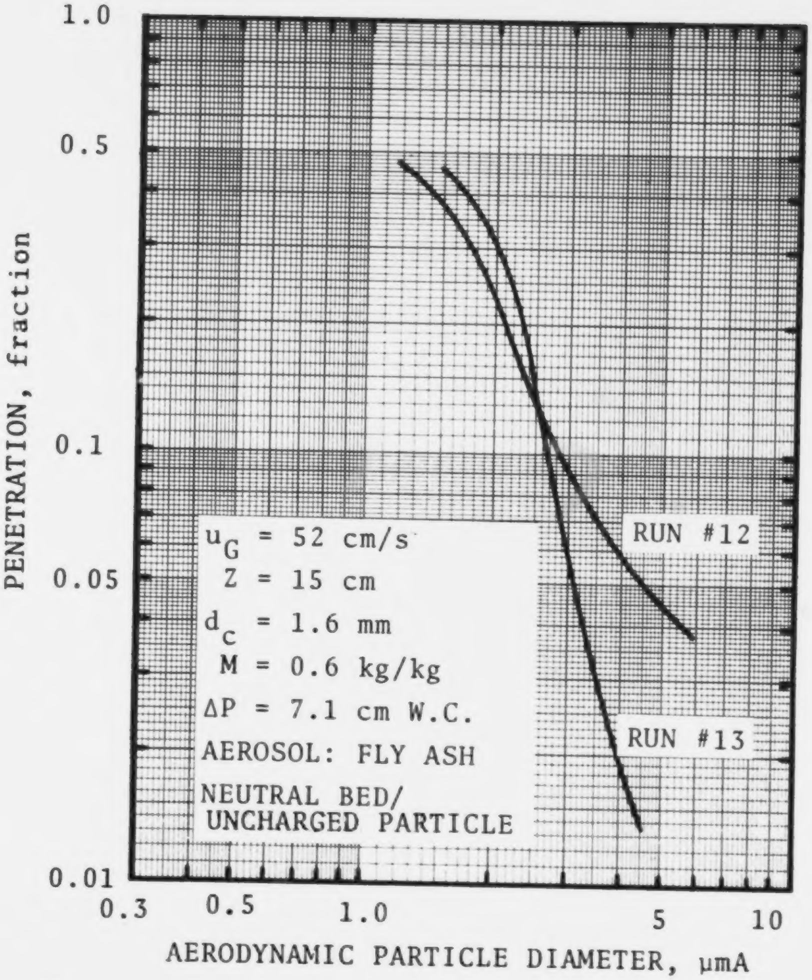

Figure C-7. Experimental grade penetration curves of the moving GBF.

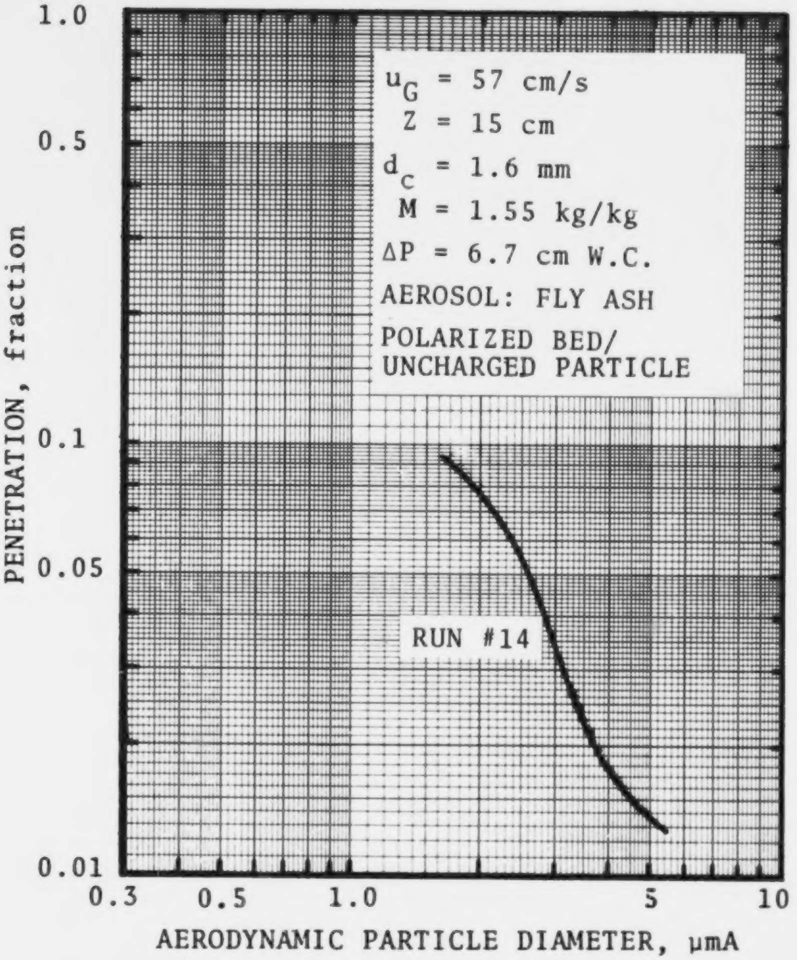

Figure C-8. Experimental grade penetration curves of the moving GBF.

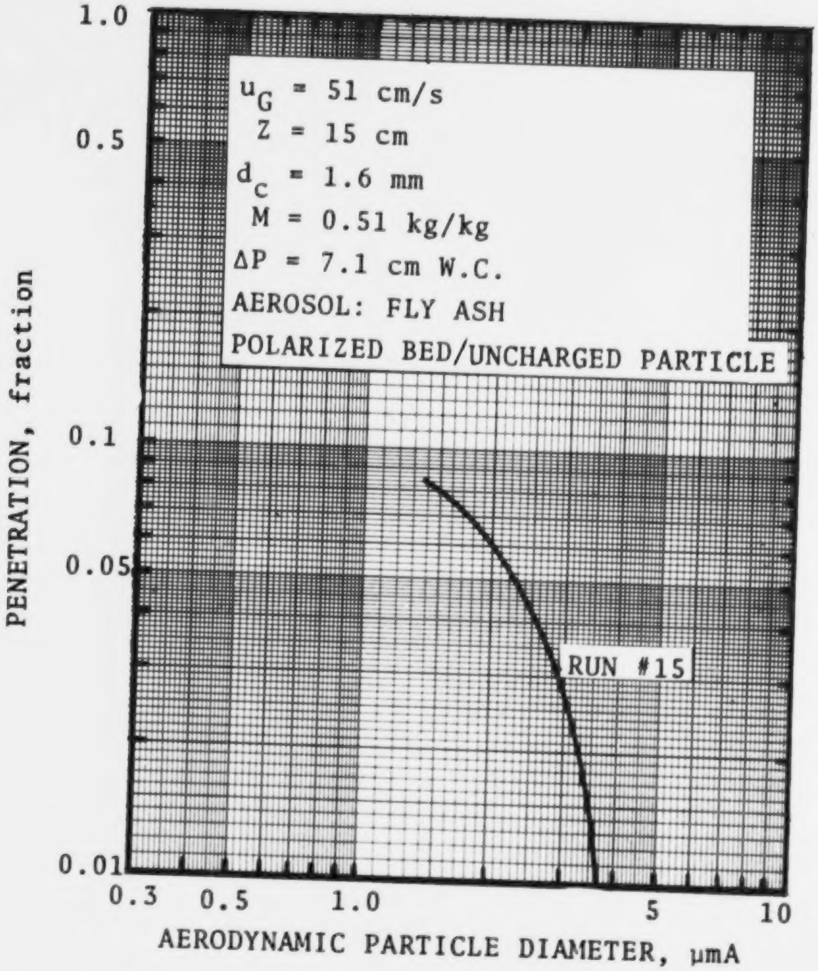

Figure C-9. Experimental grade penetration curve of a moving GBF.

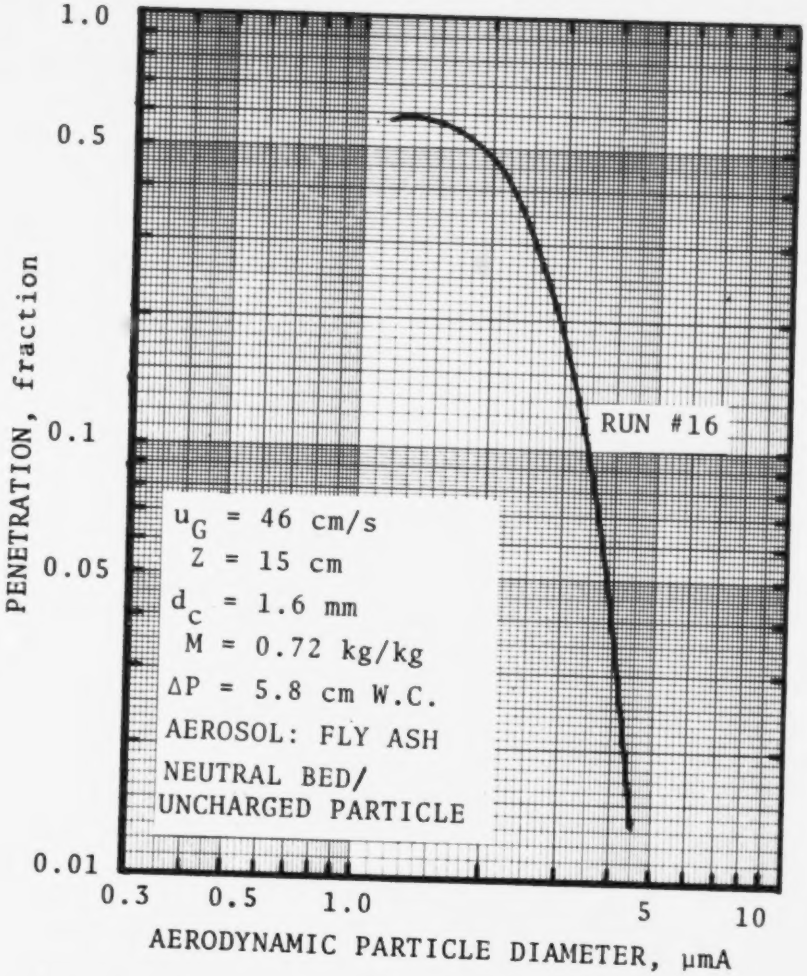

Figure C-10. Experimental grade penetration curve of a moving GBF.

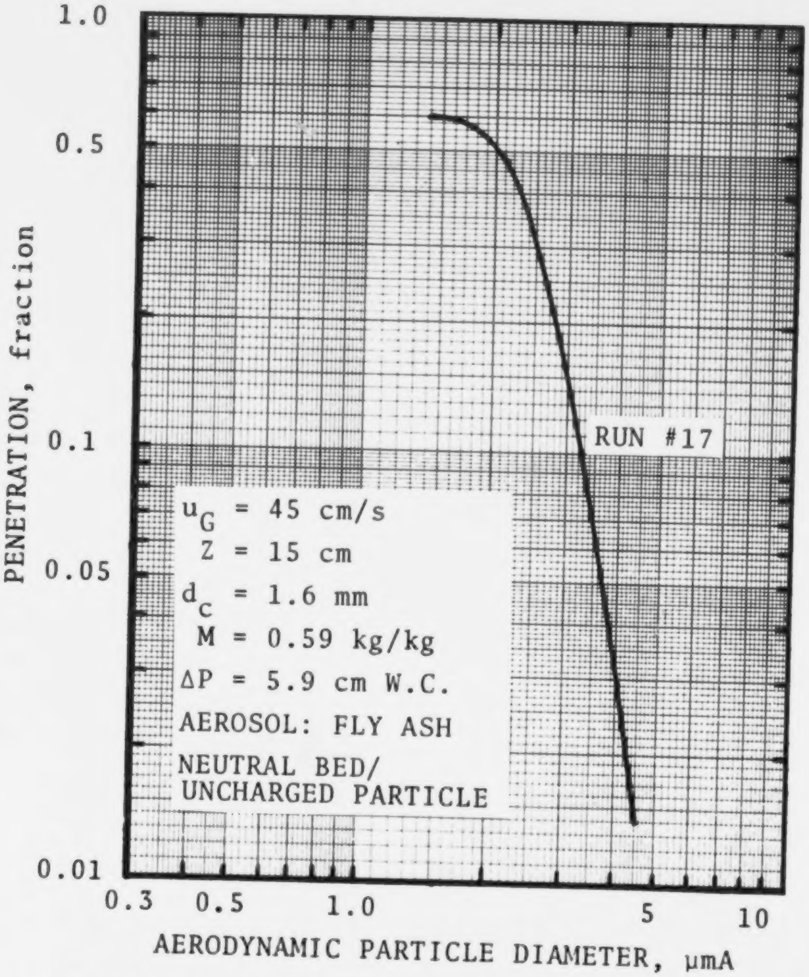

Figure C-11. Experimental grade penetration curve of a moving GBF.

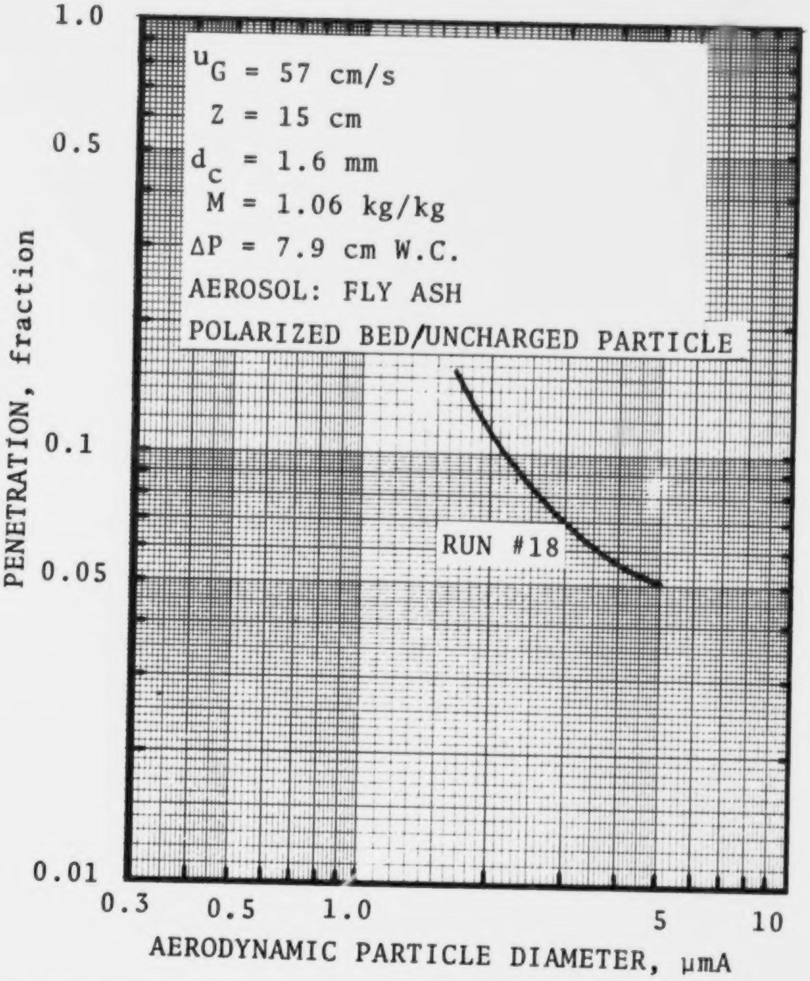

Figure C-12. Experimental grade penetration curve of a moving GBF.

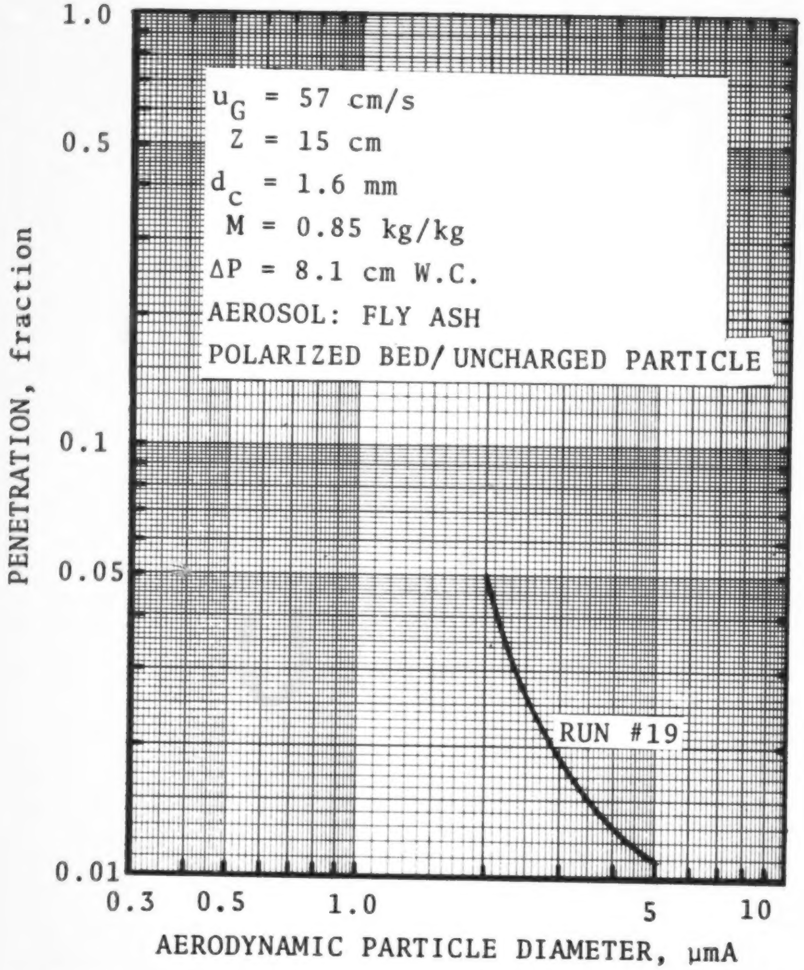

Figure C-13. Experimental grade penetration curve of a moving GBF.

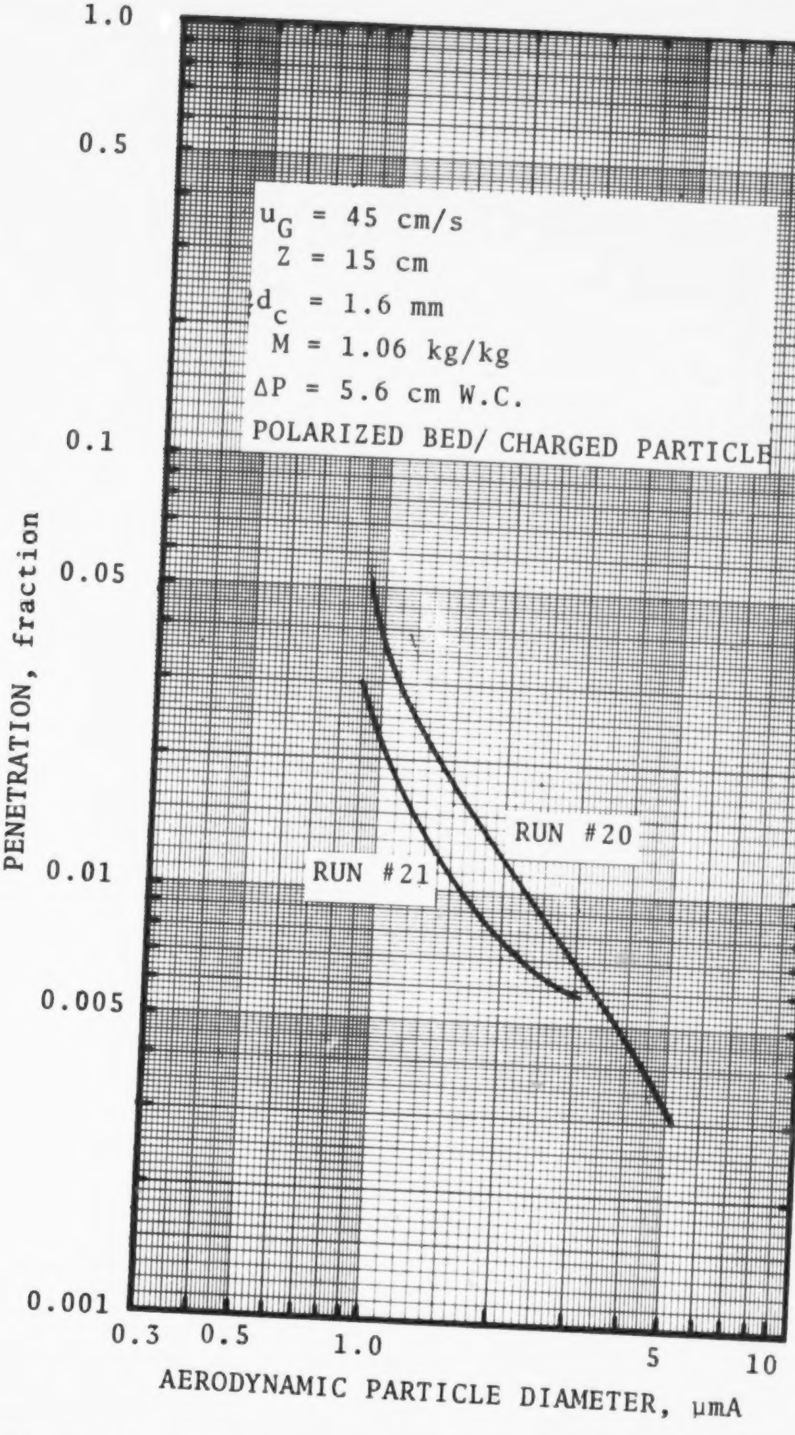

Figure C-14. Experimental grade penetration curves of a moving GBF.